

POLITECNICO DI TORINO

Master of Science in Mechanical Engineering

Master Thesis



Combustion diagnostics and calibration of the GT POWER "DI-Pulse" heat release model for a 11.0L diesel engine for heavy-duty applications

Supervisors

Ing. Roberto Finesso

Ing. Stefano D'Ambrosio

Ing. Omar Marelli

Ing. Andrea Manelli

Candidate

Giorgio Fontana

April 2021

Contents

1. ABSTRACT	6
2. INTERNAL COMBUSTION ENGINE BACKGROUND (ICE)	7
2.1. SI engine combustion process	9
2.2. CI engine combustion process	10
2.3. Diesel ideal cycle	11
2.4. Combustion in Diesel engines	13
3. GT POWER SOFTWARE.....	22
3.1. Model description	24
3.2. First model validation	27
4. TDC SHIFT	35
4.1. Beccari-Pipitone Method	37
4.2. Tazerout method	47
4.3. Jaye method	52
5. COMBUSTION MODELS IN GT POWER	57
5.1. Non-Predictive combustion model	57
5.1.1 CPOA (Cylinder Pressure Only Analysis)	57
5.1.2 TPA (Three Pressure Analysis)	58
5.2. Predictive combustion model.....	59
5.2.1 DI-Jet combustion model	59
5.2.2 DI Pulse combustion model	60
6. DI PULSE CALIBRATION PROCEDURE.....	63
6.1. Cylinder Pressure Only Analysis (CPOA) model tuning	64
6.2. Test Cell Data Analysis	69
6.3. Three Pressure Analysis (TPA) model tuning	73
6.4. DI PULSE model calibration	80
6.5. DI Pulse model validation	84
7. RESULTS DISCUSSION.....	85
7.1. CPOA results	85
7.2. TPA results.....	94
7.3. DI Pulse calibration results	96
7.3.1 Sweep optimization for 64 operating points	97
7.3.2 Independent optimization for 125 operating points	102
7.3.3 Sweep optimization for 125 operating points	105

7.4. DI Pulse validation results 106

7.4.1. Sweep optimization using 33 operating points 114

8. CONCLUSIONS 118

9. BIBLIOGRAPHY 120

1. ABSTRACT

In the last few years, emissions have become a crucial point in automotive world, stricter emissions regulations push manufacturers to design 'greener' vehicles, developing new engines with higher and higher fuel efficiency and low emissions. Current technologies such as EGR, common rail and aftertreatment system for exhaust gases are valid solutions in the short period, but these restrictions are going to be even stricter in the next future, so new technologies and a much stronger integration between vehicles and the surrounding infrastructures are necessary. These are the purposes of IMPERIUM Project (IMplementation of Powertrain Control for Economic and Clean Real driving Emission and ConsUMption), an ambitious project supplied by some of the biggest heavy-duty manufacturers in Europe, among which FPT Industries. In this thesis the engine under investigation is Cursor 11, a 11L diesel turbocharged engine for heavy-duty applications. For this engine, several operating points from test bench are provided, but the calibration of the model on GT POWER software powered by Gamma Technologies is made on 152 among over 3000 steady operation points. The aim of this thesis is the calibration and the assessment of a predictive combustion model for diesel engine on GT POWER software called DI Pulse. Once this model is calibrated, the full model engine is capable to obtain valid estimates of several combustion parameters such as the indicated mean effective pressure (IMEP), crank angle at which 50% of the fuel mass has burned (MFB50), the maximum pressure in cylinder and at which crank angle it happens, and other useful information about engine emissions (NO_x, Soot, CO₂, HC). These results are then compared with test data from rig tests provided by FPT Industries.

2. INTERNAL COMBUSTION ENGINE BACKGROUND (ICE)

At the beginning of the XX century, internal combustion engines have begun to represent a valid solution for the terrestrial propulsion: at first, these two solutions were in competition and brilliant results were obtained using electric engines: in fact, at the end of the XIX century the Jamais Contant was the first car to reach a speed higher than 100 km/h, using an electric engine. However, the electric propulsion was then replaced with the internal combustion propulsion, than still today is the most popular solution for the terrestrial propulsion. The reasons for this monopoly can be founded in its low weight-power ratio, considering the energy produced by the engine in a determinate time range. In fact, an internal combustion engine works with liquid fuels with a very high energy density with respect to other energy sources available for the propulsion, such as the electro-chemical energy used by the electrical engine and stored in batteries [1]. So, in order to define what type of propulsion system is the best, it is necessary to focalize not only on the propulsion unit, but on the whole system (engine + storage system): basing on what has been said, it is possible to see in figure *Fig. 1* that for vehicles equipped with an internal combustion engine the weight-power ratio is about 1 kW/kg, considering the whole system. On the other side, propulsion electric engines as well as fuel cells (that use gaseous fuel to produce energy) still stand on a weight-power ratio around 1 kW/kg but considering only the propulsion unit and not the whole system.

Electric motor type	Weight		Peak Power Output		Power-to-weight ratio		Example Use
Panasonic MSMA202S1G AC servo motor ^[18]	6.5 kg	14.3 lb	2 kW	2.7 hp	0.31 kW/kg	0.19 hp/lb	Conveyor belts, Robotics
Toshiba 660 MVA water cooled 23kV AC turbo generator	1,342 t	2,959,000 lb	660 MW	885,000 hp	0.49 kW/kg	0.30 hp/lb	Bayswater, Eraring Coal Power stations
Canopy Tech. Cypress 32 MW 15 kV AC PM generator ^[19]	33,557 kg	73,981 lb	32 MW	42,913 hp	0.95 kW/kg	0.58 hp/lb	Electric Power stations
Toyota Brushless AC Nd Fe B PM motor ^[20]	36.3 kg	80.0 lb	50 kW	67 hp	1.37 kW/kg	0.84 hp/lb	Toyota Prius ^[2] 2004
Himax HC6332-250 Brushless DC motor ^[21]	0.45 kg	0.99 lb	1.7 kW	2.28 hp	3.78 kW/kg	2.30 hp/lb	Radio controlled cars
Hi-Pa Drive HPD40 Brushless DC wheel hub motor ^[22]	25 kg	55.1 lb	120 kW	161 hp	4.8 kW/kg	2.92 hp/lb	Mini QED HEV, Ford F150 HEV
ElectriFly GPMG4805 Brushless DC ^[23]	1.48 kg	3.26 lb	8.4 kW	11.26 hp	5.68 kW/kg	3.45 hp/lb	Radio-controlled aircraft

Heat Engine/Heat Pump type	Peak Power Output		Power-to-weight ratio		Example Use
Wärtsilä RTA96-C 14-cylinder two-stroke Turbo Diesel engine ^[24]	80,080 kW	108,920 hp	0.03 kW/kg	0.02 hp/lb	Emma Maersk container ship
Suzuki 538 cc V2 4-stroke gas (petrol) outboard Otto engine ^[25]	19 kW	25 hp	0.27 kW/kg	0.16 hp/lb	Runabout boats
DOE/NASA/0032-28 Mod 2 502 cc gas (petrol) Stirling engine ^[26]	62.3 kW	83.5 hp	0.30 kW/kg	0.18 hp/lb	Chevrolet Celebrity ^[27] 1985
GM 6.6 L Duramax LMM (LYE option) V8 Turbo Diesel engine ^[11]	246 kW	330 hp	0.65 kW/kg	0.40 hp/lb	Chevrolet Kodiak ^[28] , GMC Topkick ^[29]
Junkers Jumo 205A opposed-piston two-stroke Diesel engine ^[30]	647 kW	867 hp	1.1 kW/kg	0.66 hp/lb	Ju 86C-1 airliner, B&V Ha 139 floatplane
GE LM2500+ marine turboshaft Brayton gas turbine ^[31]	30,200 kW	40,500 hp	1.31 kW/kg	0.80 hp/lb	GTS Millennium cruiseship, QM2 ocean liner
Mazda 13B-MSP Renesis 1.3 L Wankel engine ^[32]	184 kW	247 hp	1.5 kW/kg	0.92 hp/lb	Mazda RX-8 ^[33]
PW R-4360 71.6 L 28-cylinder supercharged Radial engine	3,210 kW	4,300 hp	1.83 kW/kg	1.11 hp/lb	B-50 Superfortress, Convair B-36
					C-97 Stratofreighter, C-119 Flying Boxcar Hughes H-4 Hercules "Spruce Goose"

Fig. 1 – Power to weight ratio for ICE and electric engine

Furthermore, focalizing the analysis to energy storage systems (fuel tanks for ICE and fuel cells, batteries for electric engines), figure *Fig. 2* shows how liquid fuels have density both in volumetric and gravimetric (ratio between the energy stored by the system and its weight – W/kg) terms greater with respect to the batteries used in electric engine propulsion: this consideration makes liquid fuels, almost all derivatives from petroleum, the best available fuel in storage terms [2].

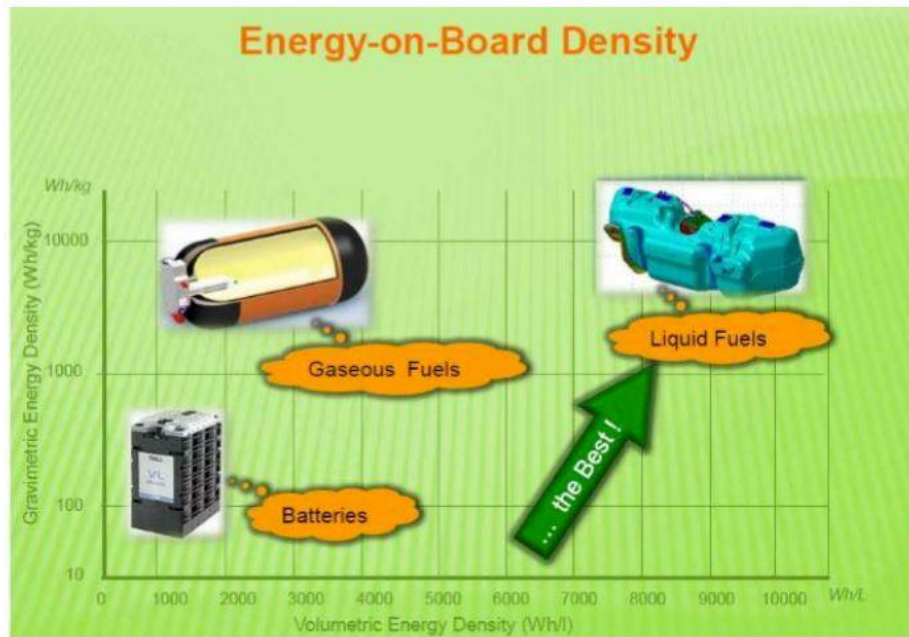
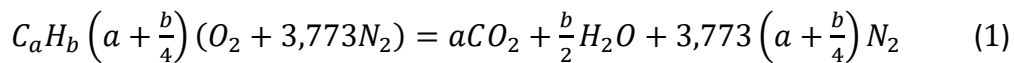


Fig. 2 – Energy on board density

Figure Fig. 2 also shows that gaseous fuels present a good gravimetric density but a worst volumetric one, due to a low storage density; in third place there is the batteries, with low values of both volumetric and gravimetric densities. For these reasons, internal combustion engines represent the best solution for terrestrial propulsion.

Internal combustion engines produce energy through the combustion: combustion is a chemical reaction in which fuel reacts with oxygen (reactants) obtaining the combustion products and chemical energy. ICE turns this chemical energy obtained by fuel oxidation in mechanical energy available for the propulsion. Fuels used for the combustion are made up by liquid or gaseous hydrocarbons that contain carbon atoms. These atoms during the combustion react with the oxygen atoms available in air in order to obtain CO₂; another product of the combustion process is water molecules, while the molecular nitrogen present in the air composition does not take part to the reaction, so it can be found unaltered among the combustion products. All the information can be summarized in the equation (1) that governs the combustion process:



Where a and b are constant value depending on the fuel type. However, equation (1) describes an ideal combustion process, while in a real combustion process internal combustion engine produces other substances such as carbon monoxide CO, unburnt hydrocarbons HC, nitrogen monoxide and dioxide NO_x, and particulate matter PM: alle these unwanted substances are *pollutant emissions* and generally correspond to 1% of all combustion products, they are toxic for the environment and for the humans [2] [3] [4]. Even if CO₂ is a product of the ideal combustion, it is a greenhouse gas and one of the main causes of the *global warming*: so, while reducing the pollutant emissions is possible acting on the combustion quality, reducing CO₂ emissions can be done only by burning less fuel, and therefore improving the powertrain efficiency.

During the years, different types of ICEs have been developed, however today the most common engines on the market are definitely *reciprocating ICEs*. These engines are characterized by the conversion of the linear motion of a piston into a cylinder closed at the top into rotational motion of the crankshaft. The piston, connected to the crankshaft through a connecting rod, moves between two extreme positions: top dead center (TDC) where the combustion chamber volume reaches its minimum value, and bottom dead center (BDC) where the combustion chamber volume reaches its maximum value [3]. The ratio between the maximum and the minimum combustion chamber volume values is called *compression ratio* (CR) and is one of the most important constructive geometric parameters in the engine development. CR is evaluated as followed:

$$CR = \frac{V_{max}}{V_{min}} = 1 + \frac{V_c}{V} \quad (2)$$

Where V is the *displacement volume*, and V_c is the *clearance volume*.

At the beginning of every cycle, it is necessary to enter fresh charge, a mixture of fresh air and liquid fuel, and to evacuate the reaction products at the end of the combustion process: in order to allow this recirculation between one cycle and another, cylinder chamber is connected with the external environment through the intake and the exhaust valves.

According to the combustion process, today on the market two different ICEs types are available:

- Spark ignition engine (SI): the combustion process start is triggered by a spark in a homogeneous mixture made by entrained air and evaporated fuel. These engines operate with fuels made by hydrocarbons with a rigid and compact structure such as gasoline and methane.
- Compression ignition engine (CI): the ignition of the fuel in these engines is caused by the elevated temperature of the air reaches with the mechanical compression. These engines operate with high-reactivity fuels, characterized by long and flexible hydrocarbons chains. The most used fuel is diesel. Due to the high reactivity of the used fuel is impossible to work as in a SI engine, so the fuel is injected few moments before the start of ignition [2].

The combustion process in both SI and CI engines evolves in the same way, described by equation (1), but the several steps followed in order to obtain the right conditions in the combustion chamber for the combustion process are quite different: below a quick discussion about the different combustion processes is made.

2.1. SI engine combustion process

In a spark ignition engine, the fuel can be injected in the intake port (PFI – port fuel injection) or directly in the cylinder (GDI – gas direct injection) [2]. However, in both case the fuel evaporates and then mixes with the entrained air: fuels like gasoline are quite volatile, which means that even with moderate pressure and temperature in-chamber conditions they easily evaporate. The injection step usually starts at the beginning of the compression stroke, so when in-chamber conditions are quite similar to the environment ones. At the end of the compression the fuel-air mixture reaches a temperature of about 700°C and a pressure of about 20 bar: these engines work

with very stable fuel, which means that even in quite high pressure and temperature in-chamber conditions they difficult ignite. So, it is necessary in order to start the combustion process to provided energy from an external source: this energy usually comes from a spark provided by a spark plug. This energy is about 1 mJ, but it is sufficient to obtain the start of the combustion (that releases over than 100 kJ per cycle). Once the first kernel is ignited, the combustion process propagates to the rest of the in-chamber air-fuel mixture in a progressive and gradual way. The first burning kernel releases a thermal flow absorbed by the adjacent layer, that reaches the ignition condition, and so on. This process is called *flame front propagation*, where flame front is referred to the thin layer that separates the burned zone, in which are present the combustion products, and the unburned zone, zone made up by the unburned air-fuel mixture (plus residual gas and eventual EGR) [2]. In the flame front the combustion reactions occur. The flame front propagation speed depends on the air/fuel ratio of the mixture and the highest speed is reached when this ratio is close to the stoichiometric ratio: the stoichiometric ratio is the exact ratio between air and fuel at which complete combustion takes place (*Fig. 3*).

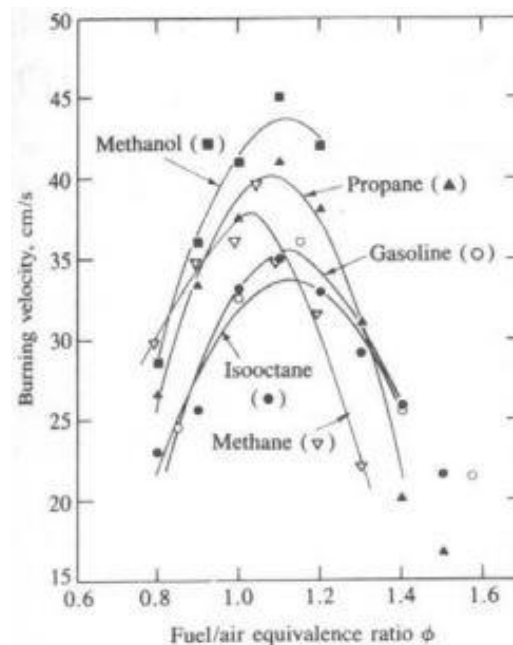


Fig. 3 – front flame laminar speed

2.2. CI engine combustion process

Compression ignition engines works with very unstable fuels, which means that even at low pressure and temperature conditions they can ignite. Due to this behaviour, it is impossible to proceed with an injection process similar to the SI engine one seen before. To avoid unwanted ignition, the fuel is injected directly in the combustion chamber (and not in the intake port, like happens for PFI SI engine) during the last degrees of the compression stroke. So, only air entered the cylinder during the aspiration step, then is compressed: when the piston is now close to the TDC, the fuel is injected at a pressure of around 800-1000 bar, which means that the fuel is injected in the chamber with a speed of hundreds m/s. When the jet entered the cylinder, it founds compressed air with a very high density, so the jet breaks into droplets [2]. These droplets now evaporate absorbing the heat flux from the compressed air, starting to mix with it. Time that interpasses from the start of injection

to the start of combustion, in which the fuel breaks into droplets, evaporates and mixes with the air, is called *ignition delay* [2], and strongly depends on several engine parameters such as the compression ratio, the rail pressure, droplets diameter, etc. While in SI engine flame front propagation, and so the combustion process, strongly depends on the air-fuel ratio, in CI engine there is not a homogeneous mixture in the chamber, there is rather a strongly inhomogeneity: in particular, there will be some zones with a lot of fuel, and other zones where the fuel is absent and there is only air [3]. Combustion process in a CI engine is a little bit more complex than the SI engine ones. In this section a quick description of how combustion works is made, the next section will analyse this process with more accuracy.

2.3. Diesel ideal cycle

Compression ignition engines follows the thermodynamic cycle developed by engineer Rudolph Diesel in 1892. Figure Fig. 4 shows the Diesel ideal cycle in a p-V diagram:

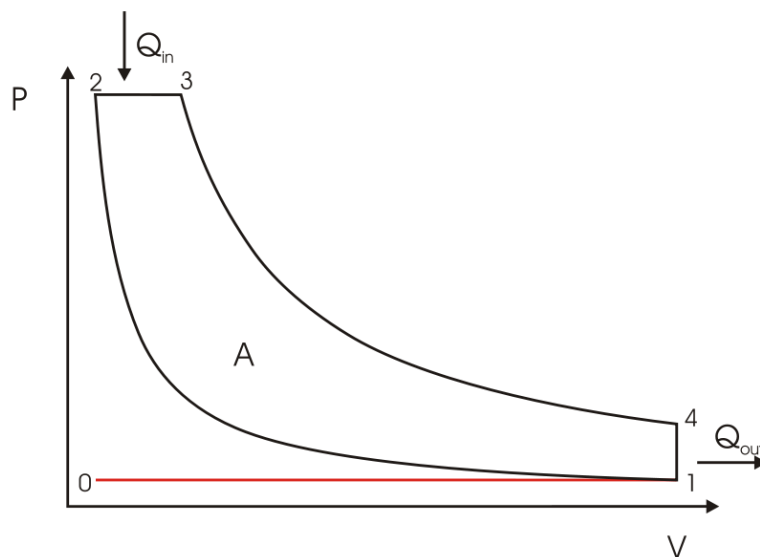


Fig. 4 – Diesel cycle

Six phases are visible on this graph:

- 1-2 transformation: adiabatic compression transformation.
- 2-3 transformation: heat absorption at constant pressure ($Q_c > 0$).
- 3-4 transformation: adiabatic expansion transformation.
- 4-1 transformation: heat release at constant volume ($Q_c < 0$).
- 1-0 transformation: forced discharge at constant pressure.
- 0-1 transformation: aspiration at constant pressure.

In this cycle, the working fluid is assumed to be an ideal gas, assuming specific heat at constant pressure c_p and at constant volume c_v to be constant and not dependent on the temperature changes during the whole cycle. The ideal fuel efficiency for a Diesel cycle is:

$$\eta_{id,Diesel} = 1 - \frac{1}{\varepsilon^{\gamma-1}} \cdot \frac{\tau^{\gamma} - 1}{\gamma(\tau - 1)} \quad (3)$$

Where ε is the compression ratio (3), γ is the ratio between c_p and c_v , and $\tau = \frac{T_3}{T_2}$. Figure Fig. 5 shows ideal efficiency curves for a SI engine and a DI engine cycles. For a given compression ratio value, ideal efficiency for Diesel cycle is always less than the Otto cycle (the cycle of a SI engine). However, in order to avoid the phenomenon of the knock, an abnormal combustion event characteristic for the SI engine where an air-fuel mixture fraction autoignites before the flame front arrives, in SI engines the used compression ratio is limited. While for a CI engine there is no limit for the used CR value [2] [3].

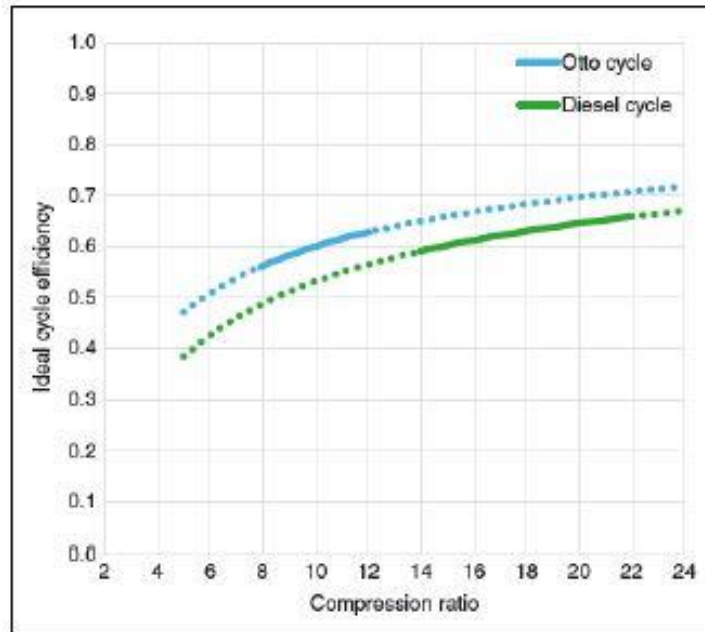


Fig. 5 – ideal Otto cycle efficiency vs ideal Diesel cycle efficiency

So, figure Fig. 5 underlines the operating areas for both engines, and it is visible that under these conditions CI engines can reach higher efficiency value. Ideal efficiency of Otto cycle is calculated using equation (4):

$$\eta_{id,otto} = 1 - \frac{1}{\varepsilon^{\gamma-1}} \quad (4)$$

A real Diesel cycle assumes the following shape:

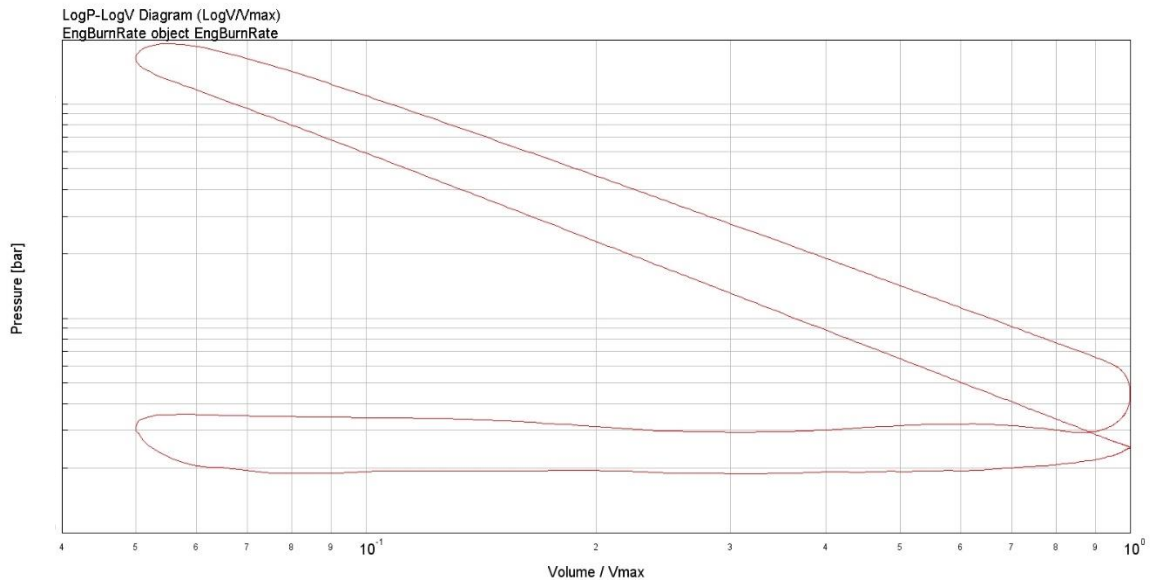


Fig. 6 – LogP vs LogV diagram for a real diesel cycle

Some consideration can be made comparing ideal Diesel cycle in figure Fig. 5 and a real Diesel cycle in figure Fig. 6: first, in a real engine when the piston is near to the BDC the exhaust valve does not lift instantaneously, but it starts few degrees earlier in order to have a bigger available surface for gas discharge when the piston reaches the BDC. Observing the real cycle, it is possible to see that the expansion isentropic transformation in the last degrees departs from the ideal one due to this valve behaviour, involving in a loss of available work. In an ideal Diesel cycle, the combustion event is instantaneous, and it happens at the end of the compression stroke, obtaining a quick pressure increase modelled as a vertical line; while in a real Diesel cycle, the combustion is quick but anyway it requests time. In order to obtain the main part of the combustion heat release when the piston is near to the TDC, the start of the combustion must be anticipated: this means that the real adiabatic compression line in the last degrees moves upward with respect to the ideal compression line, reducing the available work of the cycle. This work loss is more visible in an Otto real cycle, when the combustion event is slower with respect to Diesel combustion, due to the flame front propagation: in fact while in a diesel engine the whole air-fuel mixture when autoignites then burns quickly, in a SI engine the flame front propagation requests a longer time to burn all the in-cylinder mixture [3]. Finally, where transformations 1-0 and 0-1 overlapped in ideal cycle (Fig. 5) are now visible separately, and the formed area between them represents the *pumping loss* (*PMEP – Pumping Mean Effective Pressure*), a negative work due to the lamination losses through the valves during the working fluid replacement. All these phenomena reduce the actual work produced in the cylinder available for the crankshaft [2] [3].

2.4. Combustion in Diesel engines

Ci engines work with high reactive fuels, that is fuels that even at moderate pressure and temperature conditions can autoignite. So, differently to the SI engines injection process where air and fuel are premixed before entering the combustion chamber, in CI engines fuel is directly injected

in the combustion chamber a few moments before piston reaches the TDC. Therefore, during the aspiration phase only air entered the cylinder, and so only the air is compressed by the piston, reaching density values around 20-30 kg/m³. In order to control the combustion process, the fuel is injected with a speed of about 100 m/s using an injection pressure in the rail of about 800-1000 bar, in an environment with high-density air: this allows the jet to break into droplets with very small diameters, around 10-20 micros [2] [3]. These droplets in contact with high-temperature air (900-1000 K) start to evaporate and mix with in-chamber air, until autoignites when the threshold conditions in temperature and pressure are reached. Due to the high reactivity of the used fuel, this mixture can autoignites even with very high air-fuel ratio (i.e., with a small amount of fuel). This high reactivity characteristic of the fuel is due to its molecular structure: diesel fuel is the most common fuel used for the compression ignition engines, and it is made up by long and flexible hydrocarbons chains. Longer and more flexible hydrocarbon chains allow the pre-reaction to happen more quickly, because long chains mean that more carbon atoms are available to react with surrounding air while flexible chains mean that a single chain can react with itself. This characteristic molecular structure accelerates the combustion start, making the diesel a high-reactive fuel. All the various steps described above request a physical time to happen, even very short, and this retard the start of the combustion event. This delay that intercurrent from the starting of the injection (SOI) until the start of combustion (SOC) is called *ignition delay* τ ; this delay is necessary to allows the fuel to break in droplets, evaporate, mix, and reach the autoignition condition. Furthermore, in this time range also some pre reaction occurs. So, the ignition delay can be modelled as the sum of two terms:

$$\tau = \tau_{chem} + \tau_{phys} \quad (5)$$

A physical term characterized by the time employed for the processes described above, and a chemical term characterized by the chemical reactions within the fuel where intermediate molecules useful for the subsequent combustion process are formed. However, chemical reaction can take place during the physical phenomena, so they can overlap. In each case, between the two terms, the physical one is the most important [2] [3] [4].

During the ignition delay, the injector continues to inject the fuel in the chamber, and this fuel starts to accumulate; when the in-chamber autoignition conditions are reached, all the accumulated fuel burns generating a quasi-instantaneous in-cylinder pressure growth (this pressure peak generates vibrations, and the classical *diesel noise*). This first combustion, that can be considered almost as a constant volume transformation, allows the following injected fuel to find better pressure and temperature conditions, in order to reduce the time employed to evaporate and mix: ignition delay strongly decreases until it stabilizes on very negligible values (*Fig. 7*).

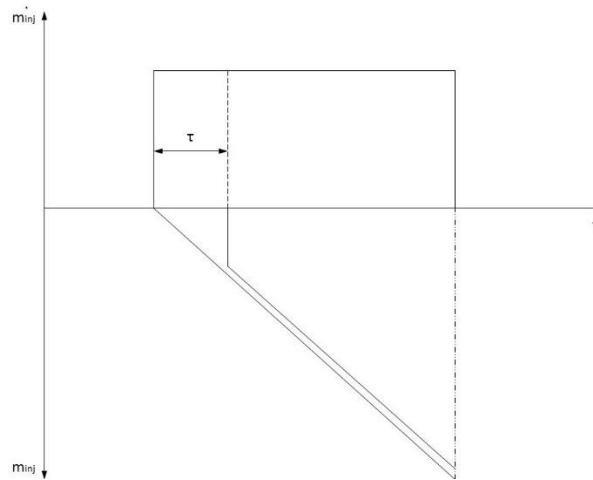


Fig. 7 – Ignition delay in Diesel engine

The typical CI engines combustion process can be characterized by the appearance of two subsequential combustion events: a first combustion characterized by a local peak, in which premix flames are present, followed by a second combustion consequential phase characterized by diffusion flames, visible in figure Fig. 8 as a lower peak but more consistent in time [2]. Observing the Heat Release Rate (HRR) in figure Fig. 8, it is possible to identify four different main steps in a diesel combustion process:

1. Ignition delay.
2. Premixed or rapid combustion phase.
3. Mixing controlled or fast diffusion-controlled phase.
4. Late diffusion-controlled combustion phase.

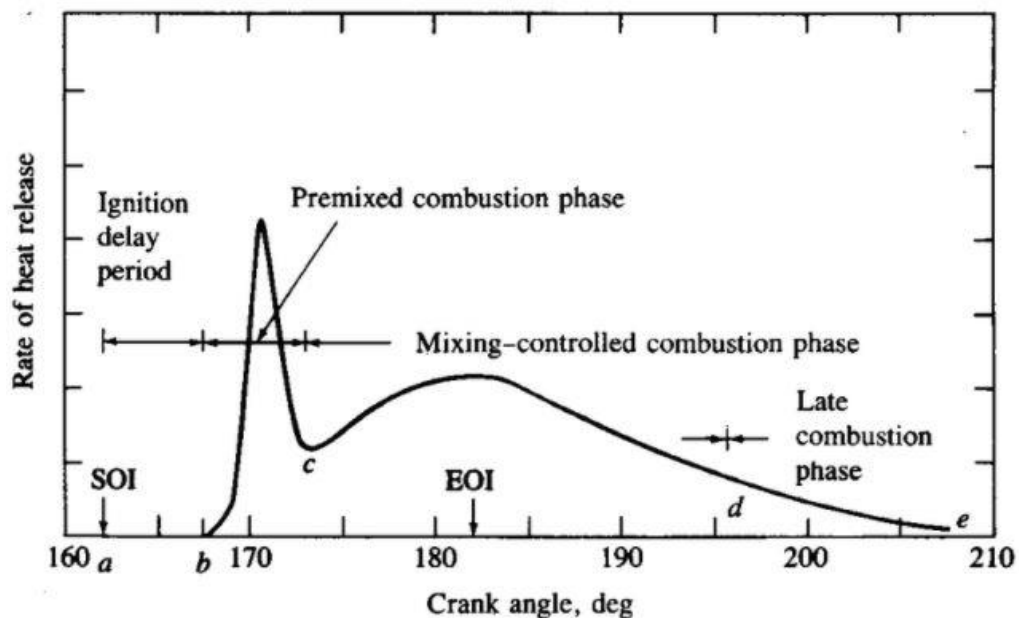


Fig. 8 – Heat Release Rate (HRR)

The ignition delay has just been described above, it is the time that intercourses between the SOI and the SOC. However, the ignition delay leads to a fuel accumulation during this first phase because the ignition conditions are not already reached, which comports a dangerous pressure increment

when all the accumulated fuel autoignites. This is the first stage of the combustion reaction, the so-called *Premixed combustion phase*. When combustion starts, due to the first air-fuel mixture kernels that reach the autoignition conditions, in-chamber temperature increases and the ignition kernels multiply, due to the acceleration of chemical and physical reactions in the fuel, causing the combustion of all the accumulated fuel. This phenomenon brings to a quasi-instantaneous pressure increase, that causes vibrations in the engine structure. In order to smooth this pressure peak, a solution could be to act on the fuel injection rate: modify the injection rate permits to regulate the fuel injected mass during the ignition delay. In particular, by decreasing the mass quantity injected, maintaining the ignition delay constant, allows to accumulate less fuel, obtaining a lower peak in the subsequent pressure trace [2]. However, decreasing the injection rate brings to a longer combustion process in angular terms, getting a worse combustion efficiency. A solution to this problem can be to use the injection rate shaping technique, where the injection rate is not constant, but it is modelled in order to achieve the best solution. For example, a valid solution can be the boot injection rate shape (*Fig. 9*), where during the ignition delay the injection rate is quite low in order to have little accumulated fuel at the autoignition moment, and a higher injection rate during the rest of the combustion process.

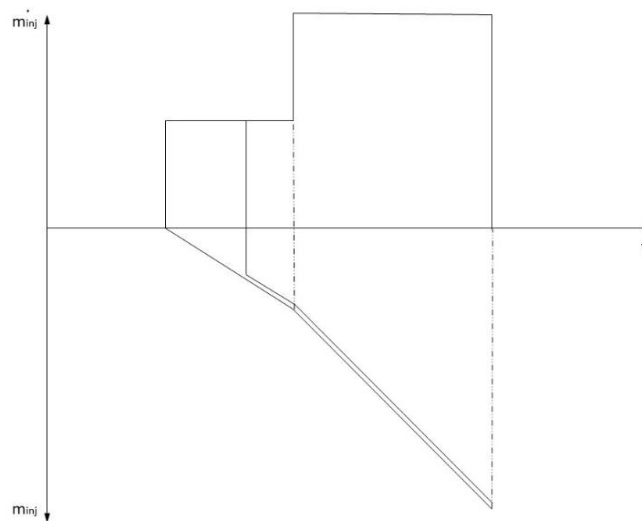


Fig. 9 – Variable injection rate

The Premixed Combustion Phase, as the subsequent combustion process described below, is characterized by the pollutant formation. In order to understand how pollutants is generated during the whole combustion process, it is useful to analyze figure *Fig. 10* that shows 10° degrees of the combustion process, from the start of injection until the full-developed combustion process.

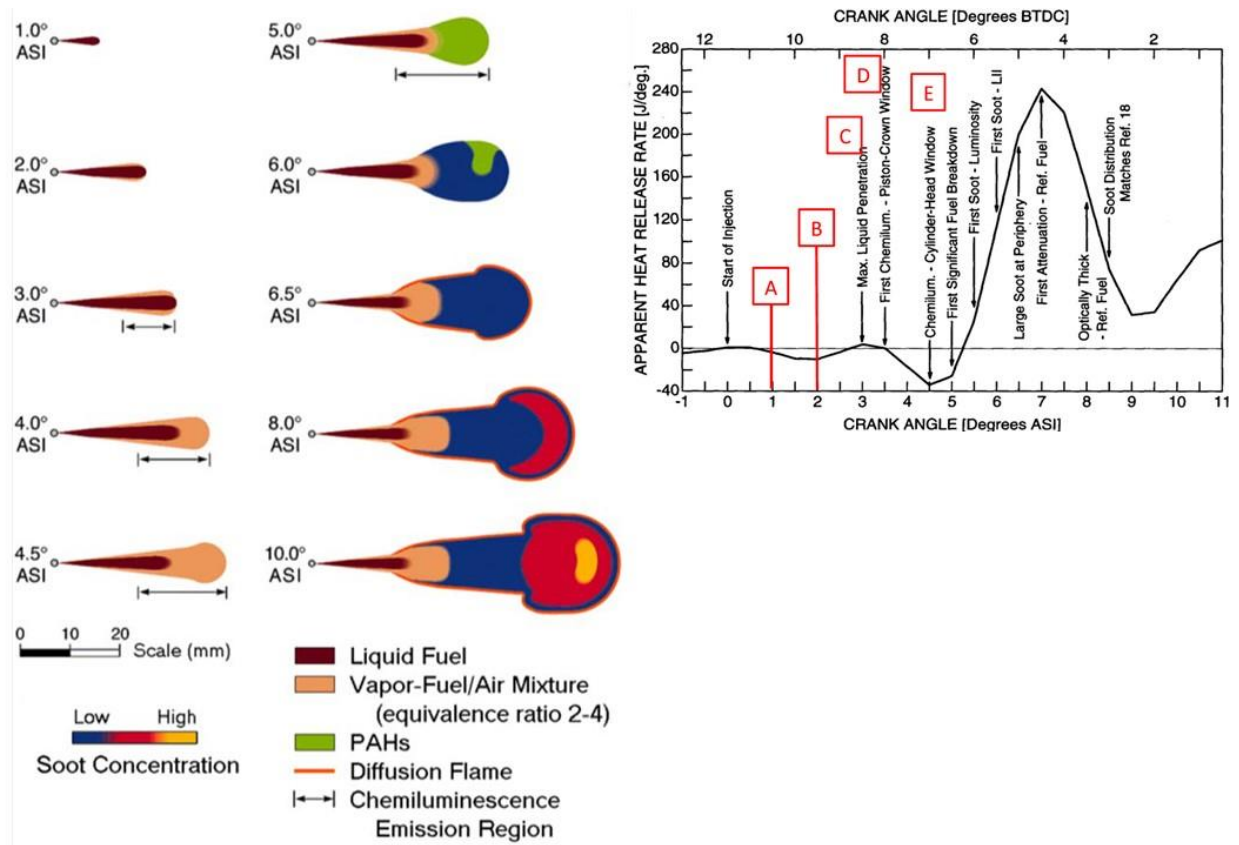


Fig. 10 – Diesel combustion process

This conceptual model describes the evolution of the combustion process in direct injection diesel engines, and it is developed by John E. Dec using advanced optical techniques [5]. For the first 2° degrees from the start of injection, the jet is still liquid, the droplets of the jet are surrounded by air at 700 K. In this condition, the injected fuel droplets start to evaporate very quickly, in fact at 3° degrees a beige halo around the liquid plume is already visible: this halo represents the air-fuel mixture. The mixing occurs only on the plume edge, because in this phase surrounded air cannot enter in the jet, due to its high density. This process continues and the air-fuel mixture zone grows more and more, while the liquid penetration stops reaching its maximum length. From 4,5° degrees after the start of injection, graph on the right in figure Fig. 10 shows a huge chemical energy release, which means that the combustion process is already started, and it happens in the vapor fuel-air mixture zone (the beige halo). The time intercurrent between the start of injection (0° degrees) and the start of the combustion is exactly the ignition delay: in this time the fuel jet breaks in droplets, evaporates, and mixes with the compressed in-cylinder air. In this example ignition delay is about 4,5° degrees long, but its length depends on many parameters [4] [5] [6].

When the combustion starts, globally in the combustion chamber there is more air than fuel, in fact λ (where λ is the ratio between the air-fuel ratio and the stoichiometric air-fuel ratio) is lean, even if in a diesel engine the max charge is reached with stoichiometric values of air-fuel ratio, so $\lambda=1$. However, combustion starts in a plume jet zone where the ϕ ($1/\lambda$) is included between 2 and 6, so where the fuel-air ratio locally is rich. The products of this first premixed combustion phase are a lot of carbon monoxide (CO), because there is not enough oxygen to complete the combustion process

in order to obtain carbon dioxide (CO_2), molecular hydrogen and also fuel fractions: the fuel fractions are made by hydrocarbon chains that only partially react with the oxygen, in minor quantity with respect to the fuel. Among these fuel fractions there are also the PAHs (Polycyclic Aromatic Hydrocarbon), peculiar hydrocarbon compounds that easily formed in environment with lack of oxygen and high temperature (in *Fig. 10* PAHs constitute the green zone). PAHs are made by hydrocarbon chains without the hydrogen atoms, that during the first combustion phase reacts in order to obtain H_2O molecules, and these molecules are important because these are the starting point from which the soot formation starts: in fact, during this phase these particles associate obtaining bigger carbonaceous particles, that is the soot. Observing figure *Fig. 10* passing from $5,0^\circ$ degrees to $6,0^\circ$ degrees ASOI (after start of injection) the green zone starts to begin blue, where blue is exactly the soot particles [5] [4]. The premixed phase combustion is ended, but if the blue zone is still present some amount of fuel fraction, and the injection is not ended, so other fuel is available; furthermore, the plume is surrounded by air, full of molecular oxygen. So, there are the right conditions to have a second combustion event. This second combustion step is called *Mixing Controlled Phase* and over the 90% of the total amount of injected fuel burns in this phase. Observing $6,0^\circ$ degrees of *Fig. 10* figure, fuel and air are in contact along the whole plume perimeter: locally air and fuel spread into each other, obtaining a thin layer; in-cylinder conditions are perfect for the combustion start, so in this layer (orange perimeter in figure) the reaction begins. The diffusion flame, however, does not surround all the plume, in fact it is visible that the perimeter of the liquid jet (brown one near the nozzle) the diffusion flame is not present: this happens because when the fuel is injected it requests time in order to evaporate, so the surrounded air is in contact with the fuel, but this last is still liquid, so air cannot enter due to the high density. This combustion is totally different respect to the premixed phase because air-fuel mixture in Mixing Controlled Phase burns in a *diffusive flame*: the burn rate of the mixture, and so the combustion rate, depends on the diffusion entity of the surrounded air into the fuel plume, hence the name diffusion flame. The diffusion flame burns with a ϕ value around the unity, so in a stoichiometric ratio, this because diffusion is quasi-homogeneous locally on the jet perimeter [4] [5]. During this second combustion all the unburned fuel from the premixed combustion burns. Observing the HRR graph (*Fig. 8*), it is possible to see both the combustion steps, in particular, the second peak is the heat release obtained by the Mixing Controlled Phase. *Fig. 11* shows the jet in its final form, it remains in this way until the injection event is ended.

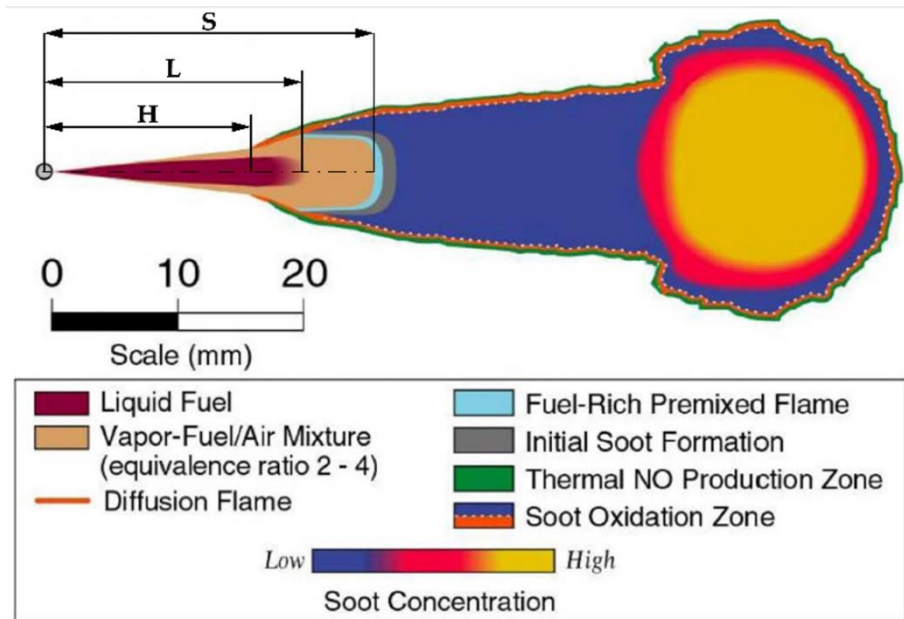


Fig. 11 – Fuel plume completely developed

If the combustion process continued without interruption, all the soot produced in the premixed phase would be burned in the diffusive phase, in order to obtain no soot at the end of the combustion. However, wall-jet interaction and jet-jet interaction suffocate the diffusion flame before that all the soot is burned, obtaining it among the others combustion products. Diffusion flame burns with a stoichiometric ratio, so the developed temperature in this second combustion steps are higher than the temperature reached in premixed phase ($\phi=2\div6$) [5] [4]. The diffusion flame is surrounded by air, where beyond the oxygen is also present molecular nitrogen: nitrogen is a non-reactive gas in ambient conditions, while becomes reactive at high temperature. So, around the diffusion flame there is a lot of molecular nitrogen in very high temperature conditions (2700-3000 K) in contact with oxygen: this coexistence brings to the NO_x formation, that depending on the time in which these conditions are maintained, can become NO₂ rather than NO. NO_x is a toxic gas that can cause serious health damage to humans, so its production must be limited, because it is difficult to totally set to zero. However, even if NO_x formation occurs in the second step of the combustion reaction, the premixed phase trend affects the subsequent NO_x formation indirectly: in fact, if the premixed combustion reaches temperature value higher than the standard one, around 1600-1700 K, the subsequent mixing-controlled combustion will reach even higher temperature, promoting and accelerating the NO_x formation process. *Fig. 12* shows a panoramic of pollutants formation in a diesel engine [4] [5].

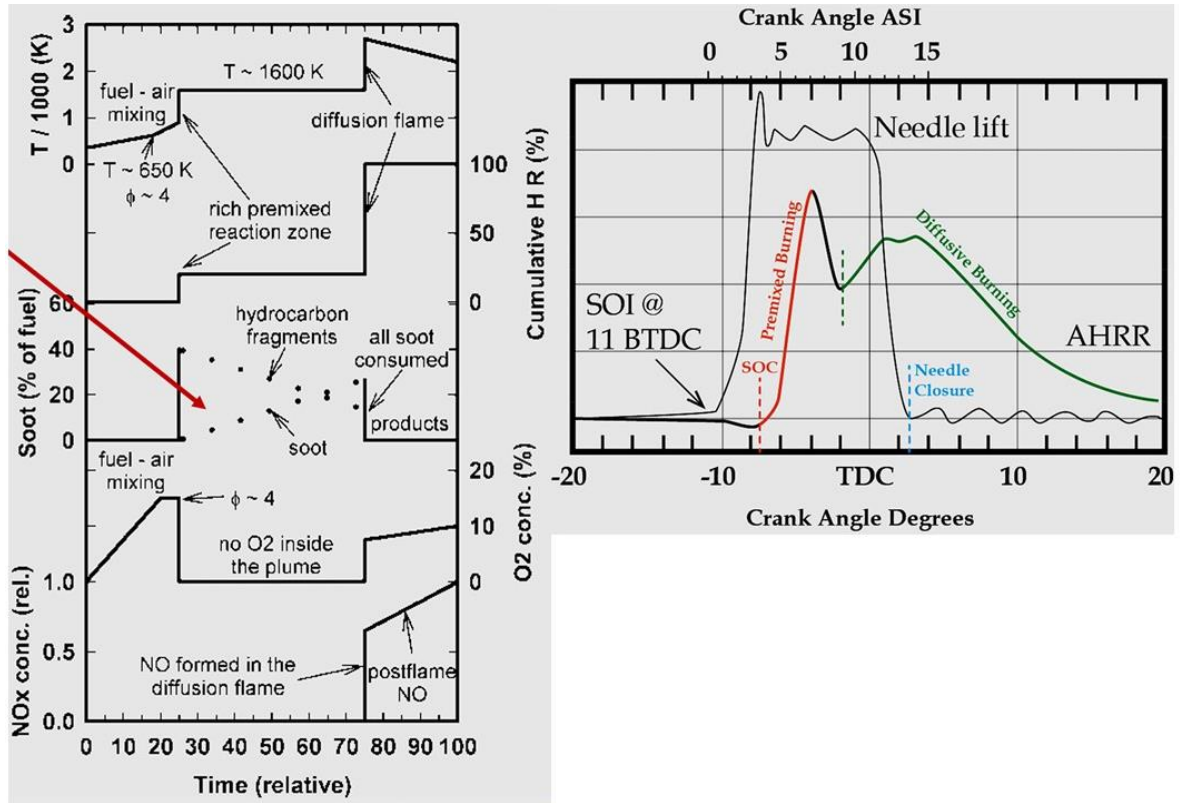


Fig. 12 – Pollutant formation process

Once the injection event is ended, in the cylinder the chemical reaction still goes. In this phase the last unburned hydrocarbons as well as the produced soot participate to the combustion. These last combustion phases are promoted by the turbulent motions within the cylinder that remix the gas in the chamber. This last phase is called *Late Combustion Phase* and must be limited in order to not negatively affects the efficiency of the cycle.

Below, several quantities that have not yet been mentioned related to the engine performances are described in order to help the readers in the text comprehension.

- *Rotational speed (n)*: indicates the revolutions number of the engine, usually in a minute, and it is measured by using a rotational encoder [3].
- *Engine Torque (T)*: is the twisting force that the engine produces, it is measured by a dynamometer.
- *Brake Power (P_b)*: is the power available at the crankshaft. It can be calculated with the following formula [3].

$$P_u = T \cdot n \quad (6)$$

Since the engine is a volumetric machine, the produced power can be also written as:

$$P_u = W_u \cdot i \cdot \frac{n}{m} \quad (7)$$

Where W_u is the work per cycle for each cylinder, i is the number of cylinders, n is the revolution number in a second, m is a factor depending on the engine type ($m=1$ for 2T, $m=2$ for 4T) [3].

- *Brake Mean Effective Pressure (bmep)*: is a parameter used to compare engine with different sizes. It is the ratio between the work per cycle and the cylinder displacement [3].

$$bmep = \frac{W_u}{V} \quad (8)$$

- *Indicated Mean Effective Pressure (imep)*: is defined as follow:

$$imep = bmep + fmep \quad (9)$$

Where *Friction Mean Effective Pressure (fmep)* is the work (normalized with respect to engine displacement) requested in order to win the frictions between engine components and for actuating the accessories.

- *Mechanical efficiency (η_m)*: is the ratio between brake power and indicated power:

$$\eta_m = \frac{P_b}{P_{ig}} \quad (10)$$

- *Fuel conversion efficiency (η_f)*: is the work produced in a cycle divided for the energy provided by the combustion of the fuel. This energy can be obtained multiplying the combusted mass of fuel per cycle and the lower heating value of the fuel Q_{LHV} , which is the amount of energy released by the complete combustion of a fuel single unit.

$$\eta_f = \frac{W}{m_f \cdot Q_{LHV}} \quad (11)$$

- *Volumetric efficiency (η_v)*: defines the entrained air amount with respect to the ideal quantity:

$$\eta_v = \frac{m_a}{\rho_a \cdot iV} \quad (12)$$

In turbocharged engines this value can assume values higher than one. ρ_a is the air density, that can be assumed as an ideal gas, and so its value can be evaluated by means of the ideal gas law:

$$\rho_a = \frac{p}{R \cdot T} \quad (13)$$

Where R is the specific gas constant and is equal to $287 \frac{J}{kg \cdot K}$.

- *Brake specific fuel consumption (bsfc)*: indicates how efficiently an engine exploits the fuel in order to produce work:

$$bsfc = \frac{\dot{m}_f}{P_b} \quad (14)$$


3. GT POWER SOFTWARE

In this thesis the software used for simulating engine operations is GT POWER, a software of the family GT-SUITE released by Gamma Technologies LLC. In GT POWER is possible to build a model of any internal combustion engine, and by using some parameters as input it is possible to foresee what conditions are achieved at the end of the combustion process. The calculation of the final condition is obtained firstly by dividing the whole volume in several sub-volumes, this phase represents the *discretization of the model*, then in each sub-volume the gas-dynamic equations which governs the fluid motions are resolved by using some numerical schemes. In every sub-volume the solution quantities (pressure, temperature, mass fractions, etc.) are calculated [7]. In GT POWER, combustion refers to the transfer of a defined amount of unburned fuel mass and air from an unburned zone to a burned zone in the combustion chamber through the front flame, releasing chemical energy [8]. This combustion event is modelled by using a combustion model: GT POWER provide different type of combustion model, which differentiate on the used fuel (obviously a diesel engine requires a different combustion model with respect to a SI engine, because the combustion event is different), and they could be predictive, non-predictive or semi-predictive model. A better description is faced in section 5. With the combustion model GT POWER allows to evaluate the chemical energy released by the fuel combustion and through the energy conversion it allows to evaluate other quantities related to engine performances, such as the IMEP (Indicated Mean Effective Pressure). Then, after an evaluation of the friction and organic losses of the engine, it is possible to evaluate even the BMEP (Brake Mean Effective Pressure). This is a quick discussion of how GT works.

The software is divided in three main parts:

- GT-ISE
- GT-Solver
- GT-Post

GT-ISE is the environment in which it is possible to build the engine model: the engine parts can be modelled using some pre-built components, called *blocks*, that can be taken from the GT Libraries. These available blocks are many for each necessity, usually every block represents a different part of the engine: there is a block for the cylinder, a block for the valve, one for the pipe and so on. Then, these parts are connected between each other using virtual links in order to allow the information passage from two (or more blocks): every type of block has a maximum number of available links in input and in output. Once the block is imported in the main template of GT-ISE these components must be tuned by setting a wide range of information which represent the real operating conditions. Building a model is about to set all this information in order to perform an analysis as closer as possible to what happens in an engine rig test in real conditions. *Fig. 13* shows an example of a block used in this Diesel engine model, in particular a part of the intake manifold.



☒ Main
 ☒ Thermal
 ☒ Pressure Drop
 ☐ Plots

Attribute	Unit	Object Value
Basic Geometry and Initial Conditions		
Diameter at Inlet End	mm	85 ...
Diameter at Outlet End	mm	85 ...
Length	mm	750 ...
Discretization Length	mm	40 ...
Initial State Name		Boost ...
Surface Finish		
<input type="radio"/> Smooth		
<input checked="" type="radio"/> Roughness from Material		smooth_galvanized
<input type="radio"/> Sand Roughness	mm	
Additional Geometry Options		
Radius of Bend	mm	ign ...
Angle of Bend	deg	ign ...
Pipe Elevation Change or 3D Acceleration Object	mm	ign ...
Number of Identical Pipes		def (=1.0) ...

Fig. 13 – Tail Pipe main template

The information is grouped in templates: Fig. 13 shows the *main template*, where general information such as the dimension of the round pipe, the used material and the pipe form must be set. Every block can request a higher or a lower number of parameters based on the complexity of that block. This data can be inserted numerically, by manually insert the wanted value, or can be provided in parameter form, where the information is parametrized in order to use different values for the same quantity: this approach is recommended where the model must work with different cases that request different input data. Alternatively, the input data can be updated in maps form, objects that allow to express the variability of this quantity as a function of other parameters, usually speed and BMEP. However, the model building is not the central point of this thesis work, so a brief description as above is sufficient.

Another part of the software is GT-Solver, the solver that the software uses for the calculation step. The equation used by this solver are referred to the Navier-Stokes's equations, a system of partial differential equations which describe the macroscopical fluid behavior step by step. The fluid must be continuous. In particular, the equation composing the system are:

- Mass conservation equation
- Energy conservation equation
- Momentum conservation equation

The solver works using a one-dimensional approach for the Navier-Stokes's equations resolution, starting as previously set by dividing the available volume in several sub-volumes, with a dimension imposed by the user (in Fig. 13 is visible *Discretization Length* which is the approximate length of each sub-volumes where the solution quantities are evaluated) [7]. Then, for each sub-volume the scalar quantities are calculated in its center and imposed constant for all the sub-volume, while vectorial quantities are evaluated as boundary conditions in order to obtain continuity between two linked blocks. The last part of the software is GT-Post for the post-processing of the obtained results.

In this software is possible to see the obtained data of all the quantities evaluated by the model, plot the results and export the values for further analysis.

3.1. Model description

The model used in this work is supplied already built, and it represents a 11 liters Diesel engine, 6 cylinders, direct injection, supercharged for heavy duty applications. *Fig. 14* shows this model.

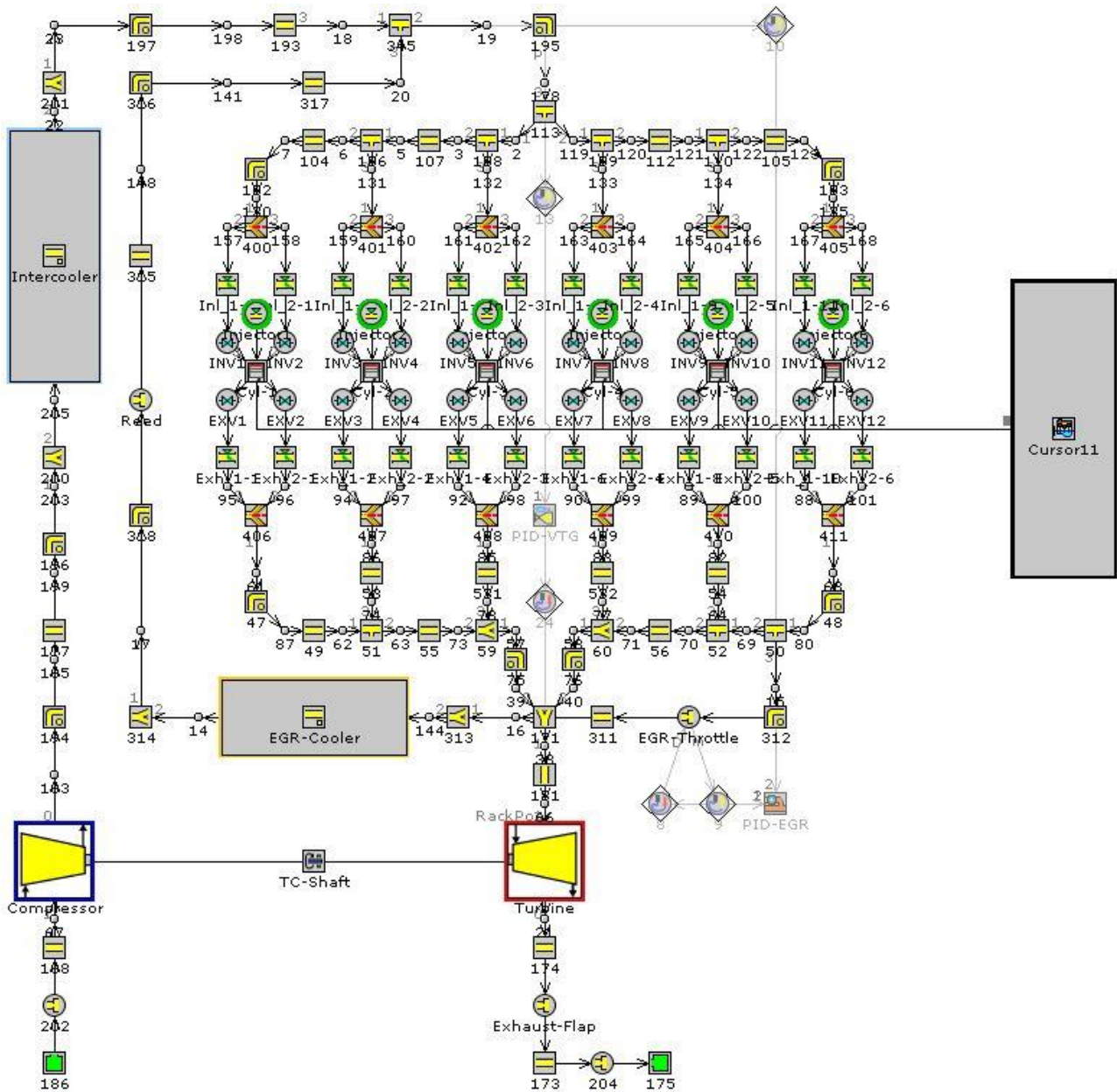


Fig. 14 – Cursor 11 model in GT-POWER

Among the classical elements that compose any engine, this model shows some components that need to be studied in deep, because are more ‘extraordinary’:

- *Variable Geometry Turbocharger (VGT)*: this is not a classic turbine, because this particular component presents rotating nozzle vanes where is possible to modify the blade angle in function of the engine speed as well as the exhaust gas flow rate [2]. Opening the turbine

nozzles (the space within two adjacent blades can be modeled as a nozzle) at high speed where the gas flow rate is huge and closing them at low engine speed where the gas flow rate is lower, allows to obtain higher supercharging level simply with a better usage of the exhaust gas' energy. Furthermore, at low load when the blades are inclined in order to obtain a very thin passage area the exhaust gas flow is very fast, and if correctly directed it can provide an increase of the generated torque, guaranteeing a huge acceleration of the turbocharger group. This solution also allows to reduce the turbo-lag phenomenon, that is the response delay due to the turbo group inertia at low load [2]. VGT presence in a CI engine provides an increase in global efficiency. Engines with fixed-blades turbine rather than a VGT, must choose a turbine size in order to maximize low-middle load efficiency at the expense of high load: in fact, when these engines reach high load, the exhaust gas flow rate is too much bigger for the actual turbine. So, in order to avoid the turbine from exploding, the turbocharger group needs a Wastegate valve, which is a valve that allows the exceed gas flow rate to by-pass the turbine. In this way the by-passed exhaust gas flow enthalpy is not exploited, and this leads to lower efficiency. Even VGT presents a Wastegate valve, but only for safety reasons. The keying angle of the blades is modified by using an electric or hydraulic actuator. This actuator is managed by a PID-VGT controller (in *Fig. 14*, the element between cylinder 3 and 4) that performs a closed loop control by comparing the actual pressure value in the intake manifold with a desired value saved in ECU maps.

- *EGR cooled circuit*: Exhaust Gas Recirculation consists in a high-pressure circuit that draws off a fraction of the exhaust gas from the exhaust manifold before the turbine and enter this fraction in the intake manifold after the compressor. This circuit is also cooled, in order to draw off a bigger exhaust gas fraction: in fact, by reducing the exhaust gas temperature its density increases, allowing to recirculate more exhaust gas in the cylinder [2]. However, there is a limit to the cooling level, because by reducing too much the temperature of the gas there is the risk of condensation droplets forming, that are dangerous for the engine performance. EGR is very important because by recirculating exhaust gases in the cylinder, it allows to reduce the peak temperature reached during the combustion event, reducing the NO_x formation (that increases with the temperature). The EGR fraction is regulated by an electrically operated pneumatic valve, which in turn is controlled by the PID-EGR controller (the one linked with block 312 in *Fig. 14*), that calculates the exact recirculation quantity based on the intake air quantity; this operation is made by using maps. Observing the EGR circuit in the model (from pipe 313 to pipe 317) it is possible to find another valve, the Reed-Valve, located after the EGR-cooler, that is a unidirectional valve that blocks the exhaust gas reflux back toward the exhaust manifold, when for some reason the intake manifold pressure becomes huger than the exhaust one [2].
- *PID-BMEP controller*: this controller allows the engine to deliver always the same desired BMEP value. In order to do that, this controller acts on the injector by modifying the injected quantity per stroke, in function of several engine parameters, such as rotational speed and entrained air, basing on internal maps. The control is the same used by the other controllers in the model, where there is a closed loop control based on a proportional-integrative sensor signal: this controller estimates the desired BMEP target at a determined engine operating

condition, and basing on the sensor signal, the PID-BMEP modifies the injected quantity acting on the injectors. *Fig. 15* shows the PID-BMEP.

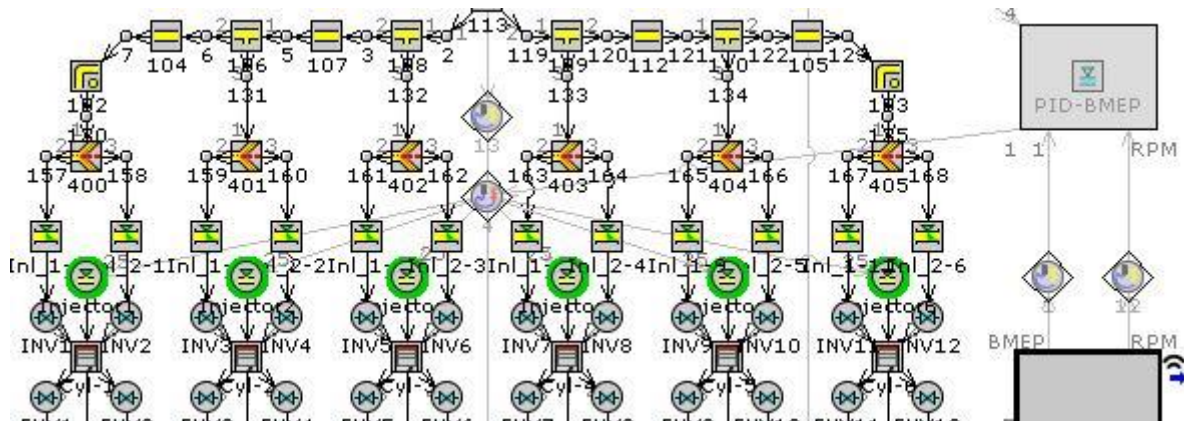


Fig. 15 – PID-BMEP controller

How it is possible to see by comparing this figure with the whole model in figure *Fig. 14*, the PID-BMEP has been removed. The reason behind this choice is that even without the PID-BMEP the simulated BMEP rests very similar to the experimental one. Beyond this medication, before starting the first validation of the model, all the maps have been substituted with parameters. How explained before, some elements in the model perform a closing loop control based on the maps. 'RLTDependenceXY' (or 'RLTDependenceXYZ') is a 'dependency reference template', used when the user wants a quantity as a function of one (or more) input signal, which does not necessarily have to be connected to the actual block. Beyond the controller, a lot of other elements work using maps in this model. These maps work by finding the value to be attributed as function of the wanted quantities, usually BMEP and rotational speed of the engine. Substituting the RLTDependence map with a parameter means to attribute at each case an exact value for any quantities: in this way the value must not be found in these maps by interpolating, because the interpolation method could be affected by errors, by selecting a wrong value. The substituted parameters are then defined in the Case Setup. In *Fig. 16* are visible some quantities that used parameters. Start of Injection (SOI), injection quantity, injection pressure and EGR fraction are some of the quantities in which RLTDependence maps are substituted with parameters for a higher accuracy during the simulation. In this engine, the main injection event is preceded by a pilot injection, and in GT POWER every injection is treated separately, so in Case Setup two SOI and two injection quantities must be defined.

Main DIPulseCalibration All							
Parameter	Unit	Description	Case 1	Case 2	Case 3	Case 4	Case 5
Case On/Off		Check Box to Tur...	<input checked="" type="checkbox"/>	<input checked="" type="checkbox"/>	<input checked="" type="checkbox"/>	<input checked="" type="checkbox"/>	<input checked="" type="checkbox"/>
Case Label		Unique Text for PL...	0	1	2	3	4
speed	RPM		2225	2100.01001	2000	1900	1800
BMEP	bar		11.08650303	14.64741993	17.10928535	19.16955757	20.11266518
BoostPressure	bar		2.32655896	2.535138977	2.671228943	2.750248962	2.791070984
TurboSpeed	kRPM		82.8	98.9	100	100	100
inlet	mm		85	85	85	85	85
outlet	mm		75	75	75	75	75
InjectionPressure	bar	Rail Pressure (Inject...	1750.640015	1905.880005	1937.939941	1974.73999	1986.130005
Fuel-Mass_pilot	mg	Injected Mass per P...	0	0	2.2	2.2	2.2
Fuel-Mass_main	mg		115.9076191	147.0424163	168.5763883	187.0461944	193.6660549
SOI_pilot	deg	Injection Timing	-30	-30	-21.2428371	-20.13026039	-18.2690194
SOI_main	deg	Injection Timing	-9.55260006	-9.215475816	-8.161099625	-7.690800133	-6.507300072
EGR_target	%	Target EGR Fraction...	10.83582557	9.363388177	8.33490088	6.957214579	5.800016174
boost_target	bar	Target	2.32655896	2.535138977	2.671228943	2.750248962	2.791070984

Fig. 16 – Case Setup

3.2. First model validation

In this work, the Cursor 11 engine will work with 152 steady state operating points. These 152 operating points are scattered all over the engine map, in order to cover all the engine conditions. Fig. 17 shows the Cursor 11 engine map with the operating points used for this work.

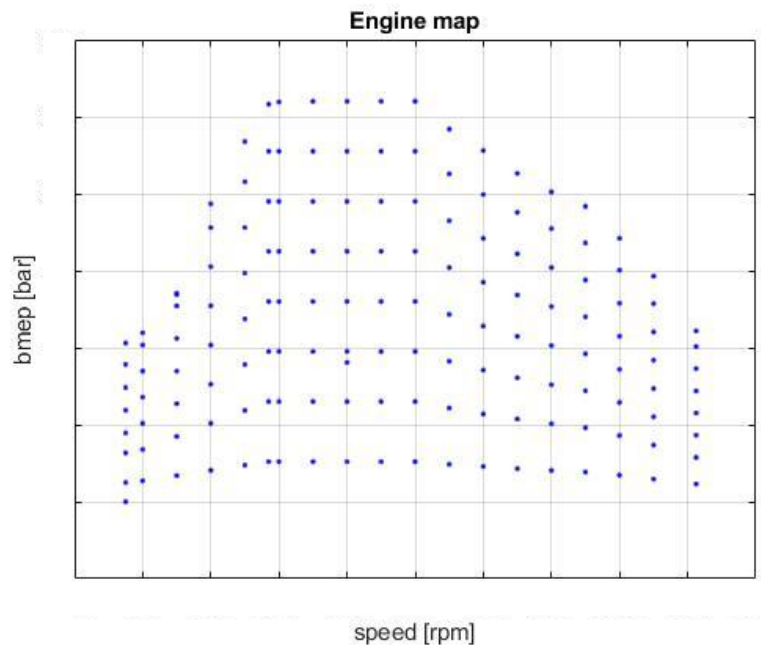


Fig. 17 – Engine map with the 152 operating points selected for the simulation

FPT Industrial provides a set of data obtained in rig tests for these 152 points, and the aim of the first part of this job is to validate the model. The validation of a model consists in compare simulation outputs with provided data obtained in a rig test, for a certain number of quantities. If experimental data and simulated data fit well, the model is validated. Before starting the simulation, it is necessary to update in Case Setup the correct number of cases, inserting a value for each parameter. Once the Case Setup is ready, the first simulation can be launched. The quantities chosen for the validation are:

- Brake Mean Effective Pressure (**BMEP**)
- Rail Pressure
- Total Injected Fuel Quantity per stroke (pilot + main)
- EGR Fraction
- Boost Pressure
- Crank Angle at which 50% of Mass Fraction is Burned (**MFB50**)
- In-cylinder Pressure Peak
- Pressure Peak Position
- Indicated Mean Effective Pressure on 720° degrees (**IMEP720**)
- Indicated Mean Effective Pressure on 360° degrees (**IMEP360**)
- Pumping Mean Effective Pressure (**PMEP**)
- Friction Mean Effective Pressure (**FMEP**)
- Lambda at EVO
- Intake Manifold Temperature and pressure
- Exhaust Manifold Temperature and pressure
- Air Mass Flow rate
- EGR Flow rate

These quantities have been selected for their relevance in the combustion process. Once the simulation is ended, GT-Post allows to export whatever output quantity in .txt form, then these data are post-processed in MatLab, where they are plotted with the experimental data provided by FPT Industries. For each analyzed couple of quantities, in order to quantify the accuracy of the simulated data, two statistic indexes are used: R2 and RMSE. R-squared (or R2) is a statistical measure that represents the proportion of the variance for a dependent variable with respect to an independent variable (or variables) in a regression model; it can assume values within the range 0 to 1, and a negative value has no mathematical meaning. R2 is evaluated by using formula (15).

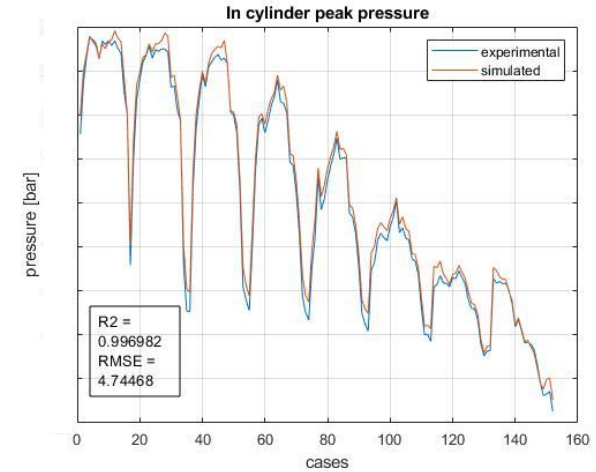
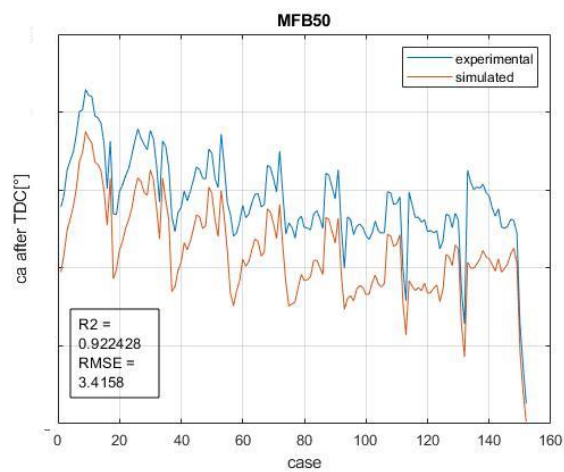
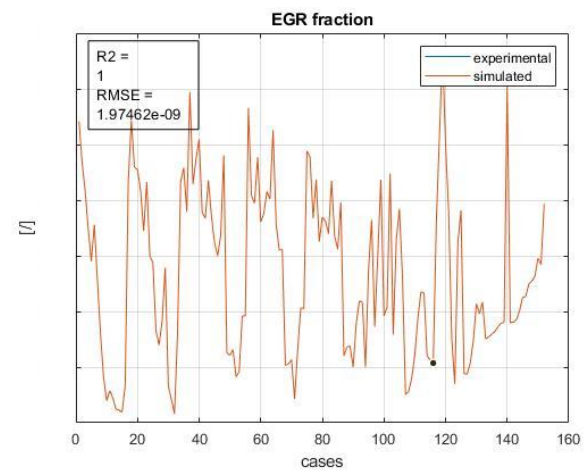
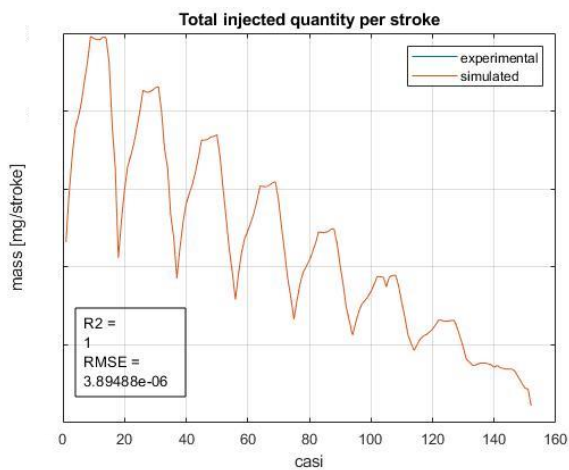
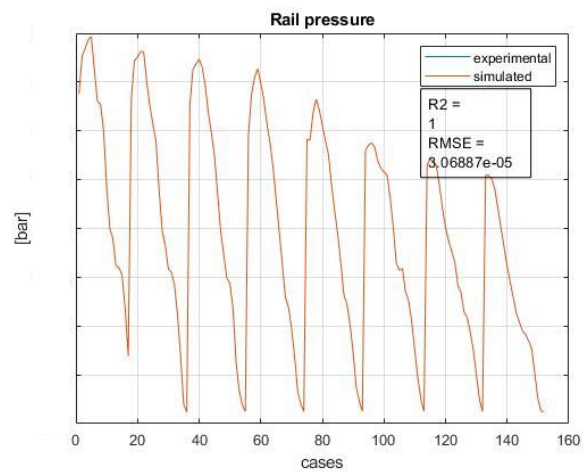
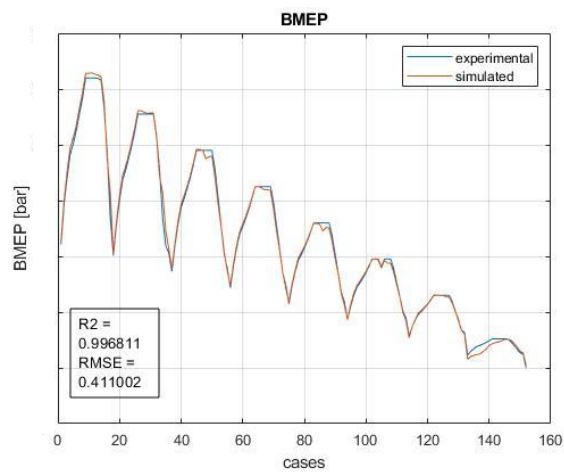
$$R^2 = \frac{SSR}{SST} = \frac{\sum(\hat{y}_i - \bar{y})^2}{\sum(y_i - \bar{y})^2} \quad (15)$$

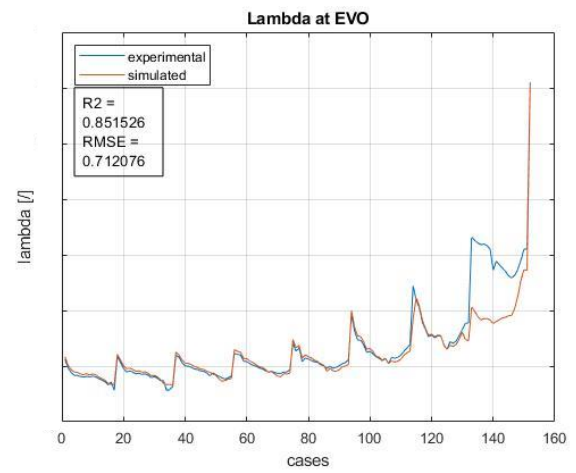
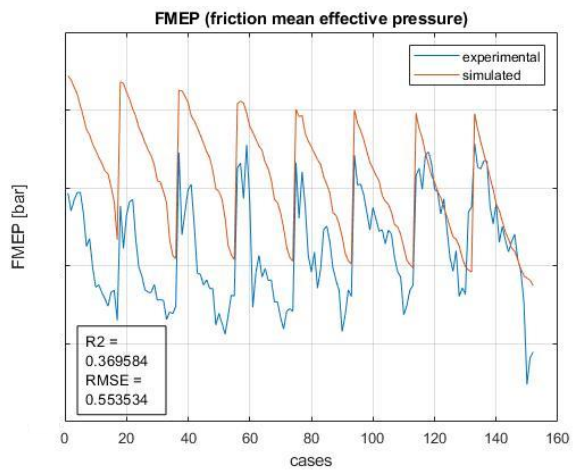
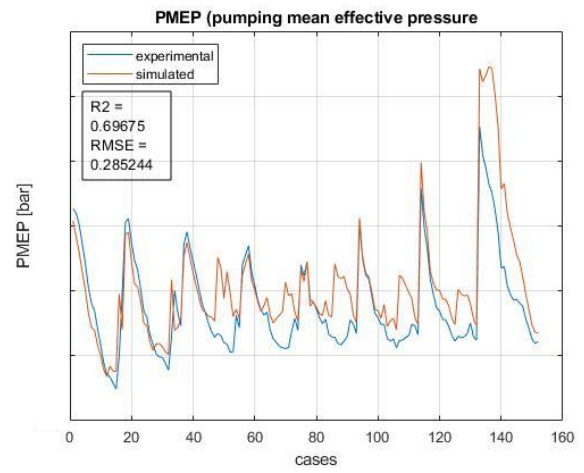
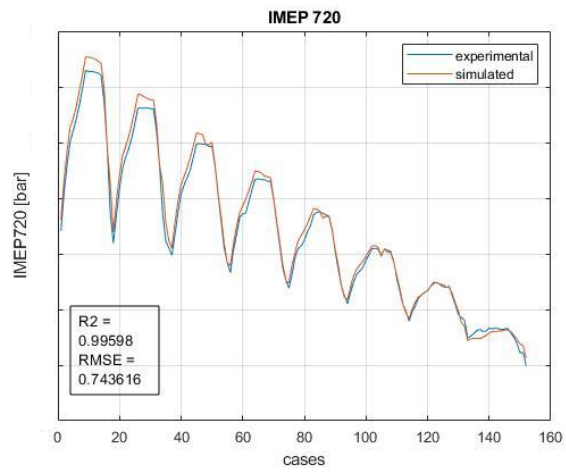
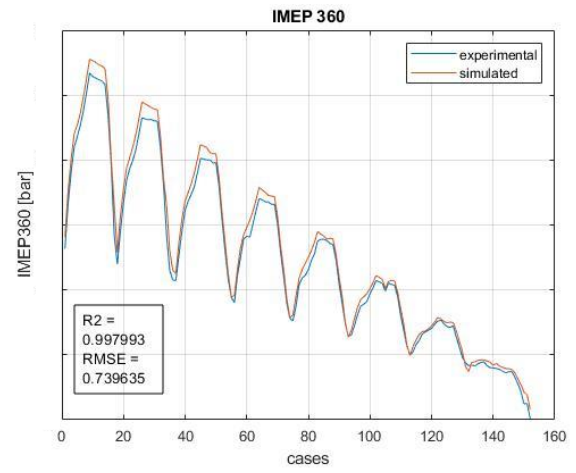
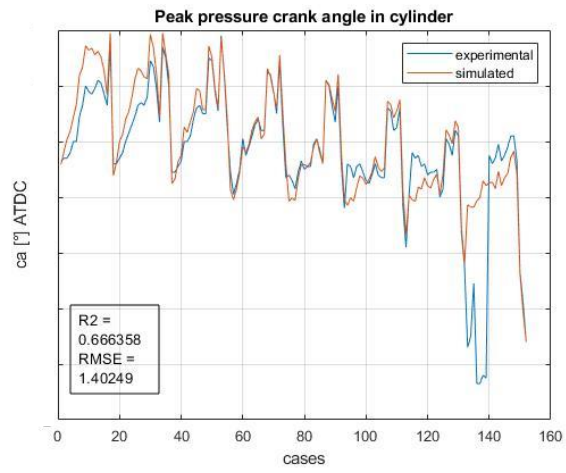
It is defined as the ratio between the regression deviance and the total deviance. Where simulated data does not fit well the experimental data, this index assumes a value near to zero; vice versa, when there is a good match between experimental and simulated R2 value is near to one. R2 equal to one means that the data are identical.

RMSE (Root Mean Square Error) is a frequently used measure of the difference between data predicted by a model and observed data. RMSE represents the square root of squares differences between simulated values and experimental values. The formula used is:

$$RMSE = \sqrt{\frac{\sum_{i=1}^n (p_i - a_i)^2}{n}} \quad (16)$$

So, it represents an average of the deviations evaluated on all the values assumed by the examined quantities. RMSE value depends on the evaluated quantities, so never compare RMSE values from different quantity analysis, because they will surely be different (depending on the quantity scale of value). Below, the results of the first validation are showed. Due to the trade secret, all the y-axis quantity values on the graphs in this work are blurred.





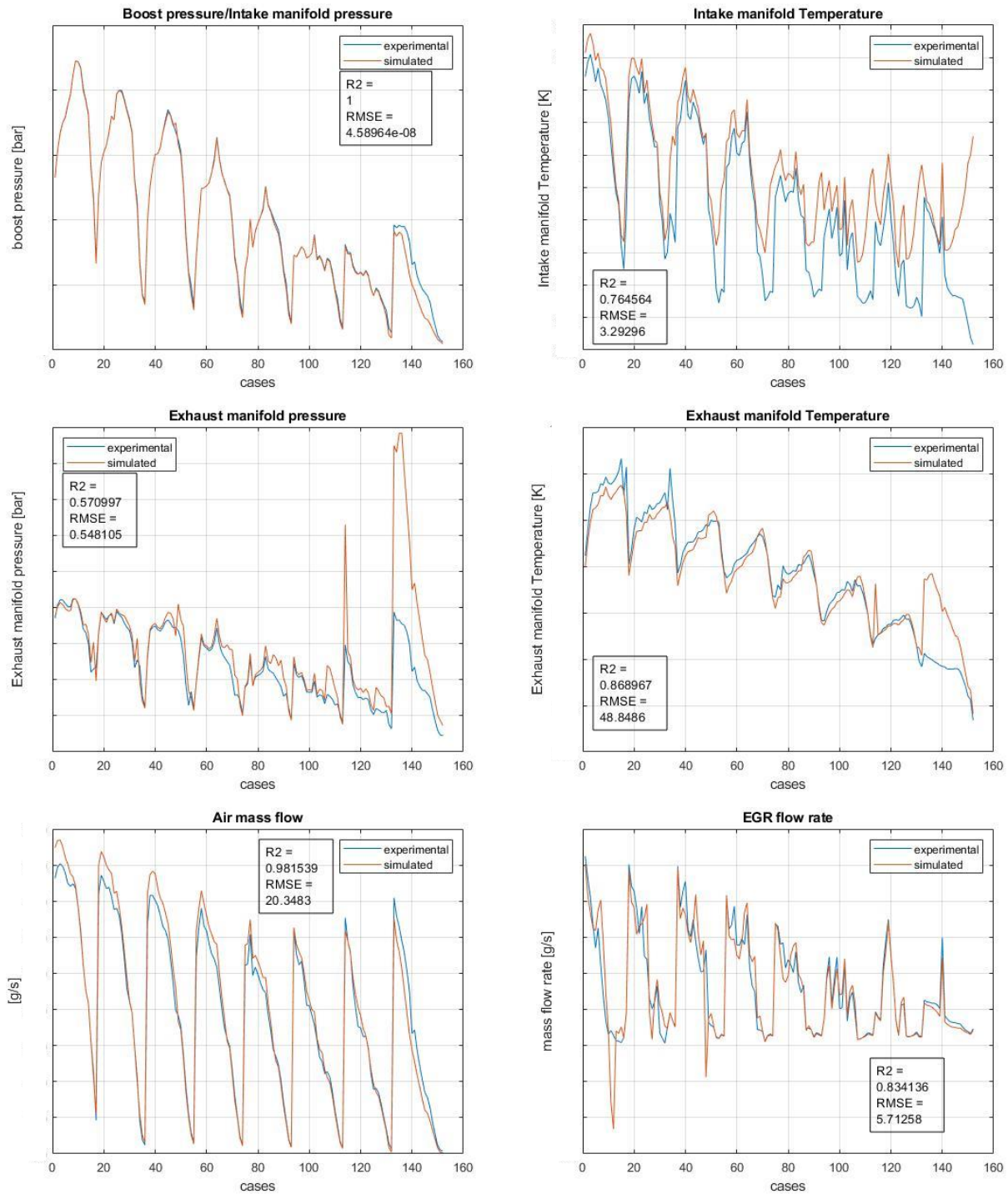


Fig. 18 – Validation results, from left to right: a) BMEP b) Rail pressure c) Total injected fuel mass per stroke d) EGR fraction e) MFB50 f) in-cylinder pressure peak g) In-cylinder pressure peak position h) IMEP360 i) IMEP720 j) PMP e) FMEP l) Lambda at EVO m) Intake manifold pressure n) Intake manifold Temperature o) Exhaust manifold pressure p) Exhaust manifold Temperature q) Air mass flow r) EGR flow rate

Among the figures, it is possible to see several quantities that reach a R2 value equal to one: this is a condition achieved only when the experimental and the simulated data are perfectly identical. In a simulation environment, even if the used model is perfect, a condition of total equality is practically unobtainable. However, the quantities with R2 equal to one, are quantities used as input in the model, defined in the Case Setup before starting the simulation: they have been analyzed in order to understand how GT POWER works: quantities such as total fuel injected quantity, rail

pressure, EGR fraction present a total overlap between the simulated and the experimental trends, because they have been used by the model as input data; while observing BMEP graph (Fig. 18 a)), that is also defined in Case Setup before the simulation start, there is not overlapping between the curves, and so the R2 index is lower than one. In fact, for BMEP parameter, during the simulation a closed loop control is performed, so if the imposed BMEP value at the beginning of the test is not achieved during the simulation, the obtained BMEP value substitutes the 'wrong one'. Using the PID-BMEP allows to obtain different results.

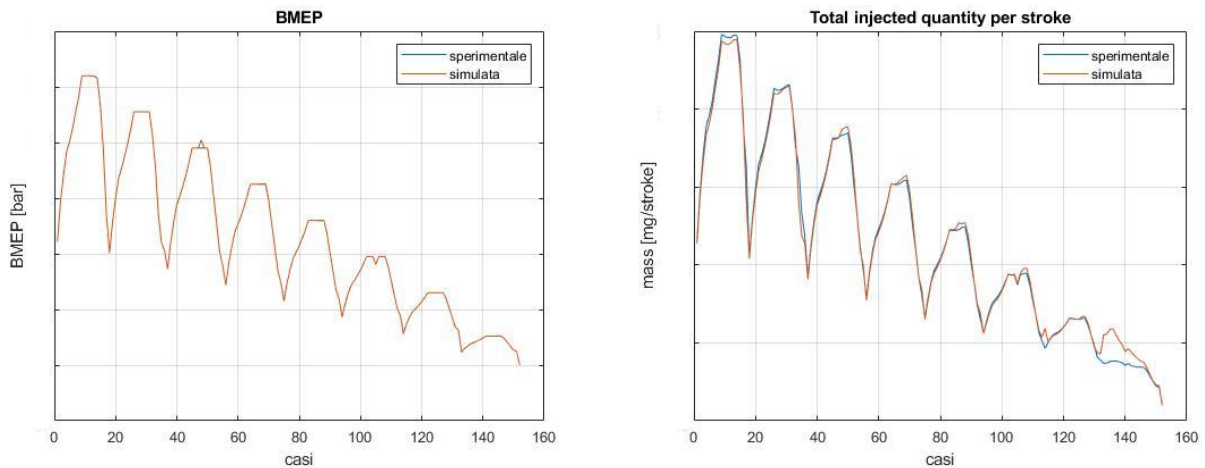


Fig. 19 – Results obtained with PID-BMEP controller a) BMEP b) Total Injected fuel mass per stroke

Fig. 19 a) shows the BMEP trend by using the PID-BMEP controller: even if the statistic indexes are not reported, anyway it is possible to see the experimental and simulated data are totally overlapped, that corresponds to have a R2 value equal to one. Vice versa, Fig. 19 b) shows the total fuel injected quantity trend obtained by using the PID-BMEP controller: comparing this result with the one obtained with no controller, where R2 index is equal to one, it is possible to understand how the PID-BMEP works. In fact, by using the controller, during the simulation in order to obtain the wanted BMEP value, it acts on the injectors by modifying their injection rate, by increasing or decreasing it depending on it wants to obtain a higher or lower BMEP value. The result of this operation is to obtain a perfect BMEP match, despite this implies a worst injected fuel trend. So, it is possible to affirm that BMEP and injected fuel per stroke are antagonistic quantities in this model (the other input quantities are not reported because they do not change with respect to Fig. 18).

By observing the output quantities graphs, it is visible that almost all the analyzed quantities present a higher R2 value, symptom that the model is modelled pretty well. In particular, by observing all the graphs it is possible to note that even if the experimental and simulated data seem to be similar for most of the cases, in the last 25-30 operating points they show dissimilar trends. This worsening in the last case of the validation can be attributed to the *exhaust flap valve* located downstream the turbine (Fig. 14). This valve can fulfil several different functions in the exhaust system: in both high and low duty applications it can be used in emission control, where this valve diverts a part of the exhaust gas flow toward the HC absorber in order to reach faster the *light-off temperature*, temperature at which HC absorbers work with the best efficiency possible. Furthermore, by closing this valve the backpressure in the exhaust manifold downstream the turbine increases, allowing the

turbine to work with a higher efficiency. In this model the exhaust flap valve is modelled as an orifice having a 95 mm diameter and a variable *forward discharge coefficient* (this coefficient simulates the valve closing); this coefficient changes in function of BMEP value, using a block called switch (*Fig. 20*): this element allows to produce an output switchable between two different values, depending on a third value, the control signal, the threshold that determinate the switch.



Fig. 20 – Exhaust flap valve with switch block for forward discharge coefficient change

In this specific case, the forward discharge coefficient is set to one if the BMEP is lower than a certain value, while is set to a RLTDependence if BMEP value is higher than the threshold. However, in the 152 operating cases used for this validation, the rig test data suggests that the exhaust flap valve is always opened, so the switch is cancelled from the model because it is useless. Even if the valve is always open for all the cases, its presence particularly affects the last cases: the reason is that these points correspond to low load operating points, and so suffer more every little changes. This work does not focalize on the resolution of this problem, but the idea is to increase the diameter value in order to reduce the effect that this valve, even completely open, has on the exhaust gas flow. More drastic solution would be to delete this valve from the engine.

Finally, an important consideration can be done by observing FMEP trends in *Fig. 21 a*). Friction Mean Effective Pressure is a parameter that represents the mean effective pressure lost due to friction: in a real engine, frictions are always positive, while for certain points in the experimental data provided, they assume negative values. This has not physical meanings.

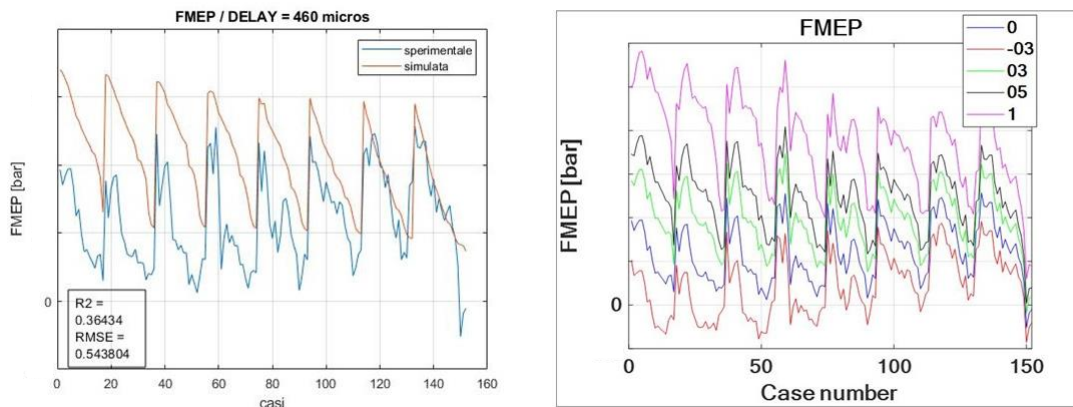


Fig. 21 – FMEP a) validation results b) trends obtained by shifting the pressure signal

Furthermore, the FMEP trend seems to be unaffected by the load, and this can be visible by observing the trend's peak (the load progressively decreases with the cases), that seem to be constant for all the cases: this is a problem, because theoretically FMEP decrease with the load.

Friction Mean Effective Pressure calculation requires accurate measurement of the cylinder pressure, mostly its phasing with respect to the Top Dead Centre (TDC). In fact, *Fig. 21 b)* shows how FMEP trend changes by shifting a little bit the pressure trace forward or backward. In particular, by shifting the pressure trace forward of just one degree (purple curve), the FMEP trend assumes only positive value and seems to decrease with the load. So, in the next chapter different techniques are evaluated in order to verify the correct pressure shift, or in case this is wrong, to find the correct one.

4. TDC SHIFT

In-cylinder pressure analysis is a valid tool in internal combustion engine research & development [9]. Starting from in-cylinder pressure trace several useful information such as indicated mean effective pressure (IMEP), indicated fuel consumption, heat release rate, mean friction pressure, mass fraction burned, and also emissions information. So, in-cylinder pressure analysis must be performed with high attention, in order to obtain a good accuracy in the results. In-cylinder pressure trace can be afflicted by different types of error, the main commons are listed below:

- Encoder error.
- Pegging error.
- Thermal shock error.

Pegging Error is an error due to the wrong choice of the pressure peg value used for the conversion of the voltage signal acquired by the piezo-electric transducer in pressure signal available for the analysis, while *Thermal Shock Error* comes from the high thermal energy amount released during the combustion phase that affects in-cylinder pressure measurement. For a more accurate description on these common types of errors, please see section 4.a. However, this section focalizes on the most dangerous but unfortunately most common source of error occurred during in-cylinder pressure measurements: *Encoder Error*. This error consists in a wrong evaluation of the crank position when the piston is at top dead centre (TDC). In order to obtain the crankshaft position, a rotary encoder is used. The encoder is an electro-mechanical sensor that translates physical motion into electrical data, and it is mounted on the crankshaft and manually calibrated. Even very small errors can cause high inconsistencies in calculated parameters: just 1° degrees before or after the real TDC can bring up to 10% evaluation error on IMEP and from 5% to 25% error on the heat released by combustion event [9]; to avoid this massive errors, TDC position must be known with a $0,1^\circ$ accuracy. Fig. 22 a)b) shows some data that can be affected by this type of error. However, it is not an easy task to obtain this value with such a high precision: in fact, when piston is close to TDC, $0,1^\circ$ crank angle corresponds to a piston movement in the order of one tenth of micron, such a teeny value to estimate.

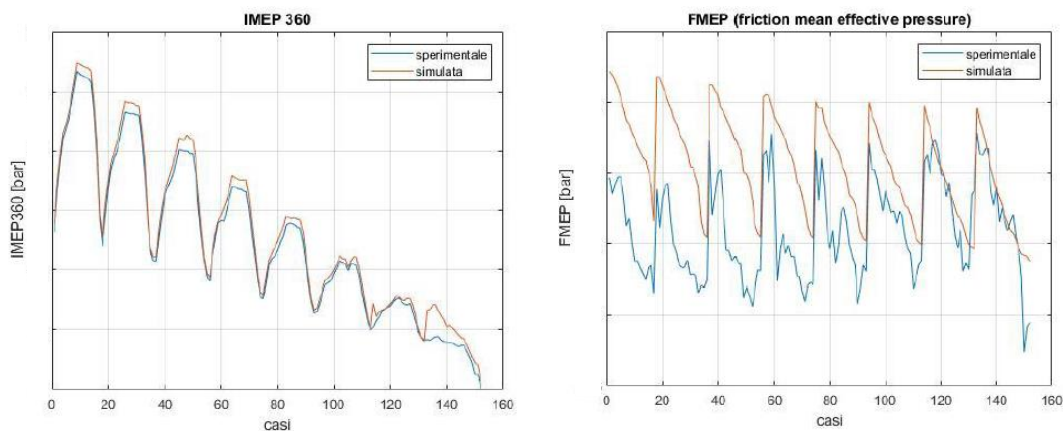


Fig. 22 – Quantities most affected by a wrong pressure phasing a) IMEP360 b) FMEP

In the past, for determining the piston top dead centre position it was used to mark a rotating component, such as an engine flywheel, coupled to the crankshaft. Then, the mark aligned with the fixed reference point gave the TDC position. However, this method suffers from inaccuracies involved with tolerance chain of the coupling between gears that brings to an incorrect positioning of the piston within the cylinder. This problem increases the position error when the shaft starts to rotate, due to inertia and elastic behaviours of the components. Another method consists in the use of a pressure transducer in order to obtain the maximum in-cylinder pressure generated while the valves are closed. Even if this method allows a very accurate real-time trace of the pressure trend in the cylinder, it hardly provides the correct TDC position. Today, a very useful tool for a very accurate TDC position evaluation is a capacitive sensor, called *TDC sensor*, which allows a dynamic measurement within the required $0,1^\circ$ precision in order to obtain reliable results [9] [10]. This method is recommended since it is not affected by errors in pressure values due to an incorrect pegging, cylinder-cylinder interaction and so on. This is an invasive method, because the sensor must be fitted or in the spark plug or in the injector hole of the cylinder; this is the main drawback of TDC sensor using, as well as the high cost of the component.

However, in this section will not be analysed data from experimental tests but different methods will be proposed in order to obtain the correct top dead centre position starting from mostly thermodynamic considerations. Literature is full of papers that used thermodynamic methods in order to evaluate TDC offset based on the in-cylinder pressure trace. Some methods can be used for fired engine, but most of them is based on motored engine cycles: a motored engine cycle is a cycle during which the engine is powered by an external source and no injection events occurs. In an ideal motored engine cycle energy exchange during the compression and the expansion strokes are completely balanced. This means that a crank angle resolved pressure data should be symmetric respect to TDC, and the peak pressure coincides exactly with top dead centre position. However, in a real motored engine cycle the peak pressure occurs slightly before the top dead centre due to heat transfer losses from the gas to the cylinder walls during the compression stroke, and due to the blowby mass leakages through the crevices. The difference between the ideal and the real TDC position is called *thermodynamic loss angle* [9].

In this paper three methods are developed:

- Beccari-Pipitone method.
- Tazerout method.
- Jaye method.

All these methods are performed on motored engine cycles, in particular FPT provides 18 different motored cycles, with the specifics listed in *Table 1*.

Op. Points	Speed [rpm]	Power [kW]	Op. Points	Speed [rpm]	Power [kW]
1	2200	-99.4	10	1300	-27.7
2	2100	-88.5	11	1200	-23.8
3	2000	-80.9	12	1100	-21.5

4	1900	-72.2	13	1000	-19.6
5	1800	-61.9	14	900	-15.2
6	1700	-53.1	15	800	-12.2
7	1600	-44.9	16	700	-10.1
8	1500	-39.5	17	600	-7.8
9	1400	-32.5	18	550	-6.5

Table 1 – Motored cycles used for the TDC position evaluation

4.1. Beccari-Pipitone Method

This method used a thermodynamic approach in order to evaluate TDC position. A motored engine can be analytically described by isolating the combustion chamber mass from the external environment and studying the energy transformation that occurs. So, after some non-reported calculation steps, the in-cylinder pressure can be evaluated as in equation (17):

$$\delta p = \frac{1}{V} [\delta Q(\gamma - 1) - \gamma p \delta V] + \gamma \frac{\delta m}{m} \quad (17)$$

Where δm is the entered mass, that in a motored engine cycle is only characterized by the blowby mass leakages from the crevices (so negative for the used convention), while δQ is the heat exchanged between the trapped mass and the cylinder walls, that depends on their temperatures. In an ideal engine, δQ and δm are both zero, so in the equation (17) pressure assumes its maximum ($\delta p = 0$) when the volume reaches its minimum ($\delta V = 0$); by integrating on the whole cycle the expansion and the compression strokes result symmetric with respect to the TDC, and the pressure peak coincides with the top dead centre position [9]. However, these assumptions are not valid for real engine, where the heat exchange between the gas and the combustion chamber's wall is not negligible, and the blowby mass leakages occur; due to these two phenomena the pressure curve results to be asymmetric with respect to the TDC, shifting the maximum pressure peak in advance with respect to the top dead centre position [9]. This angular distance between LPP and TDC is called *loss angle* (Eq. (18)), and its value depends on the amount of heat exchange and mass leakage (Fig. 23 – Teta loss). In real engine this value is bigger than 0° degrees, but usually is lower than 1° degrees.

$$\vartheta_{loss} = L_{PP} - L_{TDC} \quad (18)$$

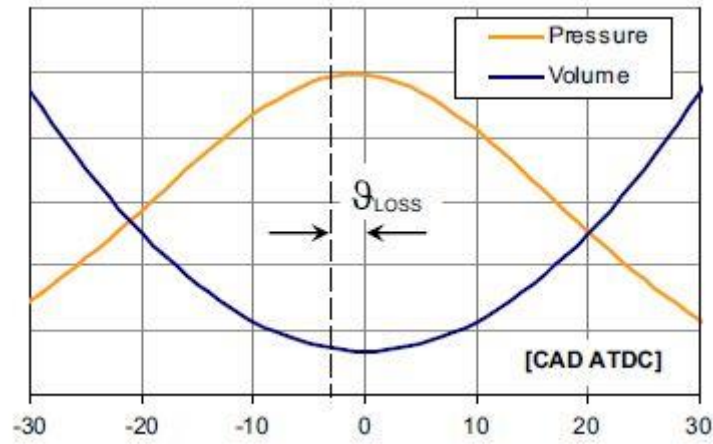


Fig. 23 – Teta loss

The loss angle value strongly depends on the heat transfer between cylinder walls and in-cylinder gas and on blowby mass leakage, these two phenomena shift the pressure trace backwards with respect to the TDC position. So, it is possible to define a function, called *Loss Function*, defined as in equation (19), that takes in accounts the amount of gas escaping from the cylinder and the capability of the cylinder's wall to exchange heat with the gas [9]. Loss function is easily evaluable used known quantities such as pressure and volume variations (Eq. (19)), the first one is obtained by rig test, the second one can be calculated by equation (20), using simple geometric consideration on crank connecting rod mechanism.

$$\delta F = \delta S + c_p \frac{\delta m}{m} = c_p \frac{\delta V}{V} + c_v \frac{\delta p}{p} \quad (19)$$

$$\frac{\delta V}{V} = \frac{\sin(\vartheta) \left(1 + \frac{\cos(\vartheta)}{\sqrt{\mu^2 - \sin^2(\vartheta)}} \right) \delta \vartheta}{\frac{2}{\rho - 1} + \mu + 1 - \cos(\vartheta) - \sqrt{\mu^2 - \sin^2(\vartheta)}} \quad (20)$$

Where ρ is the *compression ratio*, ratio between the maximum and the minimum combustion chamber volume, and μ is the *rod to crank ratio*, ratio between the connecting rod and crank radius.

Like just said, the loss function is the sum of two parameters, so its trend follows the behaviours of both δQ and $\delta m/m$ factors: Fig. 24 shows that the entropy variation starts with a positive value, because T_{gas} is lower than T_{wall} so the heat flux goes from cylinder's wall to in-cylinder gas (according to the used convention the δQ is positive when absorbed by the system), and decreases during the compression, due to T_{gas} increasing, until its minimum near TDC position, where the heat flux is maximum. While the blowby mass leakages through the crevices start from zero, due to a low in-cylinder pressure, decreasing (used convention says that mass flux is positive when enter the cylinder) during the compression, where the difference between in-cylinder pressure and carter pressure increases 'pushing away' from the cylinder a fraction of mass though the crevices. Blowby

phenomenon assume its minimum value near TDC position. Loss function trace it is the sum of these phenomena.

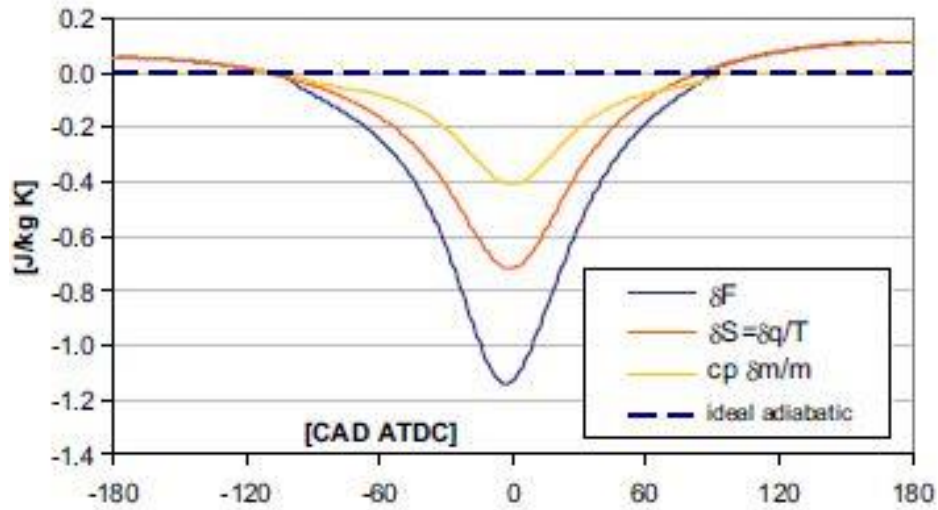


Fig. 24 – Loss function trend

The loss function is calculated in order to obtain the loss angle value: in fact, when the pressure trace reach its maximum, at LPP, in this point δp is zero and the loss function depends only on $\delta V/V$; $\delta V/V$ is note by equation (20), so, skipping some extra passages and making some approximations, it follows that the loss angle can be calculated using equation (21):

$$\vartheta_{loss} = \frac{2}{\rho - 1} \frac{\mu}{\mu + 1} \left[\frac{1}{c_p} \frac{\delta F}{\delta \vartheta} \right]_{LPP} \quad (21)$$

$$\text{with } \sin(\vartheta_{loss}) \approx \vartheta_{loss} \quad \cos(\vartheta_{loss}) \approx 1 \quad \vartheta_{loss}^2 \ll \mu^2$$

The loss angle can be easily correlated to the loss function value in LPP. Unfortunately, loss function trace is strongly affected by even small phase errors between $\delta V/V$ and $\delta p/p$. Fig. 25 shows how much loss function changes with different small phasing errors, especially around the pressure peak. This variability makes equation (21) inconsistent, and impossible to use.

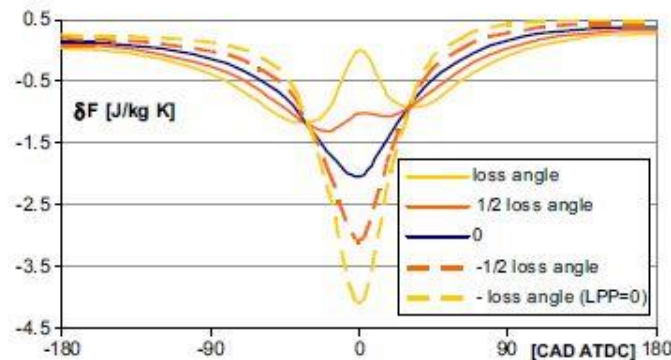


Fig. 25 – loss function trend with different loss angle

However, always on *Fig. 25*, it is possible to see that there are two zones in loss function trends that are not affected by phasing errors; in these two crank positions (about 30° before and after TDC) all the loss functions assume the same values, no matter the phasing error value. So, can be useful to find a correlation between the loss function evaluated at LPP and the loss function evaluated in these two points, in order to avoid phasing errors [9]. It has been found that for a certain engine the ratio between loss function at LPP and loss function in ϑ_1 , that is one of the two non-affected points, is almost constant (Eq. (22)):

$$\delta F_{LPP} = \phi \cdot \delta F_{\vartheta_1} \quad (22) \quad \text{with} \quad \phi = 1,95$$

Where ϕ is a proportionality constant that depends on several engine parameters, especially on compression ratio and the used heat transfer law. Using a compression ratio of 20,5 and Woschni model for the heat transfer, it has been founded that the constant ϕ is 1,95. In this work will be also evaluated ϕ value for CR (compression ratio) variations. Loss function in ϑ_1 requests calculating $\delta V/V$ and $\delta p/p$ at that crank angle: first step is to phase the pressure cycle with an initial error equal to the loss angle (setting LPP = 0°), in this way the loss function increment δF_1 in ϑ_1 can be evaluated at minimum of $\delta V/V$ function (*Fig. 26*). Please observe that the x-axis resolution is about a tenth of a degree.

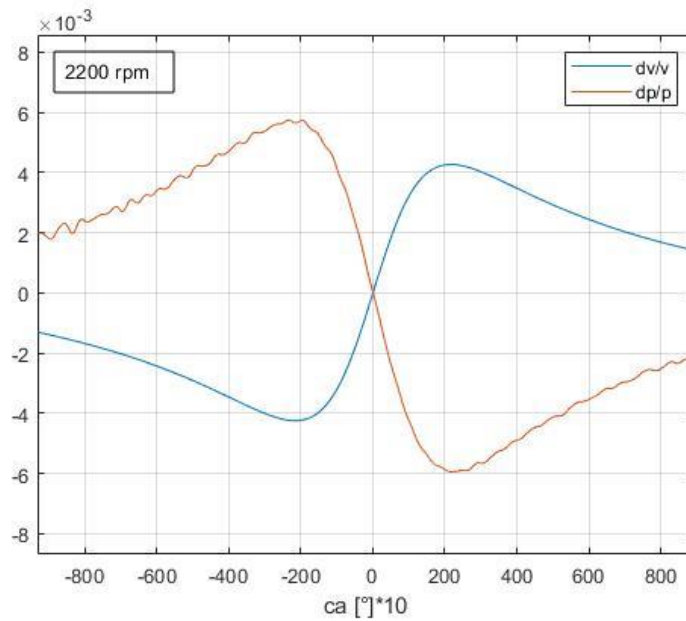


Fig. 26 – dp/p and dv/v trend

Unfortunately, both of these functions can be affected by measurement errors: in-cylinder pressure trace is detected by using a piezoelectric transducer, and the measurement, usually during the combustion phase, could be affected by some bias errors and some electric noises. While a fluctuation of the CR value, due to dimension tolerances of the combustion chamber's components, could affects the in-cylinder volume estimation [9]. Both bias errors and CR fluctuations contribute to an error in loss function evaluation in ϑ_1 . In order to avoid this error, in equation (22) is not used δF_1 , but δF_m , that is the average of loss function evaluated in ϑ_1 and in ϑ_2 (Equation (23)); in this way,

since both δF_1 and δF_2 are affected by the same errors but in opposite directions, fluctuations cancel each other out.

$$\delta F_{LPP} = \phi \cdot \delta F_m = 1.95 \cdot \left(\frac{\delta F_1 + \delta F_2}{2} \right) \quad (23)$$

Now, loss function evaluated at pressure peak (δF_{LPP}) is practically independent from the several errors discussed above and can be used in equation (21) in order to obtain the loss angle that, due to the pressure shift made in the first part of the analysis, coincides to the TDC position. The determination of the angular position ϑ_1 and ϑ_2 can be made manually on the $\delta V/V$ graph, chasing the crank angle at the minimum and at the maximum of the function (*Fig. 26*), or by using equation (24) obtained using a 2nd order polynomial interpolation on $\delta V/V$ trace:

$$\vartheta_{1,2} = \pm 76,307 \cdot \mu^{0,123} \cdot \rho^{-0,466} \quad [CAD \ ATDC] \quad (24)$$

Notice that $\delta V/V$ function is anti-symmetric respect to the y-axis, so the angular positions coincide. In this work the determination of the angular position is made using both method and comparing the results; this can be used as a check to understand if the analysis is going in the right way [9].

The Beccari and Pipitone method for the evaluation of the loss angle in this work has been developed using MatLab software to speed up the calculation step and able to perform subsequent simulations with different input parameters by changing only few code strings. Above is reported the followed procedure and the obtained results.

This method used thermodynamic consideration to obtain the correct loss angle, the angular distance between the TDC position and the LPP position. Knowing the exact position of the TDC allows to obtain information about the pressure trace with high accuracy. In this section will be summarized step by step the Pipitone-Beccari method and the results will be discussed. This method works only on motored engine cycles, so for this aim FPT has provided 18 motored cycles at different speed; the analysis is performed on all the provided cycles in order to study how speed variations affect the loss angle value. In fact, this method is developed in parallel on all the cases. More details on the input cycles are showed in *Table 1* and are visible in *Fig. 27*.

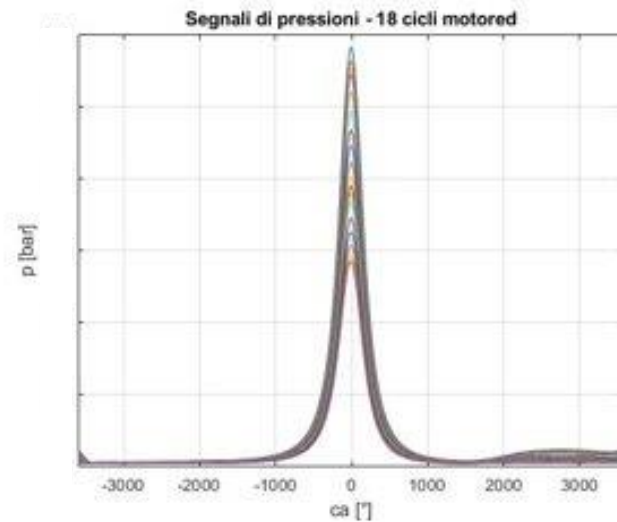


Fig. 27 – Motored cycles used for loss angle evaluation

Pipitone-Beccari method can be divided in four steps:

1. All the pressure trace must be shifted in order to have the maximum peak pressure coincident with the top dead centre (LPP = 0°). In this way, according to equation (21), the position error is exactly the loss angle itself. The pressure traces provided by rig test show the pressure peak in advance with respect to the TDC position due to thermal exchange between in-cylinder gas and cylinder walls and blowby mass fraction leakage through the crevices; however, the effect of these two phenomena is not the same at different engine speed, usually a speed increase affects leakages and heat exchange by increasing (Fig. 28). So, each cycle has the pressure peak at different crank angle, depending on its engine speed. Once all the cycles are aligned at TDC, analysis can proceed [9].

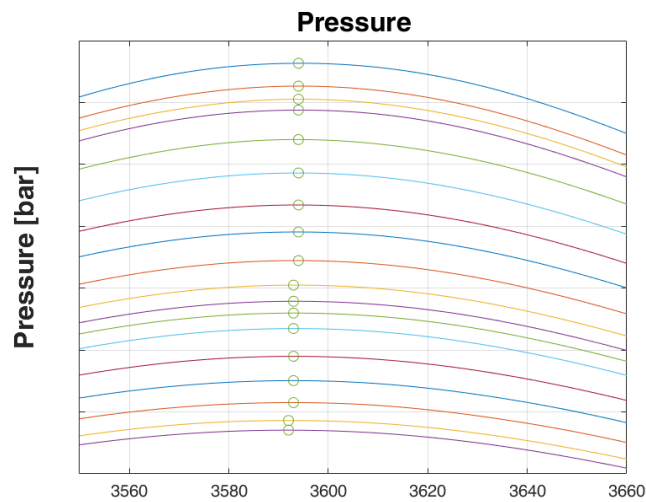


Fig. 28 – Motored cycles pressure peak positions

2. For the purpose of this work, it is not necessary to obtain all the loss function trend, it is enough to evaluate it in two points, that is in $\delta V/V$ function maximum and minimum (Fig. 26). This procedure can be made manually, by find the crank angle correspondent to minimum and maximum value of the function, or by using equation (24) proposed by

literature, obtained by using a 2nd order polynomial interpolation on $\delta V/V$ trace. Due to the shift made in the previous step, the founded $\delta V/V$ trace is quasi-antisymmetric with respect the y-axis, so ideally the maximum and the minimum are located at the same angular position, but with different signs. Using the literature approach, the formula gives $\vartheta_{1,2} = \pm 21,67^\circ$, while observing *Fig. 26* the maximum and the minimum location are founded to be $\vartheta_1 = +21,8^\circ$ and $\vartheta_2 = -21,5^\circ$: observing these results it is visible that in the second case the results are similar, but there is no symmetry. Finally, it has been decided to use the results obtained by the equation, even because there is not too much difference with the other method results [9].

3. Once ϑ_1 and ϑ_2 are founded, in this angular position the loss function, defined as in equation (23), can be calculated. With these two values, the mean value is calculated by using equation (23), that is a simple average. Beyond in-cylinder pressure and volume, loss function also needs c_p and c_v values. Specific heats (at constant pressure and at constant volume) change when temperature changes, and in a combustion chamber, even if in a motored engine cycle with no-combustion occurs, the gas temperature changes very quickly: specific heat usually increases with temperature. Anyway, the temperature trend in a combustion chamber can be obtained by using a thermal probe on the engine, as well as by using the classical known equation (13) for perfect gas, considering air in the cylinder: since pressure and volume values are known, in-cylinder temperature trace is easy to obtain [9]. Specific heat at constant pressure and at constant volume then can be obtained using equations (25)(26).

$$c_p = 1043,06 - 360,72 \frac{1000}{T} + 108,24 \left(\frac{1000}{T} \right)^2 - 10,79 \left(\frac{1000}{T} \right)^3 \quad (25)$$

$$c_v = c_p - R \quad (26)$$

However, a satisfactory approximation is equally reached if c_p and c_v are assumed to be constant; in this work both the methods are proved. The mean value is than used to evaluate the loss function in the local peak pressure LPP: for the reason explained in the previous section, the loss function cannot be evaluated directly in the peak pressure, but it must be estimated in another way [9]. For this aim, it has been found that for a certain engine and for certain conditions, the ratio between the loss function in LPP and the mean value calculated above is constant. In this work, using a Woschni model and a CR = 20,5 the proportionality constant ϕ is 1,95.

4. The loss function in LPP evaluated in step 3 can be now finally implemented in equation (22) in order to obtain the loss angle value. The obtained loss angle is, due to the shift made in the first step of this work, the position error in TDC evaluation [9].

In order to understand if there is an error in TDC position evaluation, the results obtained in this work needs to be compared with the settings used by FPT in post processing on the rough pressure

trace of the rig tests. The result of the Beccari-Pipitone method for the evaluation of the loss angle is reported in *Fig. 29*.

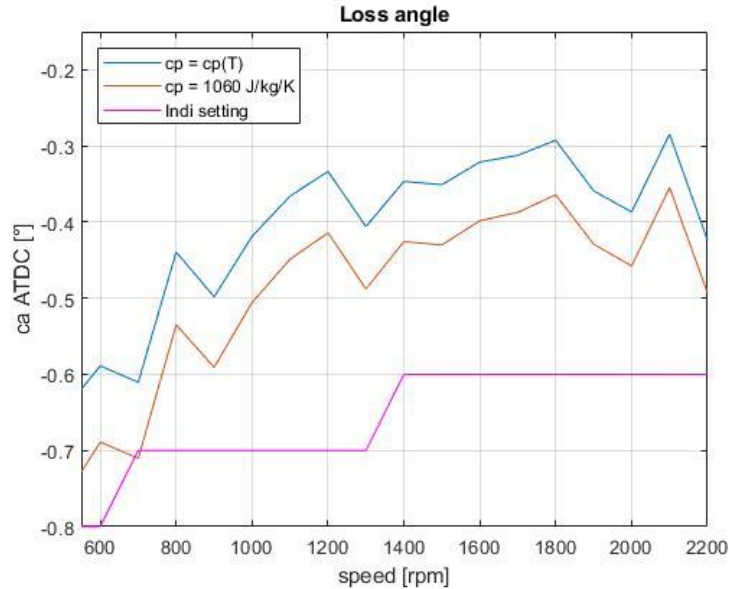


Fig. 29 – Loss angle in function of engine rotational speed

In this figure is showed the loss angle in function of the speed, obtained using specific heat as constant values as well as depending on temperature. The purple curve represents the actual used setting on rig test output pressure trace. Observing this curve, a first thing is clearly visible, the loss angle used is constant for different values of engine speed: for speed values in the range 700 rpm to 1300 rpm a 0.7° degrees BTDC (Before TDC) loss angle is used, while for engine speed from 1300 rpm until 2200 rpm loss angle is 0.6° degrees BTDC. As mentioned in section 4, as well as in this section, heat exchanges and blowby mass fractions changes with the speed, so using a loss angle constant value for different speed values can be source of error. However, even if considering loss angle constant is an error, globally its value presents an increasing trend with the engine speed. This increasing trend is also visible in the blue and the red curves, obtained by the model. Furthermore, comparing the indi setting curve and the constant specific heat curve, it is possible to see, especially after the 800 rpm, that the red curve is always greater than the purple one by a quasi-constant value of 0.2° degrees. This result is important, because suggests that the actual pressure trace used in GT POWER Cursor 11 model, is not shifted correctly: so, the pressure trace must be shifted 0.2° degrees forward. This forward shift is further justified observing *Fig. 30*, where the experimental FMEP obtained in a GT POWER simulation (*Fig. 18 k*) is parameterized respect to the in-cylinder pressure trace shift: blue curve is the one with no shift, while the others present positive and negative shifts.

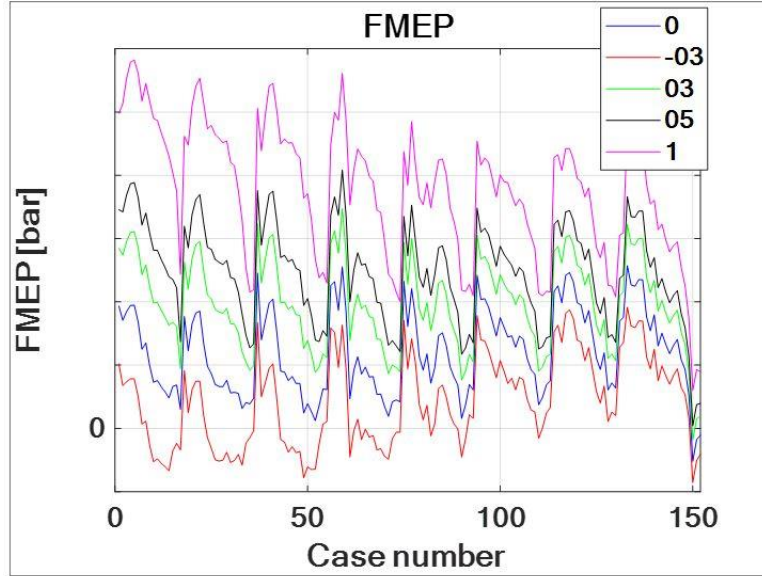


Fig. 30 – FMEP obtained with different pressure trace phasing

Observing the graph, a positive shift in input pressure trace brings to a FMEP curve shifted upward, and so with no negative values and more similar to the FMEP simulated curve obtained by rig tests (red one in Fig. 30). To confirm that what has been done in this model is correct, other two different approach are developed below.

The method description and the results useful for the purposes of the TDC correct position determination is now ended. In this second part the same analysis is performed with a different compression ratio: this analysis is useless for this section, but it will be preparatory for the next sections. In this step the used compression ratio is 20 instead of 20,5. Even if the paper used for this method () affirms that this model is not affected so much by CR variation, it can be useful to understand which parts actually changes with CR and which are not. So, it is necessary to find where CR is involved, in order to understand how it works. CR is present in equation (20) for the evaluation of $\delta V/V$ function, in equation (21) for evaluation of $\vartheta_{1,2}$, and also affects the proportionality constant ϕ , used in equation (23) to evaluate loss function in LPP.

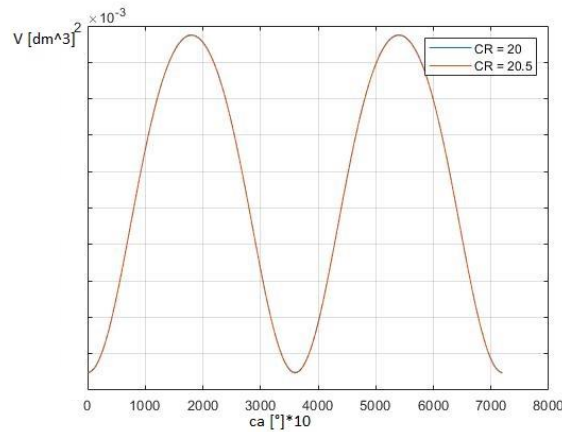


Fig. 31 – C.R. influence on chamber volume trend

Fig. 31 shows the volume trace obtained with both CR = 20,5 and CR = 20: the curves are practically the same, marking that this CR variation is too small to see relevant changes. In $\vartheta_{1,2}$ calculation formula (21), the CR (in the formula the CR is the p) exponent is very small, so it is expected that a 0,5 CR variation does not affect these values too much. The expectations are correct, because the $\vartheta_{1,2}$ angular position in which the loss function will be evaluated changing from $\pm 21,67^\circ$ degrees for a CR = 20,5 to $\pm 21,92^\circ$ degrees for a CR = 20. The last parameter affected by CR is the proportionality constant ϕ used in equation (23) to evaluate the loss function in the pressure peak. This quantity is affected by two main parameters, the compression ratio and the heat transfer law. Fig. 32 shows how ϕ changes with CR variation, using different heat transfer law.

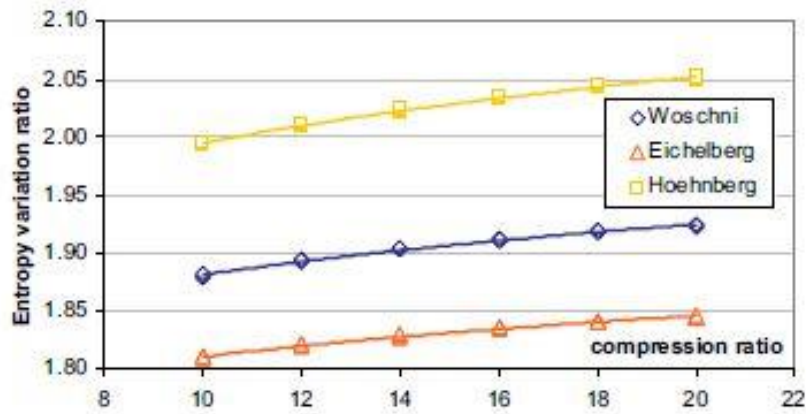


Fig. 32 – C.R. influence on ϕ

Observing the blue curve, obtained using Woschni model (that is the model used in this work), it is possible to see how flat it is: even great CR variations lead to a little variation in constant ϕ value. Once all the effects made by CR variation on this model is known, the same steps described above for the first analysis are repeated with a CR = 20.

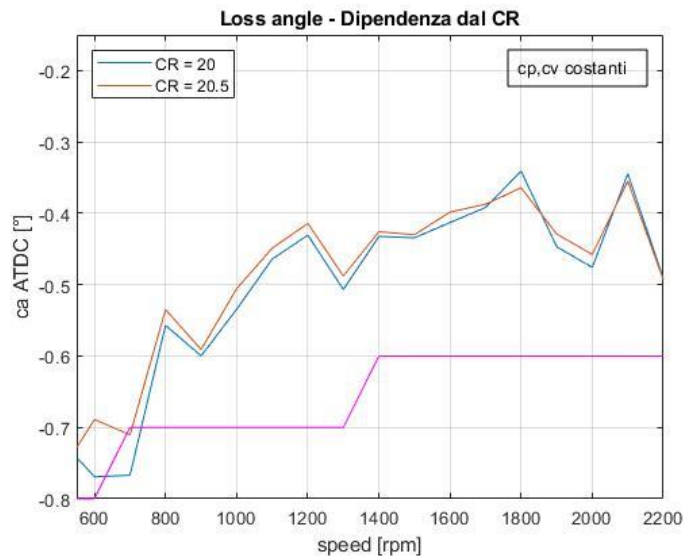


Fig. 33 – Loss angle obtained with different C.R. values

Fig. 33 shows both curves obtained with $CR = 20,5$ and $CR = 20$: while at low speed the behaviour seems to be a little bit different between red and blue curves, for speed higher than 800 rpm they assume the same trend with almost the same values. It is important to consider that the y-axis scale is about one tenth of degree, so the gap between the curves is practically negligible. Both curves are obtained using a constant value ϕ of 1,95. Changing the proportionality constant value, the result is almost the same. Observing Fig. 34, it is possible to see that even with big ϕ value changes the two curves maintain the same trend with little fluctuations in the assumed values. Furthermore, watching Fig. 34, the constant ϕ value used for this comparison for $CR = 20$ is not entirely correct: in fact, in order to show how little the impact of ϕ parameter on this analysis is, the chosen value matches with a $CR = 10$, the lower point of the blue curve in Fig. 32.

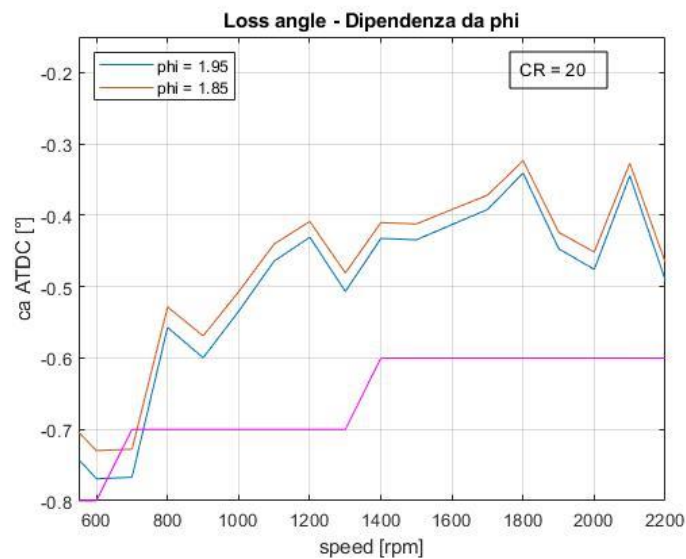


Fig. 34 – Loss angle obtained with different ϕ values

This second part of the analysis can be closed by stating that a 0,5 variation in compression ratio value is not enough to obtain a consistent change in the evaluation of the correct pressure trace TDC position.

4.2. Tazerout method

The second methodology used in this work for the determination of the correct TDC position is the *Tazerout-Le Corre-Rousseau method*. This method, as well as the first method illustrated (section 4.1), is based on first and second thermodynamic laws considerations. In a Temperature-Entropy diagram, a motored engine cycle with TDC position correctly calibrated shows a symmetric behaviour with respect to the peak temperature. Instead, when the motored cycle TDC position is not well-calibrated, the entropy trace in T-s diagram presents a loop at its peak (Fig. 35): a loop in entropy trace means that, even if in a small-time range, entropy decreases with an increase in temperature. This behaviour has no thermodynamic significance. So, below it is explained how this thermodynamic consideration can be use in order to evaluate the correct TDC position of a motored engine cycle [11].

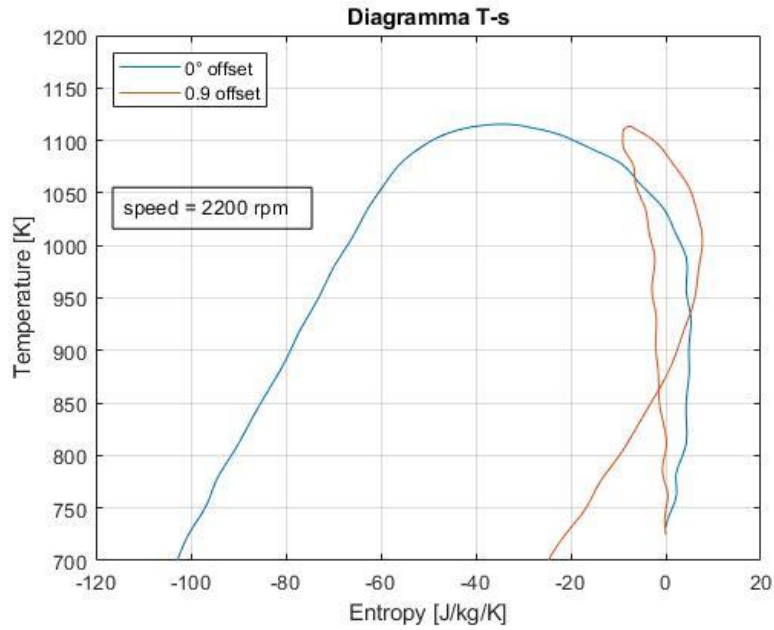


Fig. 35 – The loop occurs at the entropy peak in T-s diagram

For this work, a one-zone thermodynamic model has been developed, in order to simulate the whole cycle engine. The whole method is takes place in a T-s diagram, so temperature and entropy must be evaluated for each of 18 motored cycles available. Temperature usually is not a given data from rig test, so it must be evaluated indirectly; the easiest method is to use equation (13) for perfect gas, considering air the in-cylinder gas. In-cylinder pressure trace and volume are known, so the temperature is easily obtained (Fig. 36).

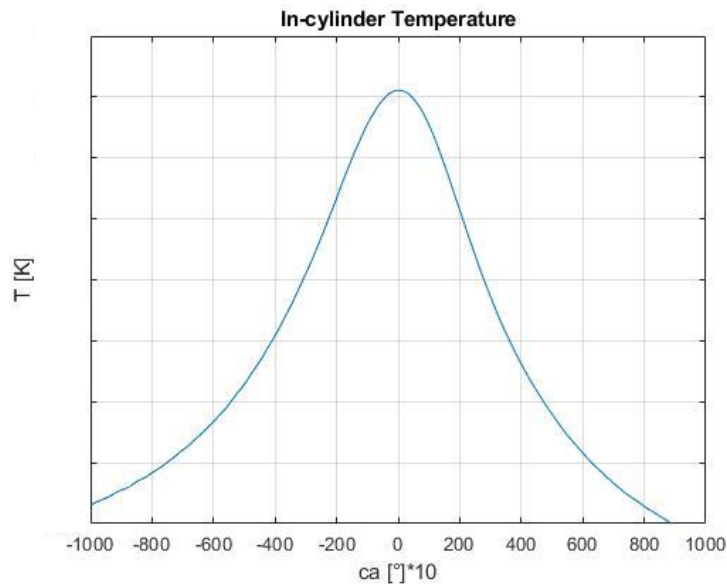


Fig. 36 – In-cylinder Temperature trend

The temperature peak is not necessary located at top dead centre. For the entropy trend evaluation some consideration can be made in order to simplify the calculation steps. Entropy must be calculated using equation (27):

$$dS = c_p \frac{dT}{T} - R \frac{dp}{p} \quad (27)$$

However, near TDC, the volume changes very slowly, so its increment can be considered null: this allows, considering equation (13) for ideal gases to obtain [11]:

$$\frac{dV}{V} = 0 \quad (28)$$

$$\frac{dp}{p} = \frac{dT}{T} \quad (29)$$

So, equation (27) can be written as:

$$dS = (c_p - R) \frac{dT}{T} \quad (30)$$

Specific heat (at constant pressure and volume) changes with temperature, according to equations (25)(26). However, temperature reach its maximum near TDC, so its increase in that range is moderate. This leads to moderate changes in specific heats value; so, it is possible in this phase to consider c_p e c_v constant [11]. During the compression stroke, equation (30) becomes:

$$\Delta S_{max \rightarrow 1} = (c_p - R) \int_{max}^1 \frac{dT}{T} \quad (31)$$

And using a first order Taylor's development:

$$\Delta S_{max \rightarrow 1} = (R - c_p) \frac{\Delta T}{T_{max}} \quad (32)$$

Same approach for the expansion stroke:

$$\Delta S_{max \rightarrow 2} = -(R - c_p) \frac{\Delta T}{T_{max}} \quad (33)$$

Where 1 and 2 are two points taken respectively in the compression stroke and in the expansion stroke, symmetrical with respect to the temperature peak. This method is based on these two entropy values: in a pressure trace with the correct TDC position, the temperature trend must be symmetric near the temperature peak, so the entropy of two specular points in absolute value must be the same (equation (34)).

$$\Delta S_{max \rightarrow 1} = -\Delta S_{max \rightarrow 2} \quad (34)$$

This temperature peak can be located before or after the TDC position, its position depends on the considered engine operating points, it is not relevant for this work. When an error exists on the TDC position, temperature in T-s diagram does not assume a symmetrical trend, it rather presents a loop

at its maximum [11]. A loop in T-s diagram has not thermodynamic significance, entropy always increases with temperature. In order to see if the under investigation motored pressure trace has a correct TDC position, two methods exist: an analytical one, in which the max compression stroke entropy value is compared to the entropy evaluated in the temperature peak; if the compression one is bigger than the peak one (Case A Fig. 37), the loop occurs so the TDC position must be shift by a constant step of 0,1° degrees. This operation is iterated until the limit angle ϑ_{lim} is reached; ϑ_{lim} is the TDC angle position at which the maximum compression entropy value becomes smaller than temperature peak entropy: the loop is disappeared (Case B Fig. 37). Finally, a further -0,45° degrees shift is applied to the pressure trace in order to achieve the best TDC position (Case C Fig. 37). This final shift is necessary to obtain a temperature trace more symmetrical near the TDC [11].

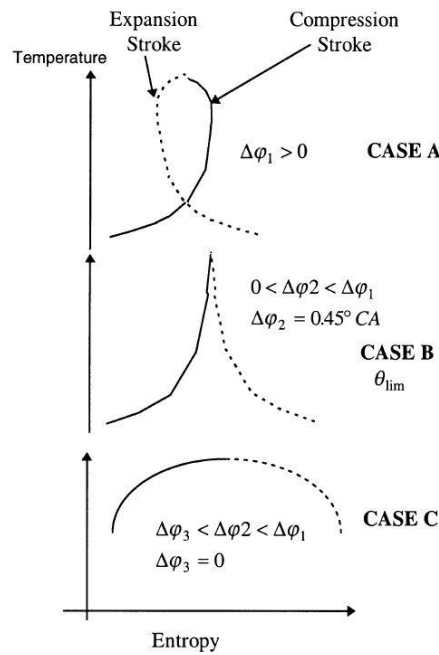


Fig. 37 – Tazerout's method for TDC correct determination

The second method, the one used in this work, is a simpler method based on observing the temperature curve in T-s diagram. Starting from the given pressure trace with its TDC position if this position is correctly phased the temperature trace should not present the entropy loop. Otherwise, if TDC is wrongly phased the temperature trace must have the loop. Like in the analytical method, a -0.1° degrees shift on pressure trace is made until the loop disappears. Once the loop is not more present, the temperature trace should take a cusp form in its peak, like CASE B in Fig. 37; this is not correct since near its maximum the temperature must be symmetrical with a smooth trend. So, in order to reshape the curve, an adding -0,45° degrees shift is needed. It must be underlined that these methodologies can be used only if the peak pressure under motoring conditions is before the actual position: in fact, the loop does not exist for negative TDC phase lag [11].

This work is performed in the same way on all the 18 motored engine cycles provided, and the results are visible in Fig. 38.

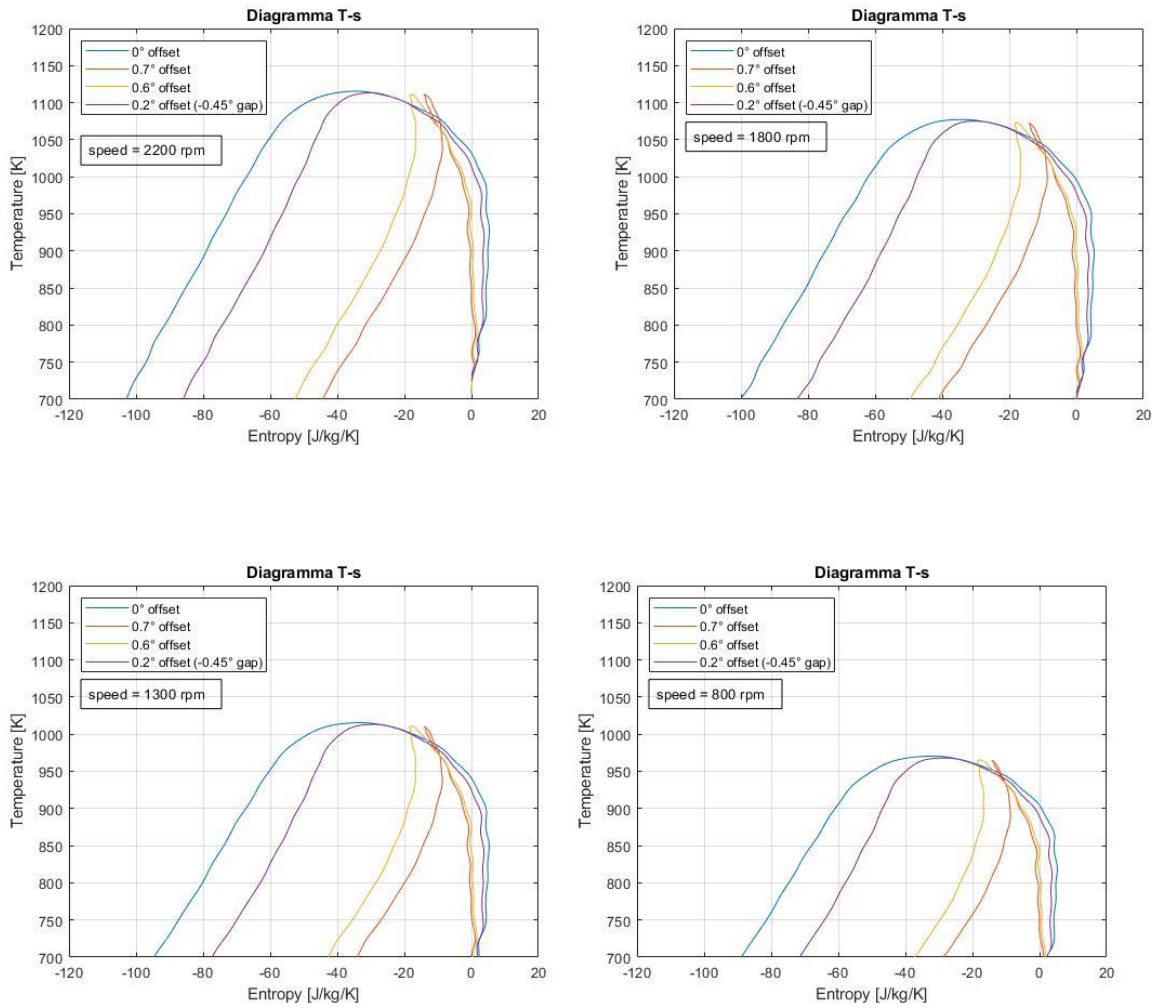


Fig. 38 – Tazerout's method for different engine rotational speed a) 2200 rpm b) 1800 rpm c) 1300 rpm d) 800 rpm

Fig. 38 a) b) c) d) show 4 on the 18 available cases. Not all the cases are reported because they result very similar to each other; only 4 cases have been chosen at different engine speed rotation in order to see how speed affects this type of analysis. Fig. 38 shows a T-s diagram with four temperature traces obtained from pressure trace with different TDC positions. The blue curve is the one obtained from the pressure data provided by FPT: this curve does not show the loop, the temperature peak is smoothed, but this is not enough to say that this is the correct TDC position. So, the approach used in this work is to start with a big shift, that is not a correct one, but it is used as a starting point, then iterating until the convergence is reached. The red curve is the first iteration step, obtained with a forward shift of $+0.7^\circ$ degrees: this temperature trace shows a little loop as its peak, that does not have a thermodynamic relevance, which means that the TDC position is not correct. Iteration continues with 0.1° degrees backward, so with a $+0.6^\circ$ degrees shift from the original pressure trace: watching the yellow curve the loop disappears, but the temperature curve is not already symmetrical. The iteration is finished, because the loop is not there anymore, and now the final -0.45° degrees shift is applied: the purple curve is the temperature curve obtained by the perfect pressure trace TDC position, and this is clear watching the smooth trend that the curve has next to the TDC: it is symmetrical with respect to its peak. So, the blue one seems to be the corrected

one before this analysis, because it has no loop, but the whole iteration process shows that the correct one is $+0,2^\circ$ degrees further on (*Fig. 39*).

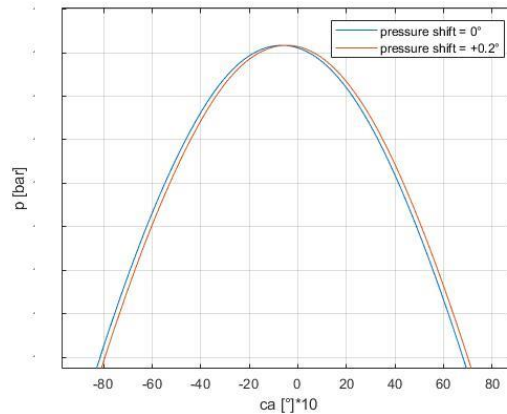


Fig. 39 – Correct pressure shift

The result of this second method proposed in this work is an excellent result, because it not only finds the correct pressure trace TDC position, but it also confirms the results obtained in Beccari-Pipitone first presented method: the pressure trace must be shifted $+0,2^\circ$ degrees forward with respect to the one provided by FPT. Furthermore, another important result achieved by this analysis is that, observing all the *Fig. 38 a) b) c) d)*, it is possible to see no difference in the curve shapes, and this means that the engine speed does not affects the model validity, but only the temperature and the entropy values assumed by the curves. In order to have a further confirmation of what has been done in this work, a third method to find the correct TDC position is now presented below.

4.3. Jaye method

The last method developed in this work is the *Jaye algorithm for determining the top dead centre location in an internal combustion engine using cylinder pressure measurement*. This is an empirical method based on the analysis of the in-cylinder pressure trace: it consists in selecting a series of several points in both compression and expansion strokes, the only characteristic of these points is that they must be chosen in order to be symmetrical with respect to the actual TDC [12]. Then with these pressure information is possible to evaluate the pressure ratio as the ratio between the compression pressure value at x angular distance from the actual reference crankshaft angle and the expansion pressure value at x angular distance from the reference crankshaft angle. The obtained pressure ratios are then plotted with respect to the x distance from actual TDC position: analysing the shape of the curve is possible to obtain information about the correctness of the TDC position. This is the simplest method developed in this work because it does not come from any thermodynamic considerations, but it is based only on empirical assumptions. In fact, this method in this work is not used in order to find the correct TDC position, but it is only used to verify that the results obtained in the previous two methods are consistent [12]. A stricter description on this method is discussed below, and it is possible to see the highlights of this method summarized in a functional scheme in *Fig. 40*.

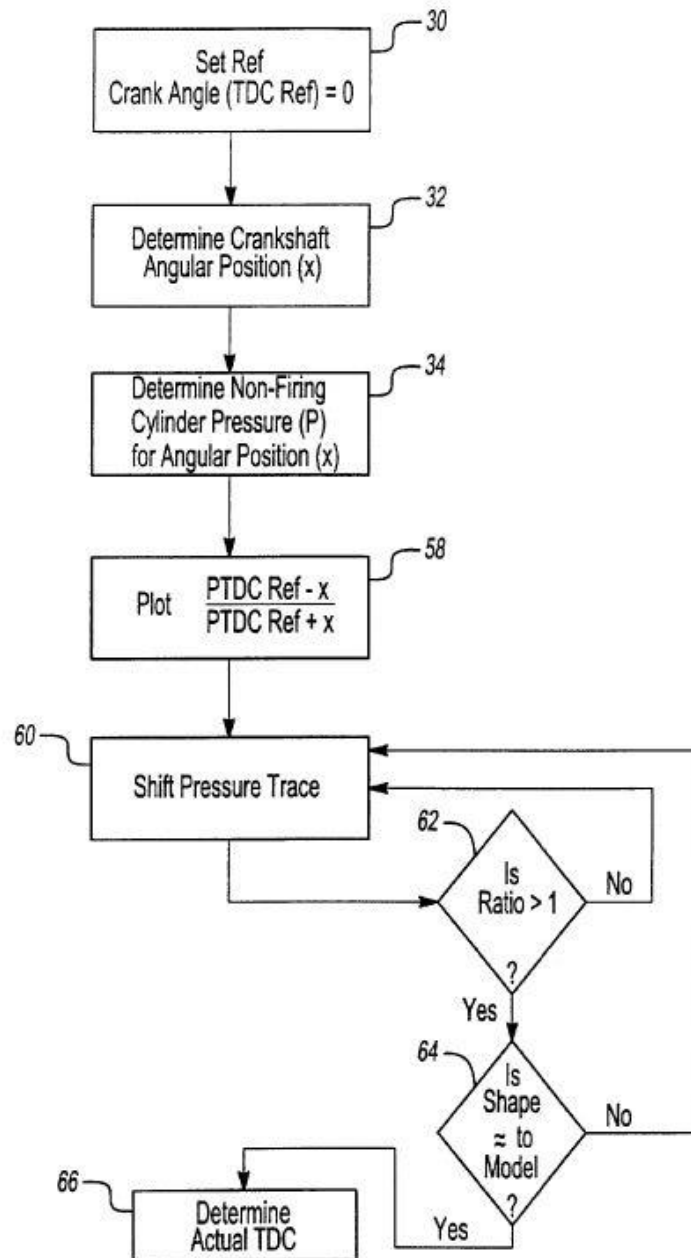


Fig. 40 – Jaye's method functional diagram

The pressure trace obtained from the rig test presents its peak in advance with respect to the TDC position, while in an ideal motored engine cycle TDC position coincides with the LPP of the pressure trace: this is due to the heat exchange between the gas and the chamber's walls and to the blowby mass fraction through the crevices. With respect to the TDC position (i.e., 0° degrees) a range of about 100° degrees in both compression and expansion strokes starting from 0° degrees are taken. It is now possible to define a pressure ratio defined as a ratio between the pressure at x number of degrees before the TDC position (in the compression stroke) and the pressure at x number of degrees after the TDC position (in the expansion stroke): this pressure ratios is now plotted in function of the x distance from the actual reference crankshaft angle [12].

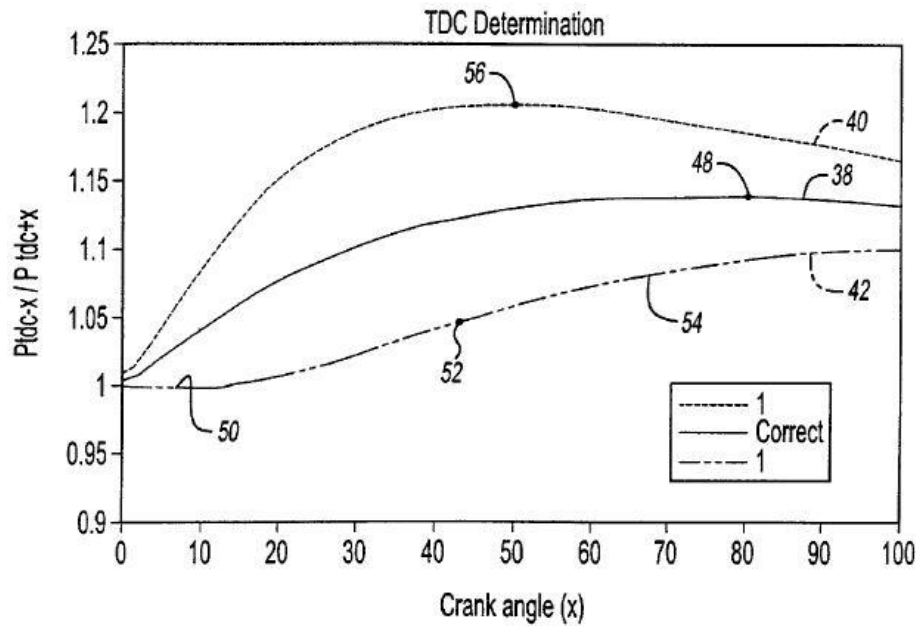


Fig. 41 – An example of the curve correct shape

Once the pressure ratio is plotted, it must be similar to the curves in Fig. 41: a curve obtained from a pressure trace with the correct TDC position should look like curve 38, while the other two plotted in this figure represent pressure ratio curves generated using incorrectly determined top dead centre position of $\pm 1^\circ$ degrees with respect to the correct TDC position [12]. Some consideration can be done observing the curve 38 obtained with the correct TDC position: all the points of the curve are greater than one; this is due to the fact that the in-cylinder pressure with a correct TDC position will be higher in the compression side for a given angle rather than the same point in the expansion side. Furthermore, the local peak of the pressure trace, like just said, occurs in advance of a few degrees or a fraction of a degree with respect to the top dead centre: this leads to a maximum in pressure ratio curve of about 1.13 when the TDC is correctly set (curve 38) [12]. The maximum value assumed by the pressure ratio curve is not fixed, but its value may vary due to some engine parameters, such as leakages, compression ratio, thermal exchange between gas and walls. However, it is good that the maximum of the curve is included in the range 1.08 - 1.18, and this value occurs around 80 - 90° degrees from the TDC shift. The position of the curve maximum value is due to the heat transfer and to the temperature of the cylinder surfaces: engines with a cooling system able to maintain the temperature near to the 373 K will show the maximum value within the 80 degrees, while hotter running engines will show this point earlier. Observing the wrong curves in Fig. 41, it is possible to see that the curve 50 obtained with a TDC position in advance with respect to the correct one presents several negative values, a concave portion for the first degrees, and the maximum is not clearly visible, but it should be around the end of the curve [12]. While the other wrong curve (curve 56), obtained with a TDC position later with respect to the correct one is all greater than 1, but its maximum value occurs too soon and with a value too much high. In conclusion, the pressure ratio curve must respect three fundamental criteria:

- Each point of the curve must be greater than one.
- The curve should be convex along its length.

- The maximum value must occur around or beyond the 80° degrees from the TDC.

If only one of these conditions is not respected, the actual TDC position is not correct, so the pressure trace must be shifted. This is an iterative process until the pressure ratio curve respects the conditions mentioned above; the used iteration step is completely arbitrary, usually a $\pm 0,1^\circ$ degrees step is recommended. As mentioned in the beginning of this section, the Jaye method is not performed in order to find the correct TDC position, but it is used in order to confirm the results obtained in the previous two methods discussed in previous sections: so, the following graphs (Fig. 42 a) b) c) d)) are obtained for a $+0,2^\circ$ degrees TDC shift with respect to the FPT provided pressure data.

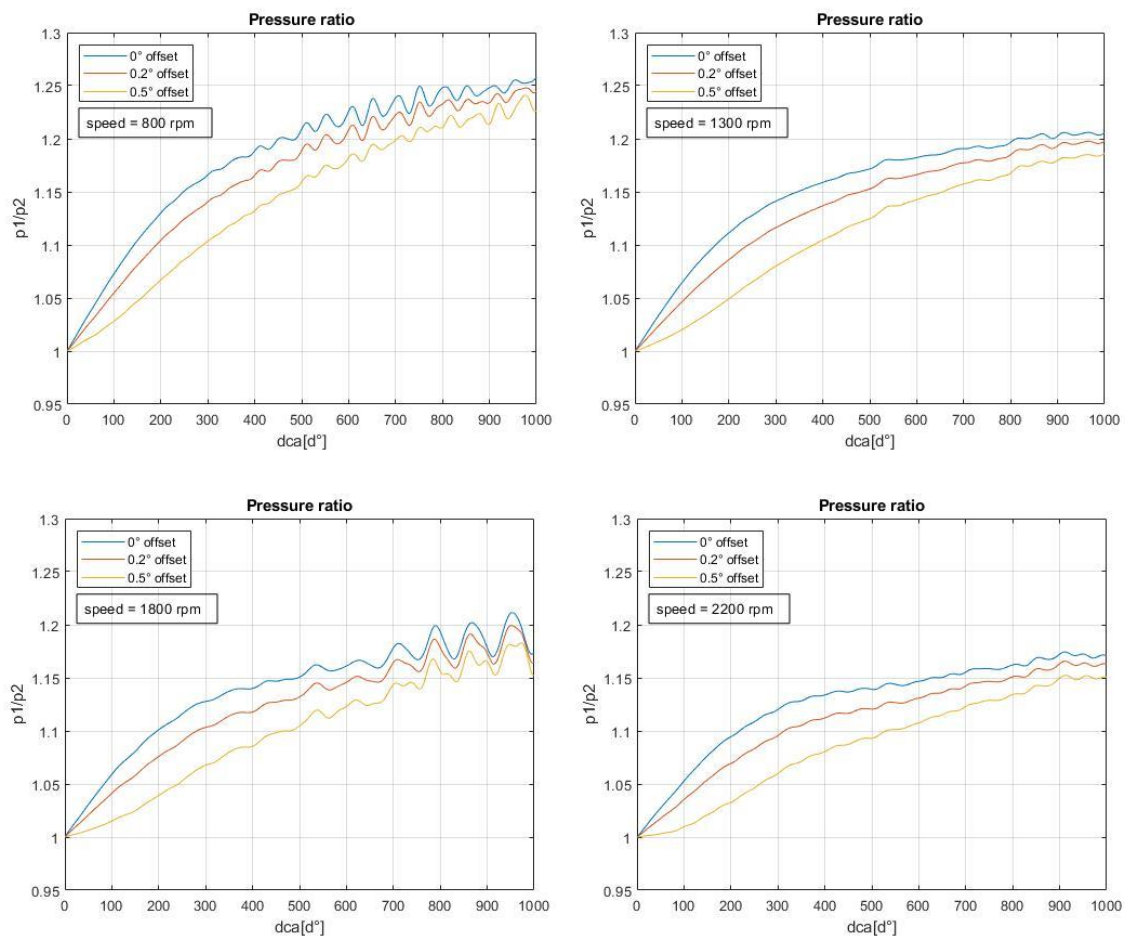


Fig. 42 – Jaye’s method results with different engine rotational speed a) 800 rpm b) 1300 rpm c) 1800 rpm d) 2200 rpm

Like for the other methods seen in this section, Jaye method is performed for all the 18 motored engine cycles provided: Fig. 42 a) b) c) d) show only 4 cases on the 18 available at different engine rotational speed, the other non-reported cases are similar to the ones reported in the above figures. Focalizing on graph Fig. 42 a), it is possible to see three different pressure ratio curves obtained for three different shifts: the blue one is obtained with no-shift applicated at the original pressure trace, while the red and the yellow ones are obtained with a $+0,2^\circ$ degrees and a $+0,5^\circ$ degrees shift, respectively. Pipitone-Beccari method and Tazerout method results give that the correct shift corresponds to a $+0,2^\circ$ degrees, so this method must verify if this shift is correct: observing the red curves in all the Fig. 42 a) b) c) d), it is possible to note that all the conditions are respected. All the

points of the curve are bigger than 1, the curve is convex along all its length and the maximum value (a perfect value is difficult to obtain due to the strong fluctuations) occurs always after the 80° degrees from the TDC position. It is possible to note how engine speed affects the curve maximum value, in particular this maximum grows with the speed. All the three conditions are confirmed, so it is possible to confirm that the actual TDC position is not the correct one, the pressure trace must be shifted forward by a +0,2° degrees shift. Furthermore, it is possible to observe watching the yellow curves in the *Fig. 42 a) b) c) d)*, that a shift bigger than 0,2° degrees (in this case the used one is +0,5° degrees) is not correct, because the obtained pressure ratio curve does not respect the above-mentioned conditions: the curve is bigger than one in all points, but in the first part the curve is not convex. The correction of the TDC position can be easily made on the provided pressure trace excel file.

5. COMBUSTION MODELS IN GT POWER

5.1. Non-Predictive combustion model

In a non-predictive combustion model, the burn rate is imposed as input of the model, so the combustion evolution does not depend on the in-cylinder conditions, always ensuring that there is enough fuel to support the burn rate. This type of model is used to study combustion aspects that are not related with the burn rate such as acoustic performances of different muffler designs, wave dynamics, boosting concepts, exhaust configuration: these parameters do not affect the combustion burn rate, so it can be imposed [8]. Moreover, non-predictive combustion model requires shorter simulation times compared to a predictive combustion model, because it does not require the burn rate calculation, since it is already known.

Engine Burn Rate Analysis

In GT Power the combustion rate is defined by the burn rate. Unfortunately, it is difficult to obtain the burn rate from bench measurements, while other quantities, like in-cylinder pressure, are easier to obtain with high accuracy. In GT Power it is possible to obtain the burn rate starting from in-cylinder pressure, and vice versa [8]. This simulation is called 'reverse run', while using the burn rate as an input to obtain in cylinder pressure is called 'forward run'. Both, reverse and forward run, use a two zones model. In this model the combustion chamber is divided in two zones: first zone called 'unburned zone' is made up by fresh air, unburned fuel, and previous cycles residual gases (plus EGR eventually) [8]. Second zone, the 'burned zone', collects all the combustion products, obtained by the progressive burning of the unburned zone's mixture. The layer that divides these zones is called flame front: all the oxidation reactions of combustion reactants take place in the flame front, while the secondary combustion reactions of the unburned products take place in the burned zone. The amount of mixture passing from unburned zone to the burned zone through the flame front is the burn rate [8].

GT Power software allows to choose between two possible methods to obtain the burn rate starting from the cylinder pressure:

- CPOA (Cylinder Pressure Only Analysis).
- TPA (Three Pressure Analysis).

While CPOA needs only cylinder pressure, TPA needs the cylinder pressure as well as the intake and the exhaust pressures, three like the name suggests. In GT Power, both methods used the same template 'EngBurnRate' called from within the engine cylinder; this template permit to insert in cylinder pressure data directly or using an external file (excel, ifile, ascii), but this will be discussed below.

5.1.1 CPOA (Cylinder Pressure Only Analysis)

Cylinder pressure only analysis calculate the burn rate starting from the cylinder pressure. To perform the analysis in GT Power it is not necessary to use the entire full model, it is enough a simpler model made up by only three components: a cylinder block, a crank train block and an injector block [8].

CPOA model methodology can be resumed in three steps:

- At the beginning, a first rough combustion burn rate is calculated making some assumptions about heat transfer.
- This burn rate is used during the forward run and the true heat transfer is calculated.
- Using the true heat transfer, the final combustion burn rate is obtained and used in the forward run to provide a pressure signal to compare with the input one.

This process runs just two cycles, but the second one is just a check to verify that results converge.

The main limitation of CPOA is the determination of some input parameters: air trapping ratio, combustion chamber wall temperatures, residual gases fraction, volumetric efficiency (indirectly). It is very difficult to obtain these values from a standard test ring, so they have to be estimated for the first try; the way they are estimated is exposed below. The main advantages of this model are that is fast, and it can be setup by knowing only few parameters (only one pressure trace), the results will be anyway consistent [8].

5.1.2. TPA (Three Pressure Analysis)

Three pressure analysis is another type of reverse run calculation used to estimate the combustion burn rate starting from a pressure trace. In this case the model is a little bit complex compared to CPOA; as the name suggests, the model needs as input three pressure, in cylinder pressure, intake pressure and exhaust pressure [8]. TPA model also requires both intake and exhaust valves, ports, and pipes. TPA's burn rate calculation process is run for multiple cycles until the model has converged: in this way trapping ratio and residual gases fraction will be calculated step by step, so there is no need to set them as input parameters; this is a big advantage respect to CPOA.

TPA simulation methodology can be resumed as following:

- For cycle 1, a rough burn rate is used, and no pressure analysis is performed.
- From cycle 2 to the end, at the start of each cycle the combustion burn rate is calculated starting from in cylinder trapped conditions at a determinate crank angle, usually IVC, along with measured pressure profile. The injection rate and the heat transfer rate come from the previous cycle. With this information the forward run simulation can start.
- The apparent burn rate obtained by the forward run of the previous step is imposed during the cycle.
- This procedure repeats until convergence is reached.

The complexity of this methodology brings to a longer simulation time.

TPA permits two types of analysis. The first and most common approach, called 'TPA steady', consists in the analysis of a steady-state operating condition over a single cycle (or several cycles' average). The aim of TPA steady is to obtain a single combustion burn rate for each operating point of the engine. The second type of analysis can be again conducted for a steady-state operating condition, but instantaneous pressure values (intake, exhaust, in cylinder) requested as input by the model are over multiple consecutive cycles [8]. The main purpose of this analysis, called 'TPA Multicycle', is to study the cyclic variation occurring on several consecutive cycles.

The main drawback of this type of reverse run is that intake and exhaust pressure traces are not always provided by bench tests: in this case TPA cannot be setup.

5.2. Predictive combustion model

In predictive combustion model, like the name suggests, the combustion burn rate is not imposed as input data in the model, but it is calculated during the simulation for each cycle based on the in-cylinder condition. This kind of simulation can be used to evaluate how much a particular variable affects the final combustion burn rate. For example, a predictive combustion model can be useful to see how burn rate changes on different operative points with different mass injection profile, since injected mass quantity and injection timing strongly affects the combustion burn rate. However, this simulation requires longer computational time if compared to a non-predictive combustion mode. GT POWER provides several predictive combustion models, for diesel engines the most useful are:

- Direct-Injection Diesel Jet Model (DI-Jet).
- Direct-Injection Diesel Multi-Pulse Model (DI Pulse).

The second one is newly developed by Gamma Technologies to take lesser computation time with a better accuracy respect to DI-Jet predictive combustion model.

5.2.1. DI-Jet combustion model

This predictive combustion model predicts the combustion burn rate in diesel engines with single or multiple injection events (GT-SUITE Engine Performance Application Manual). This model works dividing the injected fuel mass in several parts and following all these parts during all the combustion process, starting from the plume that breaks in droplets until the last fraction of fuel burning [8]. The total injected fuel mass is divided in several zones, 5 radial zones and each radial zone is divided in many axial slices. Now, all the zones present three subzones, a *Fuel Subzone* that contains only unburned fuel, an *Unburned Subzone* that contains a mixture of unburned fuel entrained air and residual gases (plus EGR, if available), and a *Burned Subzone* made up by combustion products. *Fig. 43* shows a scheme of the injection. DI-Jet works with only one injection plume, so the entire fuel mass is divided by the number of the injector nozzle orifices. At the start of an injection event, all the fuel mass is divided equally in the several zones, in particular only fuel subzones are full, while the other subzones are empty [8].

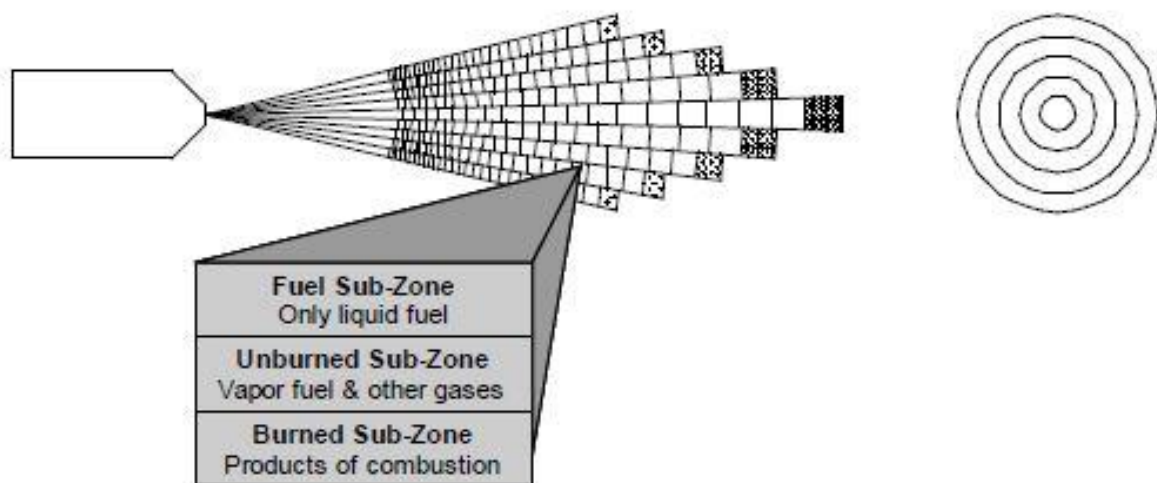


Fig. 43 – DI-Jet sub-volumes division [8]

The injection keeps it going, and the fuel plume injected at high velocity breaks into droplets finding high-pressure air in the chamber. During this phase air starts to enter the jet and mixes with the evaporated fuel; Unburned Subzones start to fill up. While all the Fuel Subzones contain same quantities of fuel, Unburned Subzones contain different quantities of air-fuel mixture, because air enters more easily in external radial zones respect to the internal ones. The entrained air causes the velocity of the zone to decrease because momentum of the zone is conserved [8]. So, during this mixing the jet deforms due to a different entrained air quantity between the external and the internal zones (Fig. 43). Combustion starts when in a zone certain conditions are reached, such as in-cylinder pressure, zonal temperature, and fuel-air ratio. Zonal temperature is the temperature of a zone and depends on the temperature of the injected fuel, the temperature of the entrained air, and the amount of evaporated fuel in the Unburned Zone. The zonal fuel-air ratio is the ratio between the evaporated fuel and the entrained air in the Unburned Subzone. Combustion takes place in the Unburned Subzones and its products move to the Burned Subzone. NO_x and Soot quantities are evaluated independently in each Unburned Subzones, and then are integrated on the whole jet to obtain the total quantity. DI Jet predictive model is not used in this work, so this is an overview of how it works, for a detailed description please consult GT-SUITE Guide [8].

5.2.2. DI Pulse combustion model

Direct-Injection Diesel Multi-Pulse model, aka DI Pulse, is a predictive model used for evaluating the combustion burn rate and associated emissions for direct-injection diesel engine, with single or multiple injection events. This model is an alternative to DI-Jet model in GT POWER, that allows to obtain shorter computational time also providing higher accuracy [8]. So, if it is possible, this model must be used rather than DI-Jet. The basic approach of this model is to track the fuel as it is injected, evaporates, mixes with surrounding gas, and burns (GT-SUITE Engine Performance Application Manual). In this predictive model, the combustion chamber is divided in three zones: A *Main Unburned Zone (MUZ)* that includes all cylinder mass at IVC (air, residual gas, EGR), *Spray Unburned Zone (SUZ)* that includes injected fuel and a mixture of evaporated fuel and entrained air, and a third zone called *Spray Burned Zone (SBZ)* made up by the combustion products (Fig. 44 a)) [8].

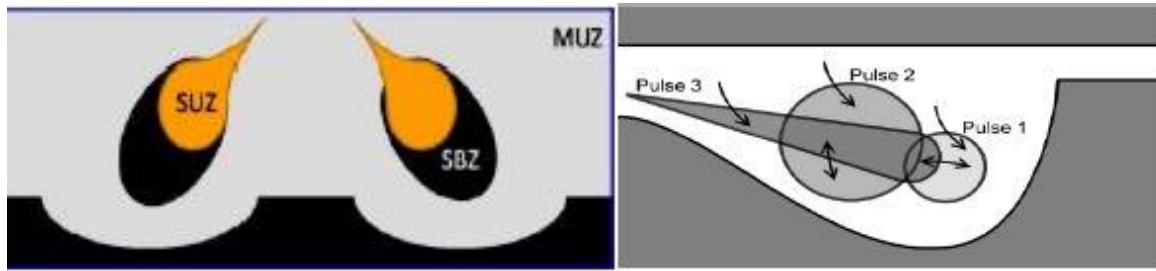


Fig. 44 – a) schematic division of SUZ, SBZ and MUZ b) How the model treats different injection events [8]

This model tracks every injection events separately from the others from the evaporation to the combustion; the injected fuel of a sub-sequent injection event is added to the *SUZ*. ‘EngCylCombDI Pulse’ template presents four parameters for the calibration of this predictive model, these parameters are:

1. Entrainment Rate Multiplier.
2. Ignition Delay Multiplier.
3. Premixed Combustion Rate Multiplier.
4. Diffusion Combustion Rate Multiplier.

These 4 parameters are multipliers used in the equations from (35) to (43) that govern different phases from the injection to the combustion; their function is illustrated below.

Fuel Injection

In diesel engine, there should be different injection events. In DI Pulse model, all the injection events are tracked separately from the others, and the injected fuel quantity is added event by event to the Spray Unburned Zone. No one of the four calibration’s parameters affects the fuel injection [8].

Entrainment

When the jet enters the combustion camera with a high speed, the interaction with high-pressure air brakes the jet into droplets. This phenomenon allows cylinder mass (air, residual gas, EGR) to enter the injection plume, starting the intermixing. The entrainment phase must not be confused with the mixture phase (in which entrained air mixes with evaporated fuel) because it happens when the fuel is still liquid, and so it is not evaporated. The entrained air causes the velocity of the zone to decrease because momentum of the zone is conserved [8]. The entrainment rate is determined by applying conservation of momentum and can be modified by the Entrainment Rate Multiplier (C_{ent}). Entrainment equations from (35) to (40) are listed below.

$$\begin{cases} u_{inj}t \left[1 - \frac{1}{16} \left(\frac{t}{t_b} \right)^8 \right] & \frac{t}{t_b} \leq 1 \\ u_{inj}t_b \frac{15}{16} \left(\frac{t}{t_b} \right)^{0.5} & \frac{t}{t_b} \geq 1 \end{cases} \quad t_b = 4.351 \sqrt{\frac{2\rho_l}{\rho_g}} \frac{d_n}{C_d u_{inj}} \quad u_{inj} = C_d \sqrt{\frac{2\Delta P}{\rho_l}} \frac{m_{inj}}{A_n \rho_l}$$

$$\frac{dm}{dt} = -C_{ent} \frac{m_{inj} u_{inj}}{u^2} \frac{du}{dt} \quad u = \frac{dS}{dt} \quad \mu = m_{inj} u_{inj}$$

(35)(36)(37)(38)(39)(40)

t	=	time	A_n	=	injector nozzle area
t_b	=	breakup time	d_n	=	injector nozzle diameter
u	=	velocity at spray tip	C_d	=	injector nozzle discharge coefficient
u_{inj}	=	velocity at injector nozzle	ρ_l	=	liquid fuel density
S	=	spray tip length	ρ_g	=	gaseous fuel density
\dot{m}_{inj}	=	injection mass flow rate	ΔP	=	pressure drop across injector nozzle

Evaporation

After the jet brakes into droplets, these droplets evaporate, and this evaporation is modelled with a coupled solution of heat and mass transfer which appropriately accounts for both diffusion-limited and boiling-limited evaporation [8]. No parameter in DI Pulse calibration is linked to the evaporation phase.

Ignition

Evaporated fuel and entrained air mix, and ignition starts when in combustion chamber temperature and pressure reach certain conditions. Time that interpasses between the evaporation and the start of ignition is called ignition delay, and chamber conditions, as well as mixture condition, strongly affect the ignition delay length. In DI Pulse the ignition delay is modelled using an Arrhenius expression, and its value can be calibrated acting on Ignition Delay Multiplier (C_{ign}) in 'EngCylCombDI Pulse' template [8]. The ignition delay is calculated separately for each injection event based on pulse conditions as well as pulse-to-pulse interaction.

$$\tau_{ign} = C_{ign} \rho^{-2} e^{\left(\frac{3000}{T}\right)} [O_2]^{-0.5} \quad (41)$$

$$\text{Ignition occurs when } \int_{\tau_0}^{\tau_{ign}} \frac{1}{\tau_{ign}} dt = 1$$

τ_{ign}	=	ignition delay	T	=	pulse temperature
$[O_2]$	=	oxygen concentration	ρ	=	pulse gas density

Premixed Combustion

When a pulse ignites, the accumulated mixture present in SUZ is ready for premixed combustion. Premixed combustion is the first step of the combustion in diesel engine (see section 2.4 for more details). The rate of this combustion can be calibrated acting on Premixed Combustion Rate Multiplier (C_{pm}) in 'EngCylCombDI Pulse' template (GT-SUITE Engine Performance Application Manual) [8].

$$\frac{dm_{pm}}{dt} = C_{pm} m_{pm} k (t - t_{ign})^2 f([O_2]) \quad (42)$$

t	=	time	k	=	turbulent kinetic energy
t_{ign}	=	time at ignition	$[O_2]$	=	oxygen concentration
m_{pm}	=	premixed mass			

Diffusion Combustion

After the accumulated fuel during ignition delay ignites during the premixed combustion, the remaining part of air-fuel mix in SUZ burns in a primarily diffusion limited phase. This second combustion phase is called Diffusion Combustion (see section 2.4 for more details), and its rate can be adjusted by acting on Diffusion Combustion Rate Multiplier (C_{df}) in 'EngCylCombDI Pulse' template. The diffusion combustion is affected by load changes, because of pulse-to-pulse interaction and pulse-to-wall interaction. Diffusion combustion rate decreases at high loads [8].

$$\frac{dm}{dt} = C_{df} m \frac{\sqrt{k}}{\sqrt[3]{V_{cyl}}} f([O_2]) \quad (43)$$

k	=	turbulent kinetic energy
V_{cyl}	=	cylinder volume
$[O_2]$	=	oxygen concentration

Now that the DI Pulse calibration parameters are known, it is possible to start with the model setup.

6. DI PULSE CALIBRATION PROCEDURE

In this section is described step by step the process followed to calibrate the DI Pulse predictive combustion model starting from the bottom. For this calibration, a total of 152 operating points were used, provided by Fiat Powertrain Technology (FPT). For these points were also provided, among others, the intake and exhaust pressure traces, that opens to a TPA. An idea is to calibrate both TPA and CPOA and see if the results go in the same direction [8]. So, the first step for the calibration of the DI Pulse is to calibrate a CPOA model to obtain the combustion burn rate starting from in cylinder pressure trace. *Fig. 17* shows the engine map with the 152 points used in this section.

GT POWER model for CPOA

CPOA needs a GT POWER model. Since in this analysis there should not be significant variations between cylinders, the full engine model is not necessary. In fact, for this type of analysis is enough a simpler model that not only reduces the input parameters but requires a shorter simulation time. This '*single cylinder model*' for the CPOA requires only an engine crank train block, a cylinder block and an injector block, as mentioned in previous section. For a single cylinder model construction, the latest block is not strictly necessary (e.g., in PFI SI the injection takes place before the intake valve, not in the cylinder), but in a diesel engine the fuel is injected directly in the combustion chamber, so the block has to be included [8]. The crank train block is taken from the full engine model to preserve some features. In Fig. 45 is represented the single cylinder model used.

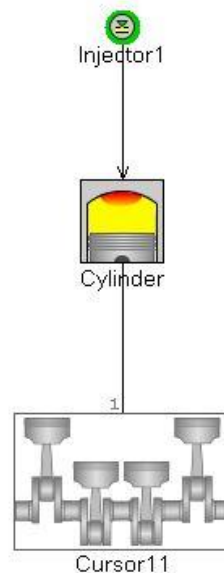


Fig. 45 – Single cylinder model

6.1. Cylinder Pressure Only Analysis (CPOA) model tuning

CPOA is a method performed in GT POWER to calculate the combustion burn rate starting from the in-cylinder pressure trace. The main drawback of this analysis is that some input parameters are hard to obtain from bench tests, so they must be estimated for the first try; moreover, because of CPOA run performs only two cycles, these parameters cannot be calculated by the model itself. These inputs are combustion chamber's wall temperature, air trapping ratio, residual gases fraction, and volumetric efficiency [8]. Last parameter usually is not obtainable from rig tests, but it can be calculated.

The process to determine the attributes mentioned above takes place as follow:

- Cylinder air trapping ratio: this quantity is the ratio between the air trapped in the cylinder and the air delivered to the cylinder. This quantity is always near to unity, only with significant overlap its value is lower than one, so for the first try it can be settled to one.

- Combustion chamber wall temperatures: as a first attempt, GT Power recommends starting with typical values of temperature that head, piston, and cylinder wall reach at full load [8]. Their values are reported in *Table 1*:

T wall first attempt [K]	
Head Temperature	550
Piston Temperature	550
Wall Temperature	450

Table 2 – Combustion chamber's temperature values for the first try

The template used is 'EngCylTWall', the 'EngCylTWallSoln' cannot be used because it needs more than two cycles to evaluate combustion chamber temperature.

- Residual gases fraction: this quantity for the first attempt can be set 3-4% higher than EGR fraction value.
- Volumetric efficiency: this quantity is the ratio of the volume of fluid actually displaced by a piston or plunger to its swept volume. Usually, this parameter is not a test ring output, but it can be calculated using known quantities, by the formula (12).

CPOA setup needs particular attention in the Main template of cylinder block. The attribute 'Measured Cylinder Pressure Analysis Object' needs a 'EngBurnRate' in which the pressure trace must be upload (the different upload types are described below). In this template there is the possibility to make different operations on pressure signal, such as shift the signal in order to match the TDC shift (widely commented in section 4 **TDC SHIFT**) or shift the signal vertically in order to have a best match between measured and simulated pressure traces: this feature is very interesting and will be discussed better later. Returning to Main template attributes, 'Cylinder Pressure Analysis Mode' must be set on 'Measured_CylP_only', and 'Combustion Object' on 'ign'. The rest of the model can be setup like any classic model. At the end, the Main template must result like in *Fig. 46*.

Attribute	Unit	Object Value
Initial State Object		Initial ...
<input checked="" type="radio"/> Wall Temperature defined by Reference Object		twall ...
<input type="radio"/> Wall Temperature defined by FE Structure part (EngCylSt...		
Heat Transfer Object		Heat_transfer ...
Flow Object		flow ...
Combustion Object		ign ...
Measured Cylinder Pressure Analysis Object		EngBurnRate ...
Cylinder Pressure Analysis Mode		Measured_CylP_only ▾

Fig. 46 – CPOA Cylinder Main template

Now the first attempt is ready to start. To reach the final burn rate, the output of the first attempt must be used as input in the full engine model to obtain the true values of the quantities mentioned

above. This iteration is made until the error is less than 2-3%. *Fig. 47* shows a functional scheme of how a correct CPOA calibration must be done.

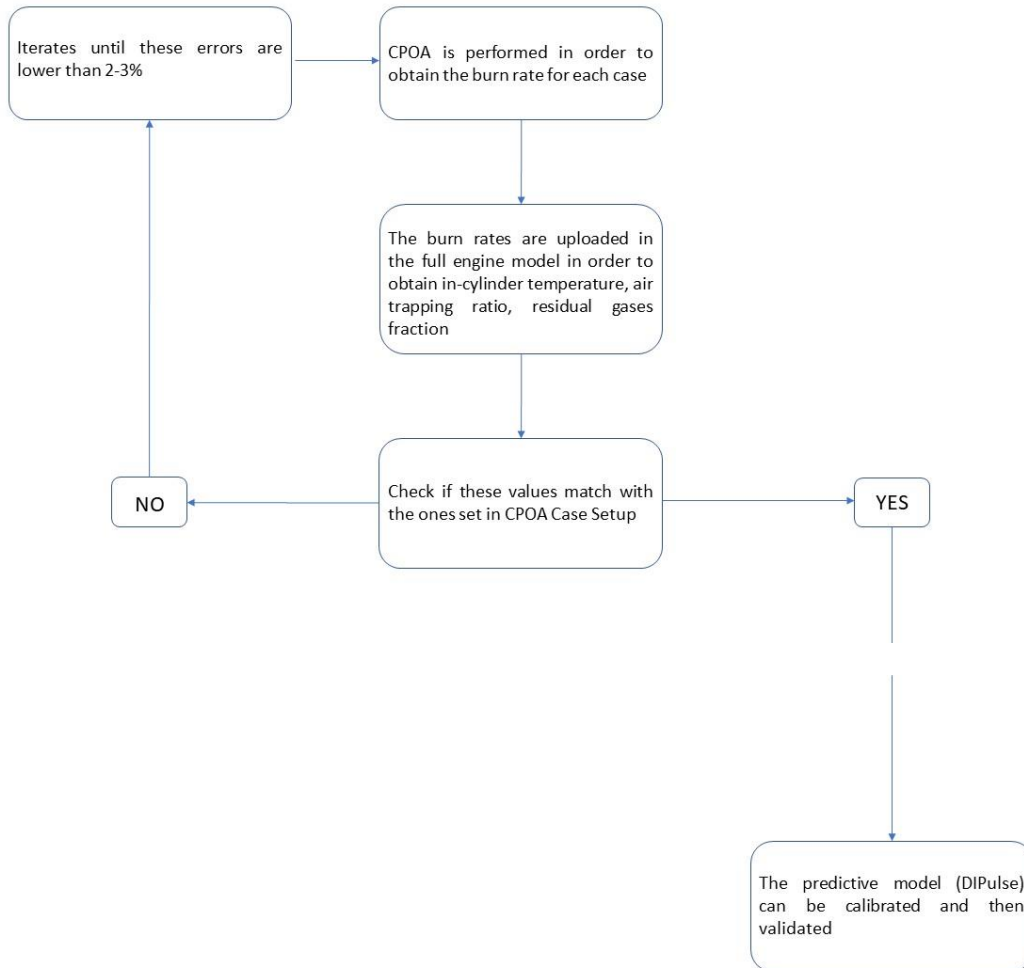


Fig. 47 – CPOA's tuning iterative method

As a result of the first of this model, a burn rate profile as function of crank angle is obtained for each of 152 steady-state points under investigation. *Fig. 48* shows two curves, the red one is the combustion burn rate, while the blue one is an input, the diesel injection rate.

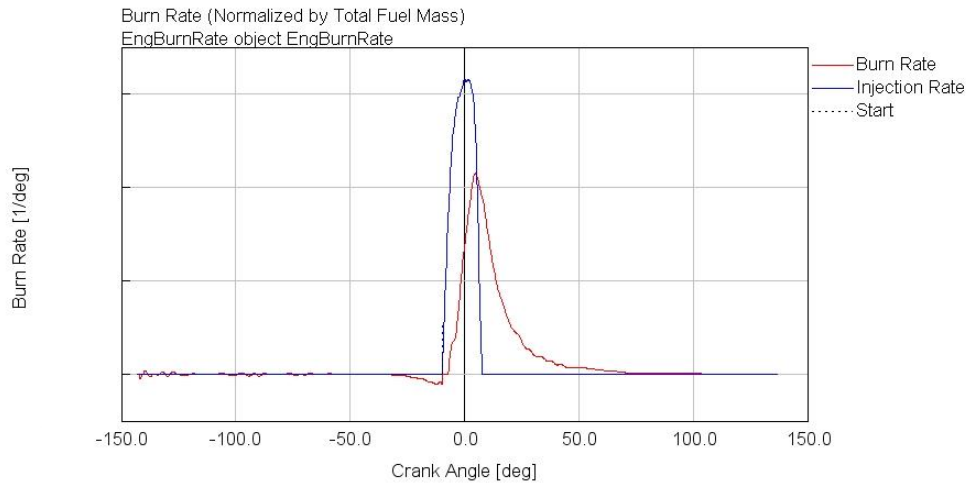


Fig. 48 – An example of combustion Burn Rate obtained by CPOA non-predictive model

Now the first attempt burn rate can be used as input in the full model engine: in this way the simulation estimates the ‘real’ values of combustion chamber’s wall temperatures, air trapping ratio and residual gases fraction. This type of simulation, where the burn rate is known, is called ‘non-predictive combustion model’. There is a GT POWER feature that helps in this transition between the single cylinder model using for the CPOA and the full model engine, generating an external file ‘filename_prof’ in which case per case is reported the combustion burn rate as function of crank angle: this external file can be used as input for the full model engine, avoiding the copy and paste part and simplifying the upload [1]. This feature is available in Output template of ‘EngBurnRate’ template; is very useful in case of several operating points (152 in this work). Fig. 49 shows how the templates looks like in the used full model engine: in ‘combustion object’ is uploaded the combustion burn rate from CPOA analysis, and ‘Measured Cylinder Pressure Analysis Object’ is set on ‘off’.

Main Advanced			
	Attribute	Unit	Object Value
	Initial State Object		Boost ...
<input checked="" type="radio"/>	Wall Temperature defined by Reference Object		Heat-Solver ...
<input type="radio"/>	Wall Temperature defined by FE Structure part (EngCylSt...		
	Heat Transfer Object		Heat-Transfer ...
	Flow Object		Flow ...
	Combustion Object		Combustion_rate ...
	Measured Cylinder Pressure Analysis Object		ign ...
	Cylinder Pressure Analysis Mode		off

Fig. 49 – Full Engine Model Cylinder Main template

Non-predictive combustion model provides the ‘true’ values of the parameters mentioned before. These values now can replace that ones used in the CPOA for the first try, and so on. The iteration process ends when the difference between the input values of the above-mentioned parameters of two consecutive iteration passages is lower than 2-3%. If not, CPOA runs again.

CONSISTENCY CHECK

There are very often a lot of errors in the calculation of the combustion burn rate using these models. An error's source can be a wrong input parameters value, or maybe an incorrect input measured pressure trace, there can be inaccuracies in used sub-models, like in-cylinder heat transfer; the error's sources are different, and it is difficult to find them. The results of the cumulated error leads to a difference between the in-cylinder fuel mass quantity used for the calculation and the predicted one. GT POWER to handle this problem introduces a multiplier, called *LHV multiplier*, that adjust the fuel energy content in order to obtain the same combustion efficiency or the same burned fuel fraction given as input in 'EngBurnExhMeasure' template. The more the cumulative error is high, the more LHV multiplier value varies from 1.0; this parameter can be seen as an indicator of the cumulative error [8]. Even if its value is near to the unity, it is recommended to verify the quality of the input data of the simulation, because it is possible that two errors can neglected each other. LHV multiplier value is reported in CaseRLT template, in 'Pressure analysis, Measure' section; this parameter gives information about the entity of the error, but no information about the source of the error [8]. This LHV multiplier is a simulation output, it cannot be used to reduce the gap between measured and simulated pressure, this is a big mistake.

Among the results of the simulation, there is also a list of consistency checks that are performed automatically and reported in CaseRLT template, 'Pressure analysis, Measure' section; this variable will be set to 0 if any of the following consistency checks made during the cylinder pressure analysis indicate a potential problem. Below are presented some of the investigated quantities:

- **Reasonable IMEP:** the IMEP calculated integrating the in-cylinder pressure trace should be greater than the BMEP calculated from the brake torque measurement; the amount of this difference must be compared to the FMEP. FMEP is known from full model engine simulations [8].
- **Pressure Smoothing:** the measured in-cylinder pressure profile should be reasonably smooth. The raw pressure trace input is smoothed by a filter that can be selected in Pressure Adjustment of 'EngBurnRate' template, under 'Smoothing Option' voice. In this simulation a cubic-fitting filter is used, with a cubic smoothing range set to 5 [8]. This value is saved in CaseRLT, and if it is >0.02 it is flagged as an error, but the consistency check of the under-investigation case is **not** set to 0.
- **Cumulative burn during compression:** during the compression stroke there should not be fuel burning, because a correct combustion event comes after the compression (i.e., during compression ending), so any calculated fuel burned is an indication of error in input data. However, in a combustion chamber in some cases it is possible to find a non-zero instantaneous apparent burn rate (it can be positive or negative) during compression, but the cumulative burn rate value is still close to zero when integrated on the whole compression stroke [8]. This value is saved in Case RLT, and if it is value in bigger than 0.02 or lower than -0.02 , the consistency check of this case is set to zero.
- **Compression slope:** the compression slope of the curve in the Log P – Log V diagram should be constant along all the compression stroke; it actually decreases during compression last crank angle due to a temperature increase. Compression slope value is connected to the

compression polytropic coefficient: the polytropic coefficient of the compression stroke depends on combustion chamber conditions. For a direct injection engine (GDI) where the fuel is injected directly in the combustion chamber the polytropic coefficient strongly changes with temperature, it is 1.4 at 300 K and decreases when temperature increases. Also EGR and residual gases fraction affects this coefficient, decreasing this value further when their fraction increases [8]. The compression slope at the beginning and at the end of the compression stroke are saved in Case RLT.

- **Fraction of fuel injected late:** this model is characterized by two injections, a main injection and a pilot injection; fuel enters the combustion chamber only during these two events in a real engine (not considering leakages). In GT POWER model if there is not enough fuel to support the predicted combustion burn rate, the injector injects an amount of fuel to fill the gap. This *amount of fuel injected late* is normalized respect to the total amount of fuel injected in the combustion chamber and saved in Case RLT [8]. If this value is bigger than 0.02 is flagged as an error, and the consistency check is set to zero.
- **LHV Multiplier:** if this parameter adjustment is bigger than 5%, it is flagged as an error and the consistency check is set to zero [8]. This parameter usage is described above.
- **Combustion efficiency and Burned Fuel Fraction:** the LHV adjustment is done to have a combustion efficiency or the burned fuel fraction at the end of analysis 100% matched with target value. It is very difficult to obtain a 100% match, usually is lower [8]. If the combustion efficiency error respect to the target value is bigger than 5% (combustion efficiency value <0.95), it is flagged as an error, but the consistency check of this case is not set to zero. Same for the burned fuel fraction, where it is flagged error when its value is bigger than 5%.
- **Apparent indicated efficiency:** if this value is higher than 50% it is flagged as an error and the consistency check is set to zero.

These parameters' checks are valid for both CPOA and TPA simulations. For TPA there are also other parameters for the validation of the consistency check, that are discussed later.

The consistency check is very useful as a warning for potential errors, helping to track the input data that are inaccurate and can be the source of the calculated burn rate error.

a. Test Cell Data Analysis

Consistency check gives an overview on simulation results. These checks are very useful to find potential errors in simulation's input data, but they do not necessarily indicate problems' source. This section suggests a series of potential common source of errors that can be found in input data and can seriously affect the simulations. Not all the following errors have the same impact on combustion burn rate, but there will be heavier errors and less important ones.

Incorrect pressure phasing

The determination of the crank angle when piston is at top dead centre (TDC) is very important to conduct a correct non-predictive analysis. For this aim, a rotary encoder is used. Rotary encoder is a sensor that translates physical motion into electrical data, and it is mounted on the crankshaft and manually calibrated. Incorrect phasing of a measured cylinder pressure trace leads to incorrect

results of several important output quantities [8] [13]. Encoder error is the amount of the angular distance between the encoder measured TDC position and the real one. Just 1 degree before or after the TDC can cause up to 10% in IMEP evaluation and from 5% to 25% in heat release evaluation; so, the correct TDC position is vital-importance target.

There are two ways to determine the encoder error:

- TDC sensor.
- Motored engine pressure trace.

TDC sensor is a capacitive sensor mounted on the injector or spark plug that turns piston movements in a voltage signal; this allows to obtain the TDC determination. TDC sensor allows dynamic measurements with an accuracy of about 0.1°. This method is recommended since it is not affected by errors in pressure values due to an incorrect pegging, cylinder-cylinder interaction and so on. The main drawback of this sensor is the high cost and that its use is not really fast, since his assembling is not so easy.

A *motored engine cycle* is a cycle during which the engine is powered by an external source and no injection events occurs. In an ideal motored engine cycle energy exchange during the compression and the expansion strokes are completely balanced. This means that a crank angle resolved pressure data should be symmetric respect to TDC, and the peak pressure coincides exactly with top dead centre position [8]. However real engines have losses in form of heat transfer, blow-by and crevices leakages. These phenomena cause a peak pressure shift within 1 degree before TDC.

Please see section 4 for more information on this topic.

Pegging Error

Usually, the best way to correctly measure in-cylinder pressure trace are piezo electric transducers. When pressure changes the transducer is deformed, and this deformation is characterized by a charge release, directly proportional to deformation intensity. This charge is converted to voltage using a digital circuit [8]. Then, a transfer function is used to obtain a pressure trace starting from a voltage trace obtained as transducer output. Transfer function depends on the used tool and can change using different transducers. Equation (44) shows a general representation of a transfer function.

$$p(\vartheta) = p_{peg} + Gain(V(\vartheta) - V(\vartheta_{peg})) \quad (44)$$

When *gain* is the sensor gain, express in bar/volt, $V(\vartheta)$ is the voltage at a given crank angle, while p_{peg} and $V(\vartheta_{peg})$ are respectively the peg pressure and the voltage at the crank angle where the pressure is being pegged. The peg pressure is a pressure value taken as reference used to shift all the pressure trace by the same value, in order to have the correct trend [8] [13]. Transfer function only converts an input voltage signal in a pressure signal, while peg pressure needs to set the correct pressure values. Chase an incorrect peg pressure affects some output quantities, such as instantaneous heat release, cumulative heat release, peak pressure value, bulk change temperature, crank angle of peak pressure, polytropic coefficient. The last parameter can be used

to check the eventual *pegging error*. In fact, polytropic exponent value is strongly linked with the rate of heat transfer across cylinder's walls and with in-cylinder gases' specific heat. In a Diesel engine, the polytropic exponent in the first part of the compression stroke, from -90 to -40 degrees before TDC, can assume values between 1,35 to 1,37. So, if input pressure trace is affected by a pegging error, the compression polytropic exponent value is out this range [13]. This range is evaluated with no EGR: when in-cylinder EGR fraction increases polytropic exponent increases.

Another way to find the pegging error, is to compare intake manifold pressure trace with in-cylinder pressure trace. Theoretically, in-cylinder pressure at BDC (Bottom Dead Centre) has the same value of intake manifold cylinder; in a real engine, this value mismatch due to leaks and friction, but the difference is lower than 200 millibar. If this difference is higher, the cause can be a pegging error.

Thermal Shock

A large amount of heat energy is released during the combustion stroke; this phenomenon can generate a momentarily change of piezo electric sensor gain, that brings to fluctuations in measured pressure trace. Usually, used sensors have very low time constants, that allows a fast recovery before the next cycle. However, if recovery is not so fast there should be cyclical variation in pressure traces. This is known as thermal shock [8] [13].

Errors due to thermal shock can be detected by analysing the Average Exhaust Absolute Pressure in exhaust manifold; the difference between measured and simulated exhaust pressure traces must be lower than 4kPa, within 240-320 ca ATDC (after TDC) interval.

Compression Ratio

Blueprint compression ratio (ratio between BDC volume and TDC volume) is always known in an engine calibration. However, in a real engine this value could not match the nominal one. This difference is due to the tolerances of the single components of the cylinder, that staked-up together can bring to a deviation from the nominal compression ratio. Furthermore, some components can be out of tolerance and some not wanted crevice volumes may be counted in CR calculation. Finally, while the geometric CR is always the same, the dynamic CR it is very difficult to evaluate, because its value change with speed and load [8] [9] [13]. A wrong evaluation of compression ratio brings to several errors in simulation output parameters, such as calculated IMEP (this parameter changes a little with CR variation) and Cumulative burn during compression (this parameter changes a lot). To find the correct CR value an iterative process can be done on CPOA model: this process is done by iterating the compression ratio to get a match between simulated and measured pressure traces in the crank angle interval that goes from compression start to start of injection (SOI), marked by a vertical dotted line. *Fig. 50* a) b) show two iterations step with CR = 20,5 and CR = 20.

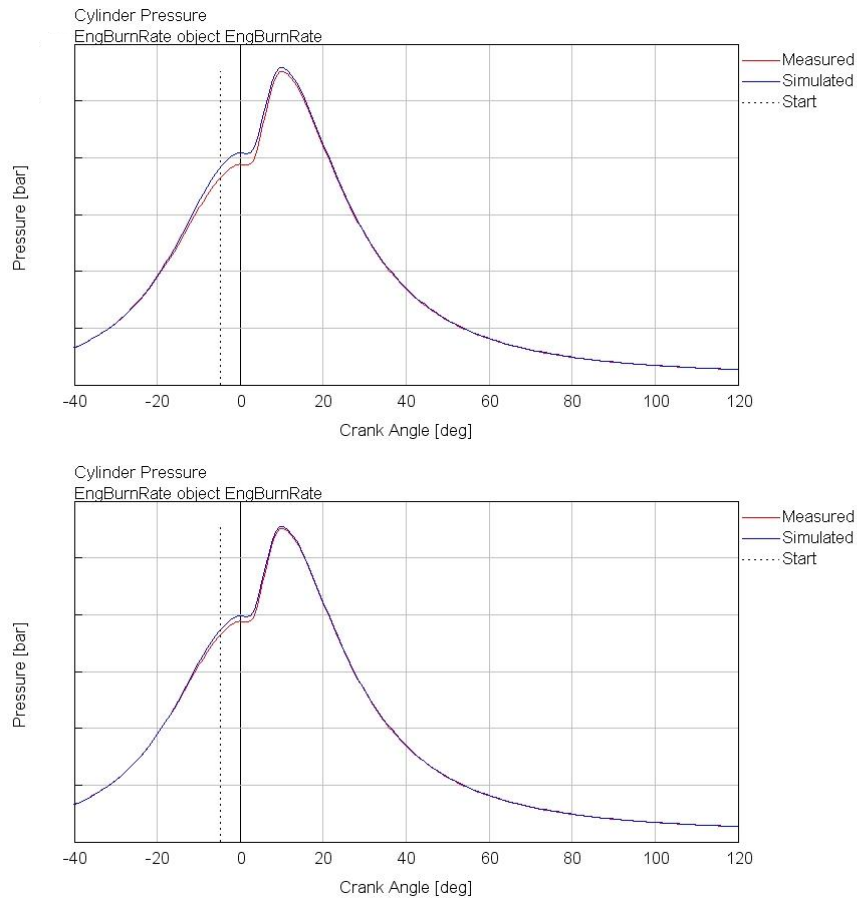


Fig. 50 – Measured vs Simulated pressure traces a) C.R. = 20,5 b) C.R. =20

CR variation effects on pressure trace can be seen on a crank-angle resolved (like Fig. 50 a) b)) or on a Log V vs. Log P diagram. Like said above, dynamic CR changes with speed and load, so simulation with several points needs several CR. However, the CR value used for the final calibration model is an average of all the dynamic compression ratio.

Fuel injection timing

The fuel injection timing is when an injection event (pilot or main) starts. There is a delay between the electric start of injection (SOIe), when the signal is emitted by the control unit, and the hydraulic start of injection (SOIh), when the nozzle opens, called injection delay. GT POWER needs SOIh as input data, while bench tests data provides SOIe. The injection delay changes with load and speed (not so much), but in this work it is considered constant for all 152 cases. Injection delay is set to 460 micros.

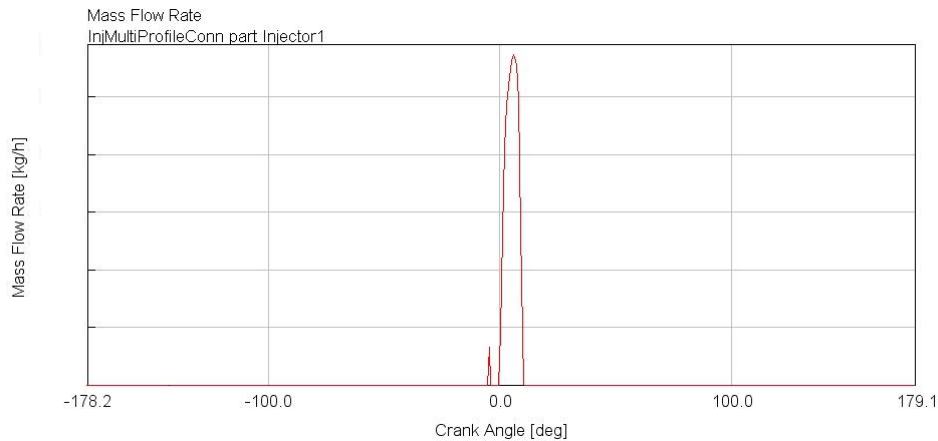


Fig. 51 – Fuel injection rate

b. Three Pressure Analysis (TPA) model tuning

Three Pressure Analysis is another reverse run model used for calculating the combustion burn rate starting from pressure traces. In this case, as the name suggests, the input pressure traces necessary for the model are three:

1. Intake pressure trace
2. In-cylinder pressure trace
3. Exhaust pressure trace

For this analysis, no estimation of combustion chamber's wall temperature, air tapping ratio and residual gases fraction need for the first try, because these quantities are calculated by the simulation itself during the iteration cycles. For the TPA methodology see section 5. This is a big advantage respect to CPOA, because in one shot TPA, if appropriately setup, gives the final combustion burn rate, no needs multiple runs until convergence. Beyond three pressure traces, TPA needs other input parameters, such as EGR fraction, intake air temperature, exhaust gas temperature, fuel injection data, spark timing (SI only). The single cylinder engine model used for CPOA is useless for TPA, because this analysis requests also an intake manifold and an exhaust manifold, or a part of them. Three Pressure Analysis can be used for two different types of analysis, 'TPA steady' and 'TPA multicycle'. In this work the purpose is to obtain a single combustion burn rate for each operating condition, no considerations on cyclic variations are requested, so 'TPA steady' analysis is chosen.

GT POWER model for TPA

The model used in GT POWER for Three Pressure Analysis is a little bit complex respect to the single cylinder engine model used for CPOA analysis, it must be integrated. Starting from the single cylinder engine model made by the cylinder block, the crank train block and the injector block, blocks for the intake manifold and exhaust manifold are added [8]. These blocks are valves, pipes, flow splits and end environments, as it is shown in *Fig. 52*; these elements should be built following normal model building procedures. In this case these elements are pasted from the full engine model, paying attention to paste only the important part and not all the intake manifold (the intake manifold of the full engine model contains intercooler, air filter, turbo group compressor, EGR flow

split are useless for TPA purposes), same for the exhaust manifold [8]. Then the pressure traces are imposed as boundary conditions using a special template created for TPA analysis purpose called 'EndEnvironmentTPA'.

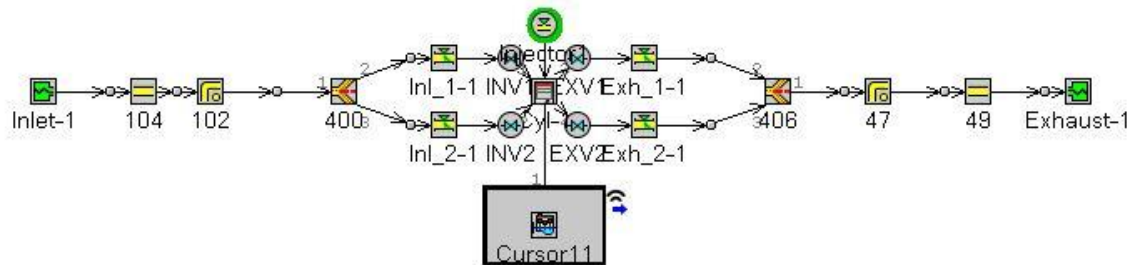


Fig. 52 – TPA model

TPA model calibration

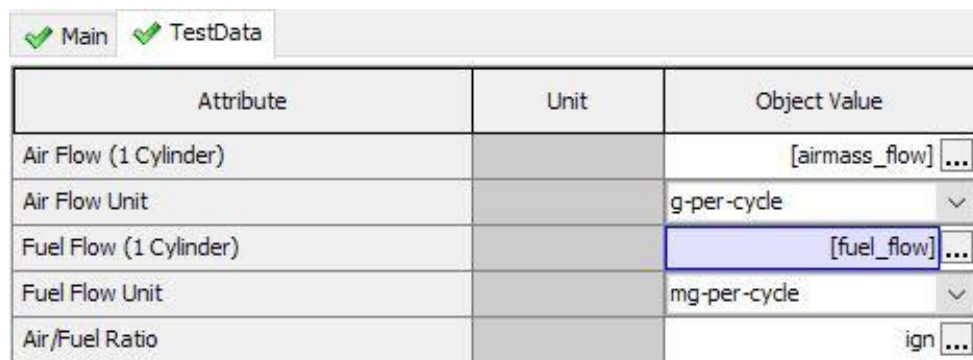
This step is very similar to the CPOA setup, because both the analysis uses the same templates. In fact, in the cylinder block, an 'EngBurnRate' object should be used for 'Measured Cylinder Pressure Analysis Object' for both 'TPA steady' and 'TPA multicycle'. The Cylinder Pressure Analysis Mode is set on TPA. In Three Pressure Analysis the combustion chamber wall temperatures are calculated so there is no needed to set a first try value, so 'Wall Temperature defined by Reference Object' needs a 'EngCylTWalSoln' object instead of 'EngCylTWal' object used in CPOA. 'EngCylTWalSoln' object is used to predict the structure temperatures, including the surface temperatures that are used in the calculation of in-cylinder heat transfer. This object is different from 'EngCylTWal' in that the temperatures are predicted by the solver rather than imposed by the user [8]. This solver object can be used because TPA operates on multiple cycles, so there is time to calculate the unknown quantities including combustion chamber's surface temperature, while CPOA runs only two cycles, so this calculation is not available. Fig. 53 shows used templates.

<div> <input checked="" type="checkbox"/> Main <input checked="" type="checkbox"/> Advanced <input type="checkbox"/> Plots </div>			
	Attribute	Unit	Object Value
	Initial State Object		Boost ...
<input checked="" type="radio"/>	Wall Temperature defined by Reference Object		Heat-Solver ...
<input type="radio"/>	Wall Temperature defined by FE Structure part ('EngCylSt...		
	Heat Transfer Object		Heat-Transfer ...
	Flow Object		Flow ...
	Combustion Object		ign ...
	Measured Cylinder Pressure Analysis Object		TPA_steady ...
	Cylinder Pressure Analysis Mode		TPA ▾
	Create Model for Simplified Pressure Analysis		<input type="checkbox"/>

Fig. 53 – TPA Cylinder Main Template

'EngBurnRate' object allows user to enter the measured cylinder pressure profile. In this object are also available some features that permit to adjust the updated pressure trace [8]. Another difference between TPA and CPOA is in 'Analysis Options' template of 'EngBurnRate' called

‘Combustion Object for Forward Run’; in CPOA this object is set on ‘def’, while in Three Pressure Analysis it has to be calibrated. A ‘EngCylCombPressure’ object is used. This object defines the combustion options to be used during the forward run portion of a simulation that also involves reverse calculation of the combustion burn rate from measured cylinder pressure. This template may only be called in models where the measured cylinder pressure and other inputs for the calculation of burn rate are defined, especially in TPA analysis where several consecutive cycles are performed [8]. While ‘Main’ template does not need any changes, in ‘TestData’ Air Flow and Fuel Flow patterns must be fill respectively with measured air mass flow rate and measured fuel mass flow rate from the same test run that generated the cylinder pressure trace in the PressureArray folder [8]. These values will not affect the pressure analysis calculations but will be used in TPA consistency check. If both Air Flow and Fuel Flow are defined, the third empty folder, Air/Fuel ratio, is calculated accordingly. These folders are filled using parameters. *Fig. 54* shows how this object looks like.



Attribute	Unit	Object Value
Air Flow (1 Cylinder)		[airmass_flow] ...
Air Flow Unit		g-per-cycle ▾
Fuel Flow (1 Cylinder)		[fuel_flow] ...
Fuel Flow Unit		mg-per-cycle ▾
Air/Fuel Ratio		ign ...

Fig. 54 – Combustion Object for Forward run

Another difference with CPOA model setup is the usage of a new type of GT POWER block called ‘EndEnvironmentTPA’; this object is used to impose boundary conditions for a Three Pressure Analysis, boundary conditions such as pressure, temperature, and composition. TPA is typically performed using measured intake and exhaust port pressure traces with a measured cylinder pressure trace and average temperature measurements in the ports [8]. This object allows the user to enter the measured intake or exhaust port pressure profile as a function of crank angle along with the measured average pressure and temperature in that port. The instantaneous pressure profile is shifted such that the entered average pressure is obtained. This object is used for both intake and exhaust boundary conditions, and they are built in the same way. The only difference is in ‘EGR Fraction’ object, that in exhaust end environment must be set to ‘def’. *Fig. 55* shows how to setup this element.

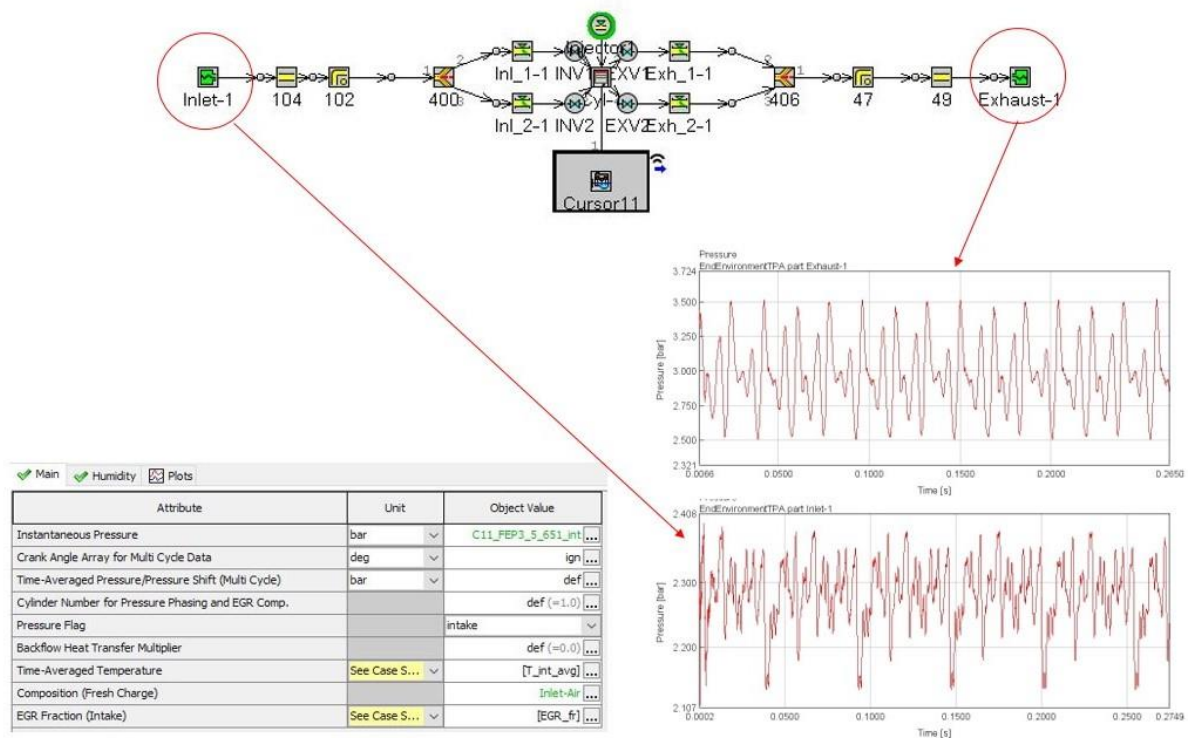


Fig. 55 – TPA EndEnvironment blocks for the upload of the intake and exhaust pressure signals

As said previously, all the intake and the exhaust manifolds of this TPA model is taken from the full model engine, to preserve some features of that model. The only parameter for a better Three Pressure Analysis to change is the ‘Discretization Length’ of all the manifold’s pipes. The *Discretization Length* is the length of each sub-volume where solution quantities (e.g., pressure, temperature, mass fractions, ...) are calculated. In a TPA the discretization length should be reduced of about 20% of the cylinder bore in intake ports and 25% of the cylinder bore in the exhaust ports. This measure is necessary to minimize unwanted noise in the pressure signal [8]. In full model engine’s pipes, the chosen discretization length is set to 40 mm, while in Three Pressure Analysis model is set to 10 mm and 8 mm, respectively for intake and exhaust manifold’s pipes (cylinder bore is 128 mm) (Fig. 56).

<input checked="" type="checkbox"/> Main <input checked="" type="checkbox"/> Thermal <input checked="" type="checkbox"/> Pressure Drop <input checked="" type="checkbox"/> Plots			
Attribute	Unit	Object Value	
Basic Geometry and Initial Conditions			
Diameter at Inlet End	mm	95	...
Diameter at Outlet End	mm	95	...
Length	mm	73	...
Discretization Length	See Case S...	[discr_]_int	...
Initial State Name		Boost	...
Surface Finish			
<input type="radio"/> Smooth			
<input checked="" type="radio"/> Roughness from Material		wrought_iron	...
<input type="radio"/> Sand Roughness	mm		...
Additional Geometry Options			
Radius of Bend	mm	ign	...
Angle of Bend	deg	ign	...
Pipe Elevation Change or 3D Acceleration Object	mm	ign	...
Number of Identical Pipes		def (=1.0)	...

Fig. 56 – Tail Pipe template

When the setup is over, TPA is ready for the simulation. In this case, compared to CPOA, the simulation time is longer, due to the high number of cycles performed by GT POWER in a Three Pressure analysis, but while CPOA needs more iteration steps to reach the final combustion burn rate, TPA needs only one simulation. Among the results, there are also the calculated values of parameters such as Air Trapping ratio, Combustion Chamber Surface's Temperatures, residual gases fraction and volumetric efficiency [8]. These values can be used as input in a Cylinder Pressure Only Analysis or, like in this work, compared with CPOA values for a further comparison. Also, in TPA there is a tool in 'EngBurnRate' output section to generate an external file *.gtm* which can be easily copied in another model.

Is very important in this calibration phase, to check the used GT POWER version; in some cases, copying a model, or only part from a model built on a different version can create problems during the simulation. In fact, during this TPA setup the elements of intake and exhaust manifold, as well as crank train object, are copied from the full model engine; full model engine GT POWER version is different from the actual v2017 version, so when TPA model is launched, the simulation does not work. This error is due to settings differences between two different version of the software. In this phase, GT POWER guide suggests a rapid check on the model settings (Run Setup, Plot Setup, Output Setup, Advanced Setup) to avoid inexplicable errors even in correct-built model. To help this check the 'Compare File' tool in toolbox can be use: this tool compares two different file and provides a list of the differences between them. Please see GT POWER guide for more information [8].

TPA Consistency Check

Three Pressure Analysis consistency check follows the same rules of CPOA consistency check, so a case for a validation must respect all the limits listed above. Beyond these ones, TPA must respect also other checks:

- **Air Mass at IVC:** only for 'TPA steady', the trapped air mass at IVC in the simulation is compared to the test data air mass entered in the cylinder. This check is available only if 'Combustion Object for Forward Run' object is a 'EngCylCombPressure' template. If simulated data differ from test data by greater than 5% it is flagged as an error, and this case can't pass the consistency check. Usually, the measured trapped air mass data come from a bench test on a full engine, then with more than just one cylinder; so, these data contain information about the whole air mass entered in all the cylinders. To obtain information about a single cylinder, this value must be divided by the cylinders number. While GT POWER works with cylinders separately, so there could be different trapped air mass values for different cylinders, and this can bring to a difference between measured and simulated bigger than 5%. Another source of error is the valve timing. In a real engine the valve timing varies as a function of speed and load due to several factors such as valve inertia, and thermal effects, while in TPA model this parameter is usually fixed for all cases. This behaviour leads to a discrepancy between the test data trapped air and the simulated one. In case of failed consistency check due to this parameter, the error can be corrected by varying valve timing until simulation and measured trapped air mass match [8].
- **Fuel Mass Injected Quantity:** only for 'TPA steady', the simulated fuel mass injected in the cylinder is compared to test data obtained from a bench test. This check is available only if 'Combustion Object for Forward Run' object is a 'EngCylCombPressure' template. Total mass means the sum of all injection events that happens in the same cycle (in this case Pilot + Main). If the difference between measured and simulated is bigger than 5%, it is flagged as an error and this cycle cannot pass the consistency check. [8]
- **Fuel Air Ratio:** only for 'TPA steady', if simulated fuel air ratio differs from measured one by greater than 5% it is flagged an error. Often in 'EngCylCombPressure' template this value is set to 'def'; in this case F/A ratio is calculated from trapped air mass and fuel mass injected values used as parameters [8].

Input file format

Usually, these types of analysis work with a large number of operating points, so upload case for case all input parameters can result a waste of time. In this work, all the simulations must run for 152 cases (operating points) provided by FPT. GT POWER, to avoid this, shows several methods to upload a large amount of information in one shot. The easiest one is the *parameter* method: this object is used to store several values under the same object name. To use a parameter is enough to insert as object of any quantity the name of the parameter wanted in square brackets. All the parameters used in a model are saved in *Case Setup* template. Fig. 57 shows several quantities used as parameter, such as time-averaged intake and exhaust temperature used in *EndEnvironmentTPA* blocks; this allows to have a different value of this quantity for each case.

<div><div>Main</div><div>All</div><div></div></div>					
Parameter	Unit	Description	Case 1	Case 2	Case 3
Case On/Off		Check Box to Turn Case On	<input checked="" type="checkbox"/>	<input checked="" type="checkbox"/>	<input checked="" type="checkbox"/>
Case Label		Unique Text for Plot Legends			
SPEED	RPM		2225	2100.01001	2000
BMEP	bar		11.08650303	14.64741993	17.10928535
BoostPressure	bar		2.32655896	2.535138977	2.671228943
InjectionPressure	bar	Rail Pressure (InjectionRateMap only)	1750.640015	1905.880005	1937.939941
Fuel-Mass_pilot	mg	Injected Mass per Pulse	0	0	2.2
Fuel-Mass_main	mg		115.9076191	147.0424163	168.5763883
SOI_pilot	deg	Injection Timing	-30	-30	-21.2428371
SOI_main	deg	Injection Timing	-9.55260006	-9.215475816	-8.161099625
HC_conc		Unburned Fuel Concentration	43.09999847	38.70000076	45
CO_conc		CO Concentration	47.5	46.5	59
filename		Filename	<C11_FEP3_...	<C11_FEP3_...	<C11_FEP3_...
EGR_fr	fraction	EGR Fraction (Intake)	0.108358256	0.093633882	0.083349009
T_int_avg	K	Time-Averaged Temperature	312.8263	313.7524017	314.2059998
T_exh_avg	K	Time-Averaged Temperature	722.4825195	779.7519897	827.907019
discr_l_int	mm	Discretization Length	10	10	10

Fig. 57 – Parameters in Case Setup

An alternative is to take data directly from an external file. This operation can be very convenient if test cell data are provided in AVL IFiles, text format (ASCII) or Excel format. Also in this case, it is necessary to call a parameter that contains the external file, to have different values for each cycle. For crank angle resolved data, such as pressure traces, where data are provided as a function of crank angle, the upload using an external file is the best solution; the procedure depends on the external file's format [8]. If this file is an Excel file, the values to upload are stacked in rows or columns; to upload these values, an array is used, defined by file name, page name, column number and the number of rows to skip. Please see Fig. 58 for a correct usage of array.

CA	deg	Crank Angle	<validation_PressureShift.xlsx_traces#1#1#2#7201> ...	<validation_P... ...
Cyl_pressure	bar	Cylinder Pressure	<validation_PressureShift.xlsx#p_traces#2#2#2#7201> ...	<validation_P... ...
T_head	K	Head Temperature	541.1369 ...	571.95996 ...
T_pist	K	Piston Temperature	691.6442 ...	733.34827 ...
T_wall	K	Cylinder Tempera...	429.9818 ...	438.27878 ...
trapping_ratio		Air Trapping Ratio	1 ...	1 ...

Fig. 58 – Array usage for excel files reading

For external ASCII text files, same procedure. Instead, external AVL IFiles uses an appropriate template, 'IFile' template. This template (Fig. 59) requires the name of the external IFile containing pressure data, in 'Filename' object, the name of the channel for the pressure array, in 'Pressure Index' object, and a name to generate an external ASCII file based on pressure data, in 'Output File Name' object. Last line can be set to 'ign'. IFiles can be opened in MatLab software using an external tool called CaTool; this allows to see all the information stacked in the IFile, that usually are stacked in subfolders called "channels". Ifiles contain not only pressure traces obtained from a bench test, but several information on tested engine's performances and geometry. 'Ifile' template can be referenced from 'EngBurnRate' and 'EndEnvironmentTPA' objects for pressure analysis such as CPOA and TPA.

Main		
Attribute	Unit	Object Value
Filename		[filename] ...
Pressure Index		p_inlet1 ...
Output File Name		ign ...

Fig. 59 – Ifile template

Different input data formats give different simulation results; in this work will be analysed Excel and AVL IFile data format, to investigate the differences. Excel format is not usually used as bench test output, but for this work they have been provided by FPT in this format.

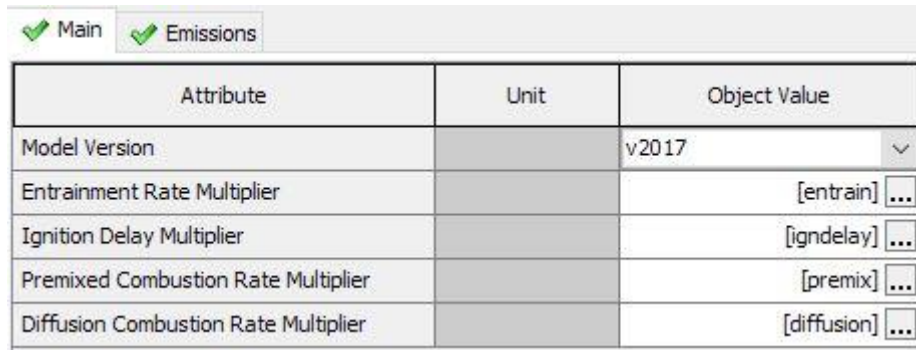
c. DI PULSE model calibration

Once CPOA and TPA results are available, the operative point that pass the consistency check can be used for DI Pulse model calibration. This model is a predictive multi-zone model able to predict the combustion process for diesel engine with single or multiple injection events per cycle. In this step of the work, is necessary to understand how some engine parameters affect the combustion burn rate, and this type of analysis is out of non-predictive model (CPOA, TPA) field, so a predictive model must be built. As express in section 5, GT POWER provides two predictive model for diesel engine, DI Pulse and DI-Jet, but the same GT POWER guide suggests always using the second one, because it is faster in the computational phase and sometimes the results are more accurate (sometimes because the quality of the results depends on input data quality) respect to the first one. Like for the Cylinder Pressure Only Analysis, DI Pulse calibration model was implemented on a single cylinder model, made by a cylinder block, an injector block, and a crank train block (see Fig. 45); this because DI Pulse performs a closed volume pressure analysis, so no gas-exchange is necessary. For simplicity, the same exact single cylinder model is recycled from CPOA, and on this model several changes have been made. First changes are on the cylinder block, the 'Cylinder Pressure Analysis Mode' object is set on Measured+Predicted, and a 'EngCylCombDI Pulse' template is used as 'Combustion Object' folder. This is the first big difference respect to a non-predictive model, in fact in CPOA the 'Combustion Object' is set on 'ign'. The calibration of DI Pulse Combustion Object consists of identifying a set of four parameters (described in section 5.2.2); these parameters are:

1. Entrainment Rate Multiplier
2. Ignition Delay Multiplier
3. Premixed Combustion Rate Multiplier
4. Diffusion Combustion Rate Multiplier

These allow to control crucial steps of the combustion process from the injection to the combustion end. In 'EngCylCombDI Pulse' template these multipliers must be defined using parameters, in this

way they can assume a different value for each case (see *Fig. 60*). These parameters cannot be empty, so they must be initialized with some values: GT POWER guide suggests initializing these multipliers with plausible values, such as the average of the extreme values of ranges listed in *Table 3* [8].



Attribute	Unit	Object Value
Model Version		v2017
Entrainment Rate Multiplier		[entrain] ...
Ignition Delay Multiplier		[igndelay] ...
Premixed Combustion Rate Multiplier		[premix] ...
Diffusion Combustion Rate Multiplier		[diffusion] ...

Fig. 60 – DI Pulse Main Template

GT POWER guide suggests typical range values (*Table 3*):

Multiplier	Min	Max
Entrainment Rate Multiplier	0.95	2.8
Ignition Delay Multiplier	0.3	1.7
Premixed Combustion Rate Multiplier	0.05	2.5
Diffusion Combustion Rate Multiplier	0.4	1.4

Table 3 – DI Pulse Multiplier Extreme values

The best possible set of these four multipliers can bring to a better match between the measured data set and the simulated match in terms of matching simulated and measured cylinder pressure, burn rate, IMEP, and so on. First step of DI Pulse calibration is a Run Optimization in order to find the best set of multipliers for every operating point (obviously by changing the operating point, change the set) [8]. An optimizer tool called ‘Direct Optimizer’ available in GT POWER is used in this phase: this optimizer finds an optimum output by varying one or more input parameters, defined by the user. This tool works by running an iteration process: the dependent variable is evaluated using the input parameters (independent variables), then using an intern algorithm new parameter values are updated, and the simulation starts again. This process is repeated until the best value is found under certain convergence criteria or until a maximum number of iterations is reached, this value can be imposed by the user. The choice of the dependent variable used to find the best match between measured and predicted burn rates is not so easy, because a lot of CaseRLT parameters can be used, however GT POWER suggests the ‘Improved Burn Rate RMS Error (Meas vs Pred)’, in ‘Pressure Analysis, Predicted’ folder. For this type of optimization, the Advanced Direct Optimizer (ADO) is used; the objective of the simulation must be set to ‘Minimize’. As explained above the *Improved Burn Rate RMS Error (Meas vs Pred)* parameter can be use as ‘Dependent Variable RLT’ object [8]. However, GT POWER guide suggests further checks on the average result error about three quantities: IMEP, maximum pressure, MFB50. These errors must be lower than a threshold, as visible in *Table 4*, and can be a further test to confirm the robustness of the model.

Parameter	Error limit
IMEP [%]	±5
Max pressure [bar]	±5
MFB50 [deg]	±2

Table 4 – Other must-checked quantities

For ‘Search Algorithm’ template GT POWER guide suggests a ‘Genetic Algorithm’ object and the subsequent folders filled as in *Fig. 61*.

Main Ind_Variables Constraints		
Attribute	Unit	Object Value
<input type="radio"/> OFF		
<input checked="" type="radio"/> Advanced Direct Optimizer		
<input type="radio"/> Simple Optimizer		
Number of Objectives		
<input checked="" type="radio"/> Single Objective		
<input type="radio"/> Multi-Objective (Pareto)		
Case Handling		
<input type="radio"/> Optimize Each Case Independently		
<input checked="" type="radio"/> Case Sweep and Cross-Case Studies		
Single Objective Setup		
Dependent Variable RLT		parmserr2br:Cylinder ...
Objective		Minimize v
Case Weighting		def (=1.0) ...
Search Algorithm		
Search Algorithm		Genetic Algorithm v
Population Size		30
Number of Generations		34
Show Genetic Algorithm Settings		<input checked="" type="checkbox"/>
Crossover Rate		def (=1.0) ...
Crossover Rate Distribution Index		def (=15.0) ...
Mutation Rate		0.5 ...
Mutation Rate Distribution Index		15 ...
Random Seed		def (=random) ...
Advanced Direct Optimizer Options		
Faster Runtime (Local Runs Only)		<input checked="" type="checkbox"/>
Maximum Number of Parallel Iterations		1
Timeout Duration (minutes)		60
Save Iteration Files?		<input type="checkbox"/>
Automatic Data Suppresion (Recommended)		<input checked="" type="checkbox"/>

Fig. 61 – Advanced Direct Optimizer Main Template

When the ‘Main template’ is ready, it is time to pass to define the independent variables in ‘Ind_Variables’ template. The independent variables are the multipliers of DI Pulse model: Entrainment Rate Multiplier, Ignition Delay Multiplier, Premixed Combustion Rate Multiplier, and Diffusion Combustion Rate Multiplier. Direct Optimizer tool allows two types for case handling:

- *Single-set or sweep optimization*: a single set of parameters for all the operation points.
- *Independent optimization*: every case has its own multipliers set.

In order to select one of these two options, 'Case Handling' folder must be set on *Sweep* for the first one, or on *Independent* for the second one. 'Case Handling' folder is available only if 'Case Sweep and Cross-Case Studies' box in *Main template* is checked; in order to perform an *independent* analysis, if GT POWER version is v2017, the box must be unchecked, while for previous versions *Case Handling* must be set on 'Independent'. Selecting *Sweep* option rather than *Independent* one, brings to a longer computation time to obtain the optimal values, because every parameter must be validated for each case. 'Lower Value of the Range' and 'Upper Value of the Range' folders must be filled with the listed values in *Table 3 (Fig. 62)* [8].

<div> <div>✓ Main</div> <div>✓ Ind_Variables</div> <div>✓ Constraints</div> </div>						
	Attribute	Unit	1	2	3	4
	Parameter to be Varied		entrain ...	igndelay ...	premix ...	diffusion ...
	Case Handling		Sweep ▾	Sweep ▾	Sweep ▾	Sweep ▾
<input type="radio"/>	Parameter Range					
<input checked="" type="radio"/>	Lower Value of the Range		0.95 ...	0.3 ...	0.05 ...	0.4 ...
	Upper Value of the Range		2.8 ...	1.7 ...	2.5 ...	1.4 ...

Fig. 62 – Independent Variables Template in ADO

In literature, a rule for the choice of the correct operating points number for DI Pulse calibration does not exist, it strongly depends on how much points pass the non-predictive model consistency check. Usually, using 50% of the total amount of valid operating points could be a correct choice. These points can be chosen totally random on the engine map, but for a better final result, the selected cases must cover as many different engine conditions as possible (high and low velocity, high and low charge). However, GT POWER guide suggests to performs calibrations, when it is possible, with an amount of at least 25 operating points; furthermore, using a large amount of points the computational time increases, so it is necessary to find a compromise. As it is possible to read in section 6.1 the operating points valid for CPOA consistency check are 125 on 152 available, so for DI Pulse calibration a variety of 64 points all over the engine map (*Fig. 76*), are chosen (51.2% of the total amount of points).

In this work, three different DI Pulse optimization approaches are simulated:

- **Sweep optimization for 64 operating points**: the optimization is performed in order to obtain a single set of multipliers for all the operative points.
- **Sweep optimization for 125 operating points**: like for the previous analysis, however the simulation is performed for all the points that pass non-predictive model consistency check. The output of this optimization will be only one set of multipliers, valid for all the cases.
- **Independent optimization for 125 operative points**: the optimization is performed in order to obtain a different set of multipliers for each of the 125 available operative points.

First two simulations provide a single set of multipliers valid for all cases, while the last optimization provides a set of multipliers for each used case. These simulations are running in parallel in order to understand how multiplier values' fluctuations affect the model behaviour. Furthermore, optimizing a single set of multipliers using both half operating points and all the operating points can be useful in order to understand if an optimization with more involved points can improve the multiplier values accuracy, or the added computational time (these simulations require a computational time in the order of the days, so doubling the operating points mean a very long computational time) is not worth.

Once the optimization work is done, a single set (in case of sweep opt.) or different sets once for each case (independent opt.), are obtained in order to minimize the *Improved Burn Rate RMS Error (Meas vs Pred) parameter* [8]. These values can now be used as input in the same model used for the optimization, in the defined parameters in Case Setup folder. Results of this simulation are available in GT-SUITE.

d. DI Pulse model validation

Once the calibration phase is ended, the correct multiplier values have been evaluated, so the DI Pulse is ready to be used. For the validation, the full engine model is used (*Fig. 14*), and the DI Pulse just calibrated is selected as Combustion Object in Cylinder block main folder, as visible in *Fig. 63*.

Main Advanced			
	Attribute	Unit	Object Value
	Initial State Object		Boost ...
<input checked="" type="radio"/>	Wall Temperature defined by Reference Object		Heat-Solver ...
<input type="radio"/>	Wall Temperature defined by FE Structure part ('EngCylSt...		
	Heat Transfer Object		Heat-Transfer ...
	Flow Object		Flow ...
	Combustion Object		DI-Pulse ...
	Measured Cylinder Pressure Analysis Object		ign ...
	Cylinder Pressure Analysis Mode	off	▼

Fig. 63 – Full Engine Model Cylinder Template for DI Pulse validation

Validation means to test the just calibrated combustion predictive model in order to verify its robustness by comparing the obtained results with the rig test data provided by FPT industries.

5. RESULTS DISCUSSION

In this section, both predictive and non-predictive combustion simulation results are illustrated.

7.1. CPOA results

Cylinder Pressure Only Analysis is the first non-predictive simulation done. Starting from a the only in-cylinder pressure trace, it allows to obtain the combustion burn rate. How to calibrate a single cylinder model is explained above step by step (in section 6.1.), so in this section results starting from different setup types are discussed. Since CPOA runs only two cycles for case, some input parameters values must be estimated for the first try. These parameters are air trapping ratio, combustion chamber walls temperature and in-cylinder residual gases fraction. When the model is totally built, simulation starts. Output of this simulation is an external file which contains the crank angle resolved combustion burn rate for each operating point; these burn rates are used as input in full model engine to obtain the true values of first try estimated parameters.

For the first try, the estimated values are:

- *Air Trapping Ratio*: this parameter is usually near to the unity, so for the first try it can be set to one.
- *Combustion chamber walls temperature*: for this purpose, combustion chamber is divided in head, piston and wall and their temperatures are estimated separately, because during combustion stroke not all the combustion chamber reaches the same temperature. The used values for the first attempt are showed in *Table 2*.
- *Residual Gases Fraction*: for this parameter GT POWER guide suggests a value 3-4% higher than EGR fraction value, that is usually provided by a bench test.

This iterative process is repeated until air trapping ratio, cylinder walls temperature and residual gases fraction values reach a constant trend, i.e., the error of a parameter value in two subsequent attempts is lower than 1-2%. Once the iterative process converges, it is time to observe the consistency check. This consistency check is automatically generated by CPOA simulation in 'Pressure Analysis, Measured' folder in CaseRLT template. *Fig. 64* shows the results for each operating point in the engine map: the green ones are the cases that respect all the checks while the red ones do not pass one, or more, checks. Please see section 6.1. for all the check performed during the simulation process.

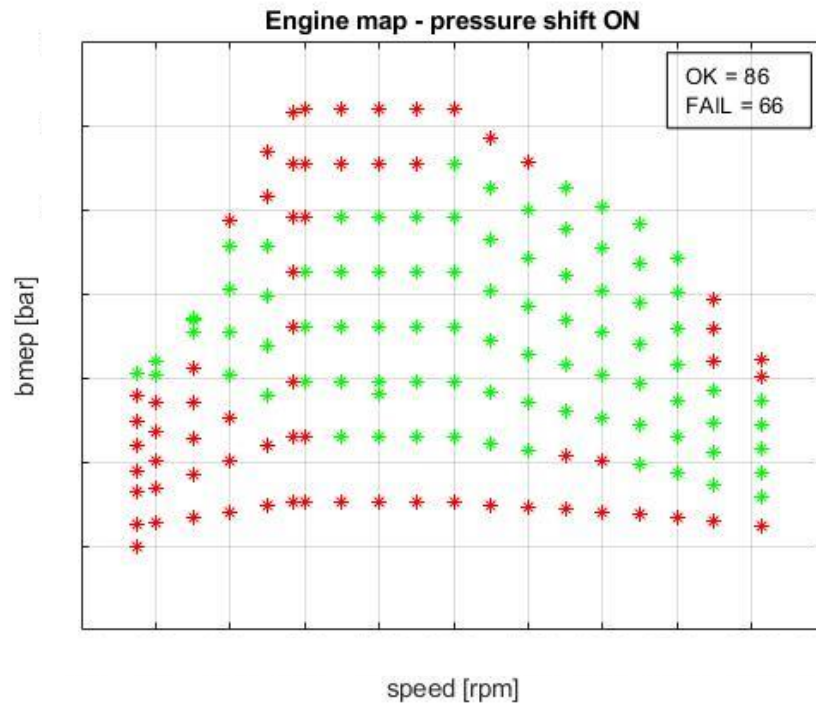
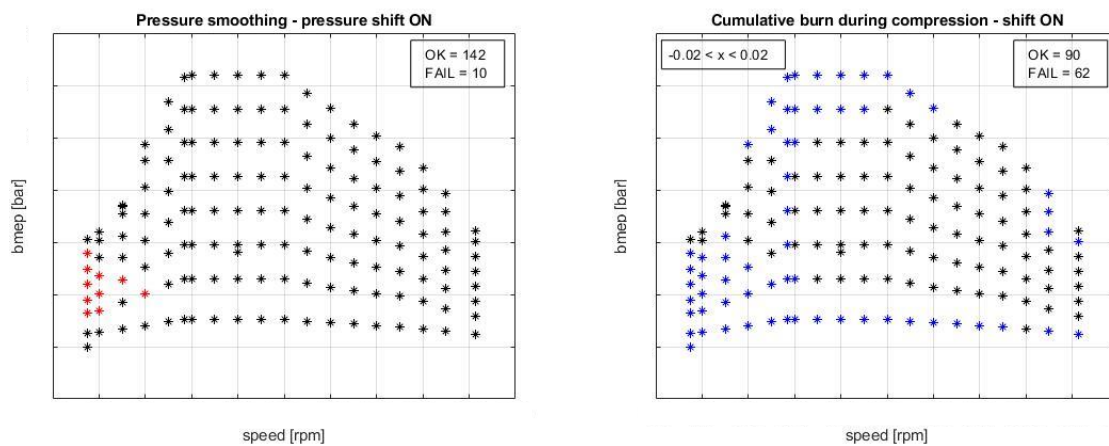


Fig. 64 – Engine map showing cases that pass the Consistency Check

On 152 operating points, 66 of these do not pass the burn rate input data consistency check: observing the engine map it is possible to note that a big part of the points that do not pass the C.C. are located at high load and at low load.

Consistency check is a useful tool to understand which engine operating points can be used for the next DI Pulse calibration process and which presents several errors in input data. However, consistency check does not investigate the source of error. So, each red point on the engine map in Fig. 64, needs a thorough analysis to find the parameter, or the parameters, that exceeds the limit imposed by GT POWER; this analysis is made on all checks made by consistency check listed in section 6.1. Fig. 65 a)b)c)d)e)f)g)h), show all the parameters involved in consistency check.



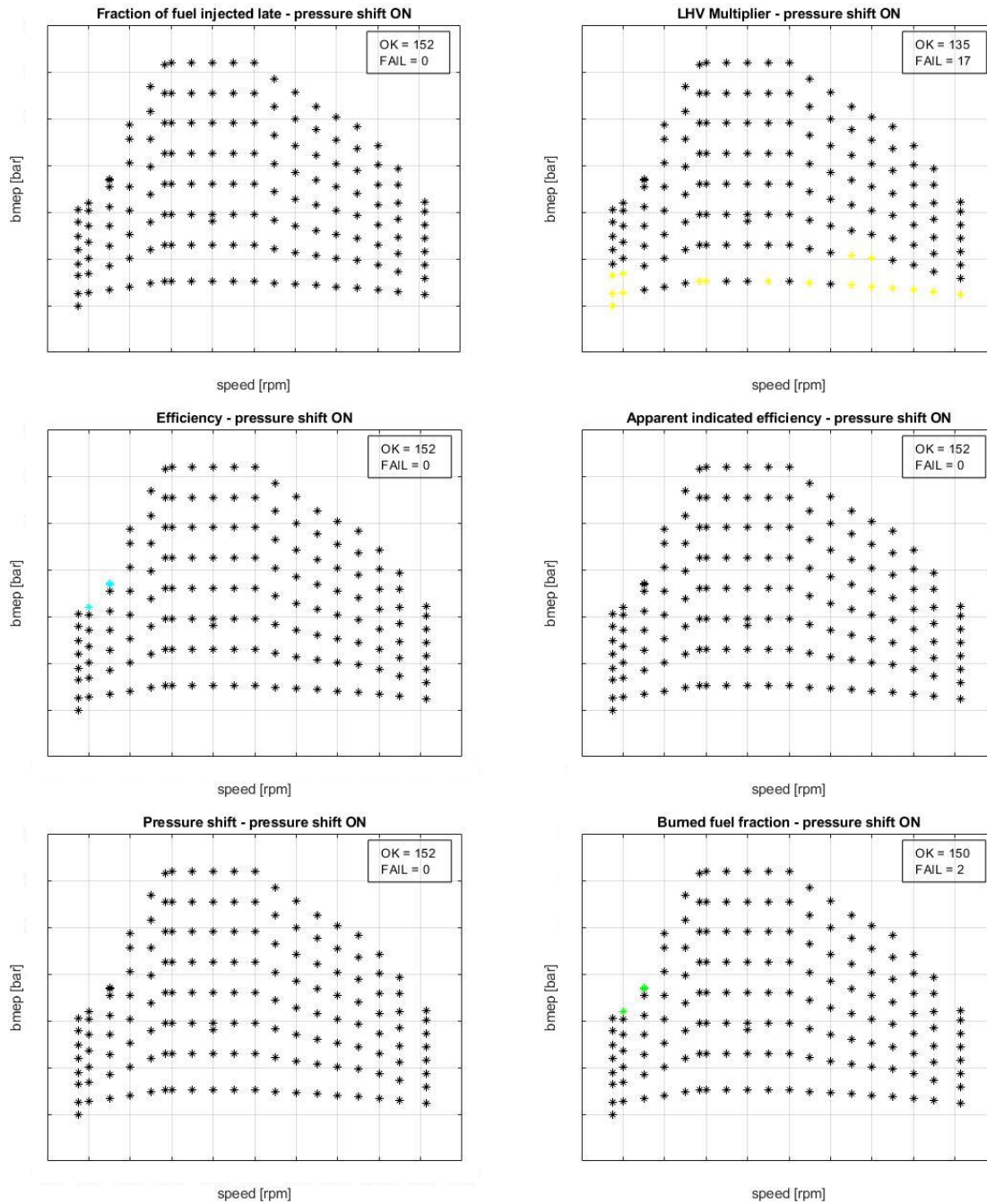


Fig. 65 - Consistency Check a) Pressure smoothing b) Cumulating Burn During Compression c) Fraction of Fuel Injected Late d) LHV Multiplier e) Combustion Efficiency f) Apparent Indicated Efficiency g) Pressure Shift h) Burned fuel fraction

These diagrams show the source of the errors. In particular, most of the errors are due to Cumulative Burn during compression (62) and a part to LHV multiplier (17). LHV multiplier errors mean that during the simulation, GT-Power had to make some adjustments to the fuel energy content in order to match the predicted fuel burned to the measured one. In case of big mismatch between measured and predicted, the request adjustment is bigger, and so the LHV is: consequently, if LHV multiplier is too big (or too low) the consistency check marks the case as not valid (red light). Beyond LHV Multiplier, the main part of the errors is due to Cumulative Burn during compression: this parameter indicates the amount of energy released during the compression before the combustion begins. In a combustion chamber during the injection and the compression stroke there should not

be energy released, so even a little amount of released energy in this phase is considered by GT Power as an error. It is important to report that the thresholds used in every check are provided in GT POWER Guide, and even if according to these thresholds some cases do not pass the check, in *Fig. 64* these cases are then signed with green light, they have passed the final cumulative consistency check. This because not all the checks have the same weight on the consistency check, some parameters are necessary to the final validation, while others are just warnings. On 152 available operating case, nearly half of the available points do not pass the consistency check: this is a signal that there is something wrong in the input data. However, consistency check is useful to flag a potential problems, but it is not able to indicate the source of this problem. As discussed in section 4.a, the most common problems detectable in input data are:

- Incorrect pressure phasing
- Incorrect gauge pressure
- Incorrect compression ratio

For errors linked with an incorrect pressure phasing, section 4 is totally dedicated to find the correct TDC position. However, CPOA model is performed for both pressure traces (no shift and a correct shift = $+0,2^\circ$ degrees) in order to obtain a further confirm about the shift value. *Fig. 66* shows the engine map for both the consistency checks.

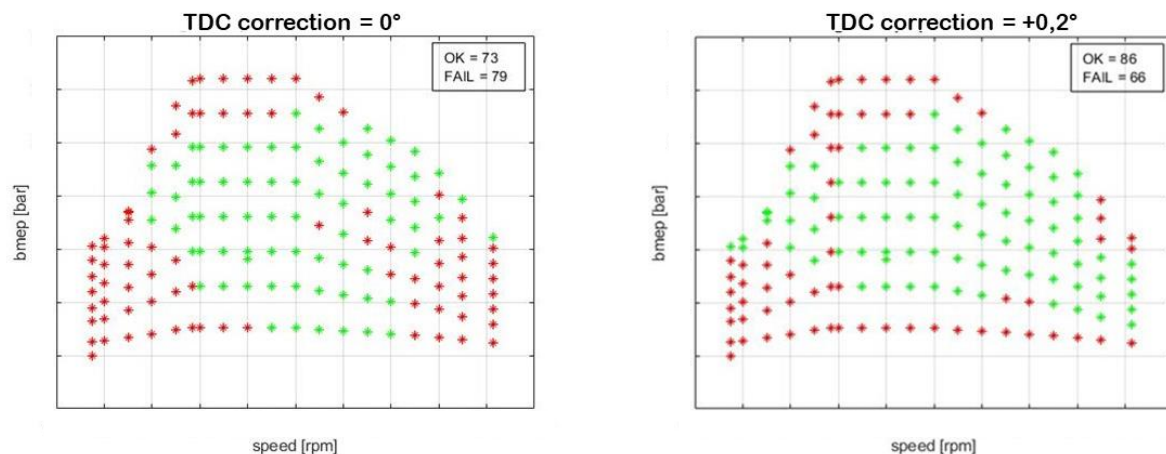


Fig. 66 – CPOA comparison results a) Pressure Shift=0° b) Pressure Shift=+0,2°

This comparison shows that the correct pressure trace (TDC correction = $+0,2^\circ$) provides better results with respect to the old pressure trace (no shift): in fact by observing the consistency check map for both the pressure signal, the one obtained with the correct pressure signal presents more valid operating points (86 on 152) with respect to the one obtained from the old pressure signal with 'only' 73 valid cases on 152. This is a further confirm of what has been done in chapter 4.

Regarding incorrect gauge pressure, errors can be made during the pressure measurement, especially during the conversion from measured signal (in volt) to pressure signal: by choosing an incorrect reference or 'gauge' pressure value, the whole signal can be wrongly shifted up or down by the amount of the error. An easy way to find if the pressure signal has been shifted correctly is to evaluate the polytropic exponent during the initial part of the compression process, between -90

and -40 degrees BFTDC, and verify that this value is in the range 1,35 to 1,37 [13]. However, this index is affected by dilution, so in engine where EGR is used this range is shifted vertically upward according to the amount of the recirculation fraction. Polytropic exponent is evaluated by using formula (45):

$$n = \frac{\ln p_{cyl}(\vartheta_i) - \ln p_{cyl}(\vartheta_{i+1})}{\ln V_{cyl}(\vartheta_{i+1}) - \ln V_{cyl}(\vartheta_i)} \quad (45)$$

These values are reported in *Fig. 67*.

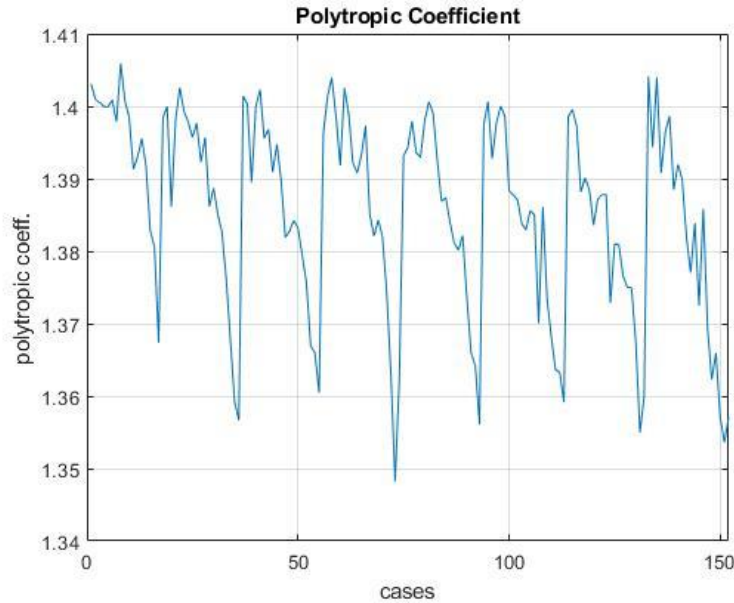


Fig. 67 – Polytropic Coefficient for each used operating point

The considered 152 operating points work with EGR fraction that fluctuate from a few percentage points to about 15%, so the range must be shifted. *Fig. 67* shows that the polytropic coefficients for each case, and it is visible that these values oscillate between 1,35 and 1,41, consistently with the presence of EGR dilution in combustion chamber [13]. So, it is possible to affirm that no errors occur due to an incorrect gauge pressure evaluation.

The last analysis concerns the compression ratio selected for the tests: the geometric compression ratio of an engine is constant for each cycle; however its value can change due to tolerances and inaccuracies that affect the engine components. Furthermore, the geometric value is constant for each condition, the dynamic compression ratio changes with load and speed. So, it is necessary to check the correct C.R. value in order to obtain consistent results. A simple way to evaluate the correct C.R. for each cycle is to iterate its value in order to get a good match between simulated and measured pressure traces in a CPOA or TPA simulation: in particular, these pressure traces must match during all the compression stroke until the SOI. In the same way, the LogP – LogV diagram can be checked in order to find the best case in which simulated and measured traces overlap the compression curve most accurately. Furthermore, since a wrong compression ratio value brings to several errors in model output, these outputs can be used as a flag in order to understand if the iteration process works: in particular, in CPOA analysis a wrong C.R. value strongly affects

Cumulative Burn During Compression parameter, which in the previous consistency check represents the most common error, by invalidating 67 cases on 152. So, the iteration process is performed in order to minimize the *Cumulative Burn During Compression* error. So, three cases at different operating conditions are selected on the engine map (Fig. 68) in order to show how a C.R. change affects the pressure trends.

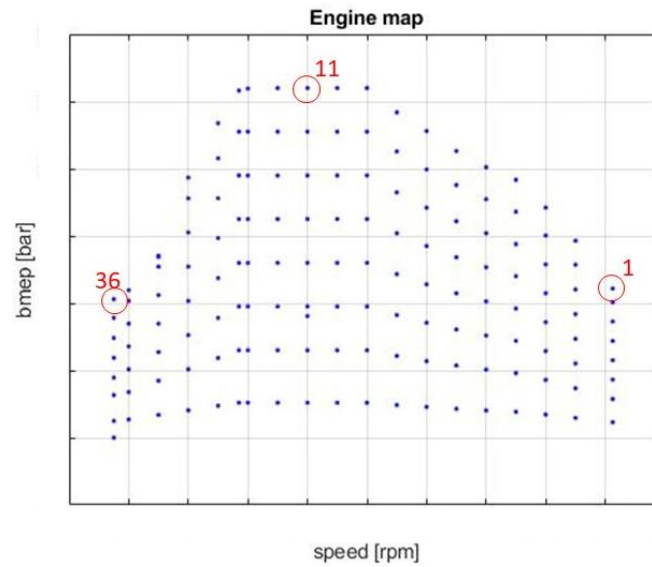
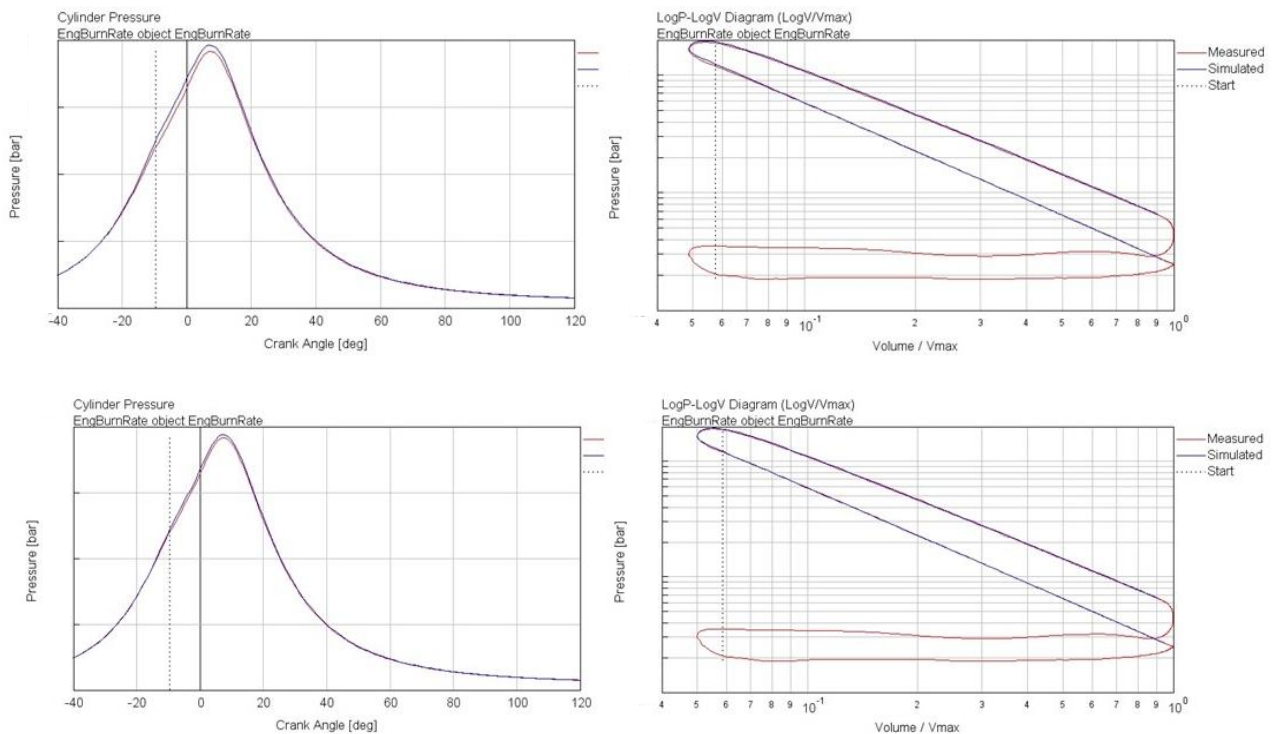


Fig. 68 – Selected cases for C.R. variation effects



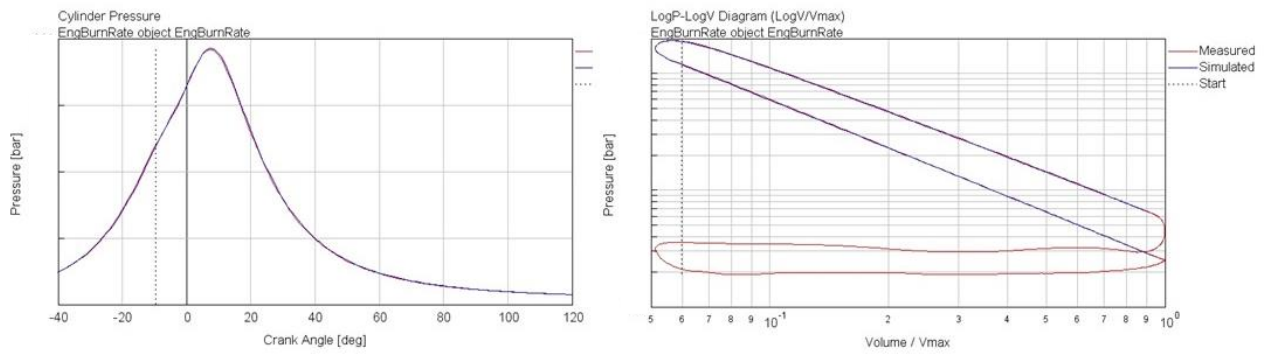


Fig. 69 – Case 1 (2200x11) results a) C.R.=20,5 b) C.R.=20 c) C.R.=19,5

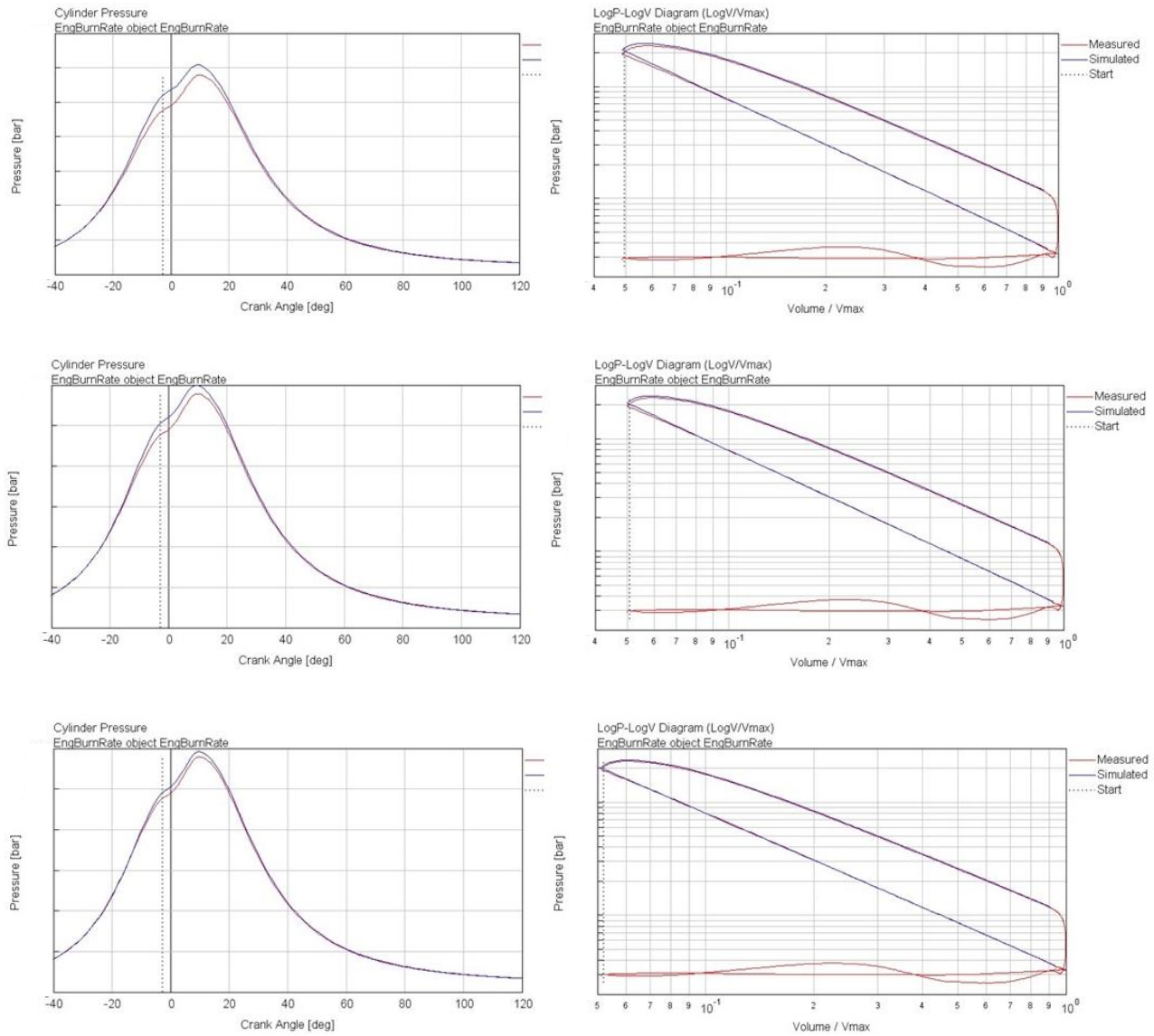


Fig. 70 – Case 11 (1200x26) results a) C.R.=20,5 b) C.R.=20 c) C.R.=19,5

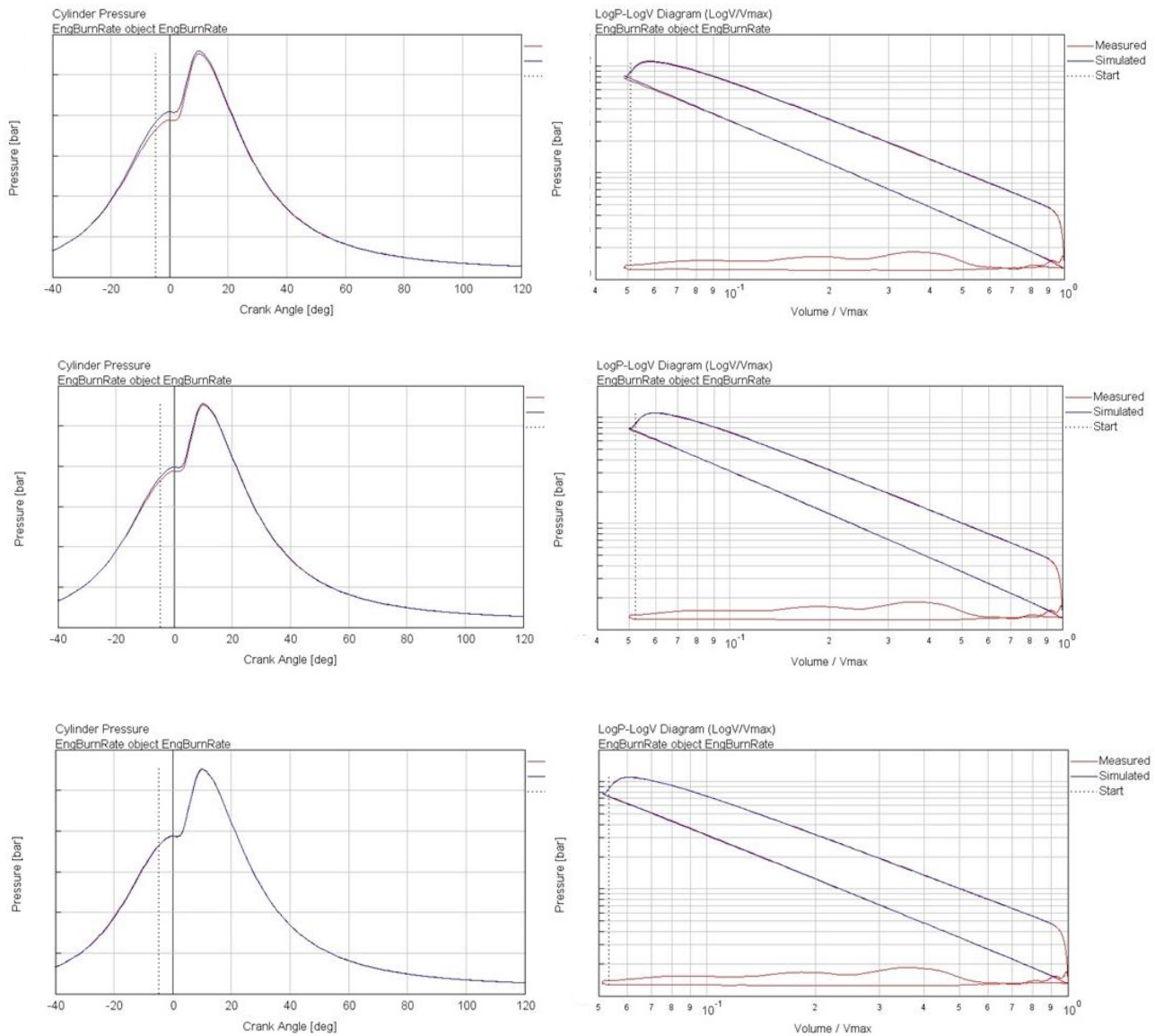


Fig. 71 – Case 36 (550x10) results a) C.R.=20,5 b) C.R.=20 c) C.R.=19,5

Each case is plotted using three compression ratio, starting from the blueprint one (20,5) and decreasing by 0,5 per each iteration step, for a total of three iterations. Observing these figures it is possible to note that step by step the gap between measured and simulated pressure traces in the compression stroke until the SOI (vertical dotted line) decreases until it almost disappears; the same behaviour can be observed in the Log P – Log V diagram where at the end of the iteration process the compression stroke of both curves are totally overlapped. In order to have a numerical feedback, Table 5 shows how the *Cumulative Burn During Compression* value decreases with the compression ratio.

	C.R. = 20,5	C.R. = 20	C.R. = 19,5
2200 x 11 (1)	-0,026	-0,013	0,0029
1200 x 26 (11)	-0,038	-0,027	-0,015
550 x 10 (36)	-0,016	-0,008	7,94e-04

Table 5 – Cumulative Burn During Compression values at C.R. changing

Remembering that GT POWER considers error for values that are not included in the range -0,002 to 0,002, the table shows how, by decreasing the C.R. value, the error disappears for all the reported cases, obtaining a parameter value near to zero. Table shows only three cases, but this iterative process must be conducted for all the available operating cases. Then the final compression ratio is represented by an average of all the obtained value. The figures reported above show only iterations by reducing the C.R. value, however the same process must be done by increasing this value, because a priori is not known if the used C.R. value is underestimated or overestimated. Finally, with the correct C.R. value the CPOA is performed in order to analyse the consistency check results.

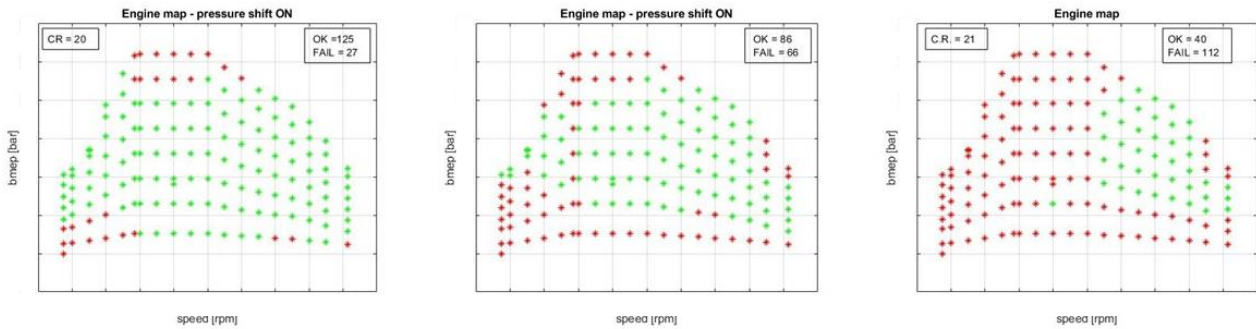


Fig. 72 – CPOA Consistency Check results with different C.R. a) C.R.=20 b) C.R.=20,5 c) C.R.=21

Fig. 72 shows the consistency check for three different compression ratio values. It is clearly visible how increasing the current C.R. value is not worth, because the actual number of valid cases goes down from 86 to barely 40. Vice versa, there is a substantial improvement in the consistency check by reducing the C.R. value by just 0,5 points, passing from 86 to 125 valid cases. The reason of this improvement is that with a compression ratio equal to 20 the *Cumulative Burn During Compression* value for many cycles re-enters in the valid range, like explained above, allowing the consistency check overcoming.

Finally, in order to complete the analysis, a last case has been evaluated, by setting C.R. equal to 20, but using the old pressure trace, the original one without the shift: a crossed analysis can be useful in order to understand how the pressure shift and the C.R. value affect each other.

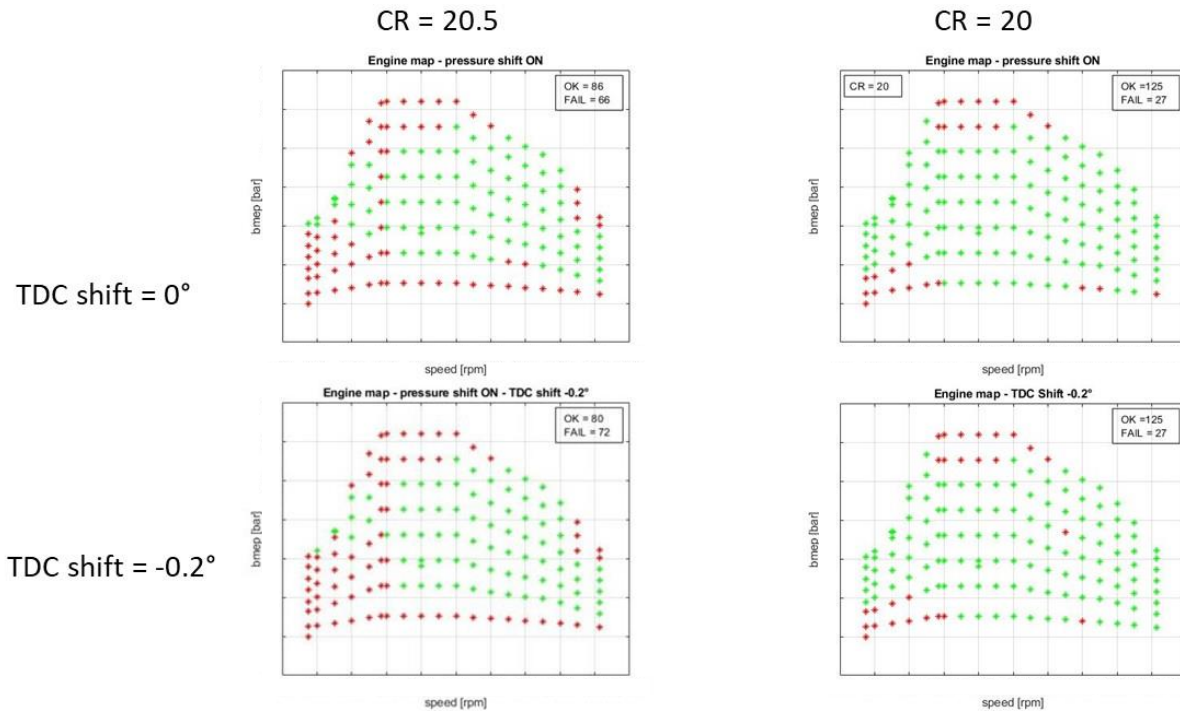


Fig. 73 – CPOA Consistency Check crossed analysis

Comparing results in Fig. 73 it is visible that the two phenomena are completely decoupled: pressure shift does not affect the consistency check results, in fact about the same results came from simulations starting from two different pressure traces. Vice versa, different compression ratios seem to strongly affect the results, by increasing a lot the number of available points for the next DI Pulse calibration step.

a. TPA results

Beyond CPOA, GT POWER provides a further non-predictive model that allows to evaluate the combustion burn rate starting from a pressure signal: TPA. Three Pressure Analysis (TPA), like the name suggests, is a little bit more complex with respect to the CPOA, because beyond the in-cylinder pressure trace it also requires intake and exhaust pressure traces. These signals are not always measured in rig tests, so when they are not provided TPA is not available and CPOA must be performed. In this case these signals are provided, so this model can be built. The advantages of Three Pressure Analysis with respect to the Cylinder Pressure Only Analysis is in the simulation process: CPOA performs just a single cycle in a single cylinder model composed by a cylinder, the crank train, and the injector, so some quantities such as the air trapping ratio, the cylinder's wall temperature and the residual gases fraction must be estimated for the first try and then evaluated with an iteration process. Instead TPA performs several cycles for each case in a more complex model, that in addition to the single cylinder model also includes intake and exhaust manifold (whole or part of the full model engine), so these above-mentioned quantities can be evaluated during the simulation process, avoiding the iteration process: in this way the results can be obtained in one shot. TPA and CPOA are two different methods that lead to obtain the same results: in this work TPA is performed in order to verify and confirm what obtained in CPOA and discussed in the previous section.

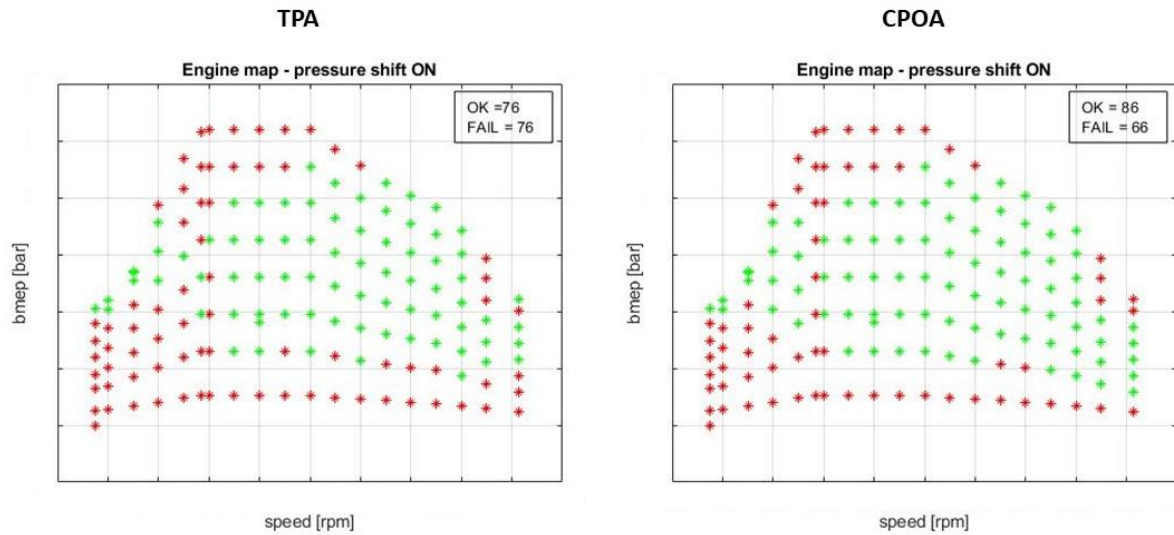


Fig. 74 – Comparing TPA and CPOA results

Fig. 74 a) shows the consistency check of Three Pressure Analysis using a C.R. equal to 20,5. Comparing these results with the ones obtained in CPOA (Fig. 74 b)), with the same boundary conditions, it is clearly visible that these are completely comparable. Even if with the CPOA more points pass the consistency check, 86 with respect to the 76 of the TPA, the two engine maps are very similar and the red zones are practically the same: the 10 operating points of difference between the two approaches might depend on different settings in model's setup, anyway the results are satisfactory. In the previous section it has been founded that the correct C.R. is 20 rather than 20,5, so also for TPA is performed an analysis by using this correct value.

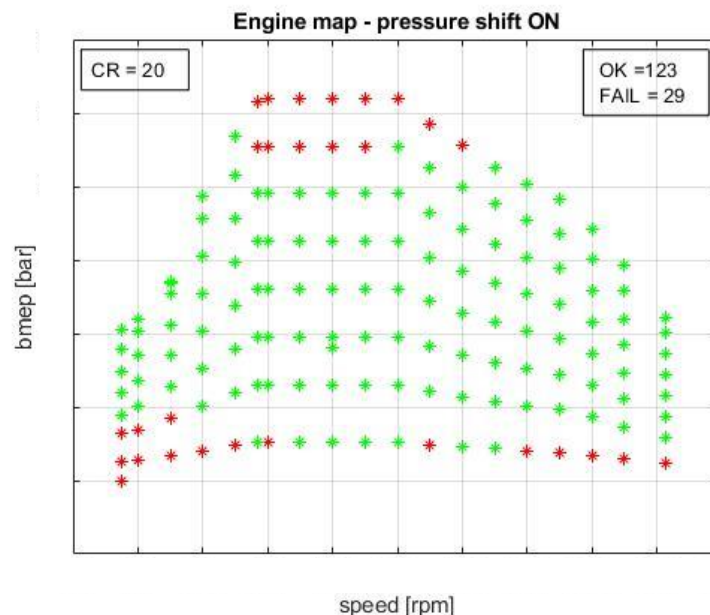


Fig. 75 – TPA results with C.R.=20

The obtained results showed in Fig. 75 confirms how said previously, in fact by using a C.R. of 20 the operating points that are able to pass the consistency check increase significantly, reaching a value of 123 on 152, very similar to CPOA results, where the valid points are 125 (Fig. 72 a)).

From these results it is possible to affirm that CPOA and TPA are two different methods that allows to obtain consistent results in both cases. It is not possible to say firstly what non-predictive model is the best, because they run in parallel and depend on which data are provided from rig tests: CPOA is the simplest model, it can be built in few minutes and does not request particular input data. However, the iteration method requested in order to evaluate the estimated values that the model is not able to calculate, can extend the effective computational time requested to obtain correct results. TPA, on the other hand, requests a more complex model and a better knowledge of GT POWER using, because, for example, in this model new blocks are introduced for the first time (TPAEndEnvironment). However, once that the model is correctly setup, it returns the final results in a single simulation, because this approach does not need the iteration process. The main drawback of Three Pressure analysis is that usually the intake and exhaust pressure traces are not provided for each cycle, so this type of analysis cannot be used.

The operating points that pass the consistency check, are now ready to be used for the calibration of the DI Pulse predictive combustion model.

b. DI Pulse calibration results

In order to obtain a valid DI Pulse combustion model, the DI Pulse calibration process is divided in two subsequent steps:

- Calibration of the model.
- Validation of the model.

The calibration step is made using GT POWER Advanced Direct Optimizer tool on a single cylinder engine model, that allows to obtain the best set of DI Pulse parameters, minimizing the error on *Improved Burn Rate RMS Error (Meas vs Pred) parameter*. The calibration can be made in order to obtain a single set of multipliers valid for all the cases, or different sets of multipliers, one for each case. In this work, three different calibration processes are considered, in order to find the best fit and test the model robustness: in fact, obtaining similar results in different simulations means that the model is very flexible and well adapts to different operating conditions. But, before starting with the results' analysis, it is necessary to chase the correct case number to considerate for the calibration. Like said in section 4.c, there is not a correct number of points to use for the calibration, this can be randomly chase; in fact, once that an operating point passes the consistency check, it can be used in the DI Pulse model calibration. GT POWER suggests using at least 25 points. On 152 operating points provided by FPT (*Fig. 17*) and tested in the non-predictive model, 125 among these correctly pass the consistency check with no errors; in literature, usually half of the total amount of points is used for the validation, in order to leave a consistent number of points for the subsequent validation. So, on 125 available operating points, 64 points are chosen for the DI Pulse predictive model, paying attention to take points across the whole engine map in order to cover all the operating conditions of the engine. *Fig. 76* shows the engine map with the 64 chosen points.

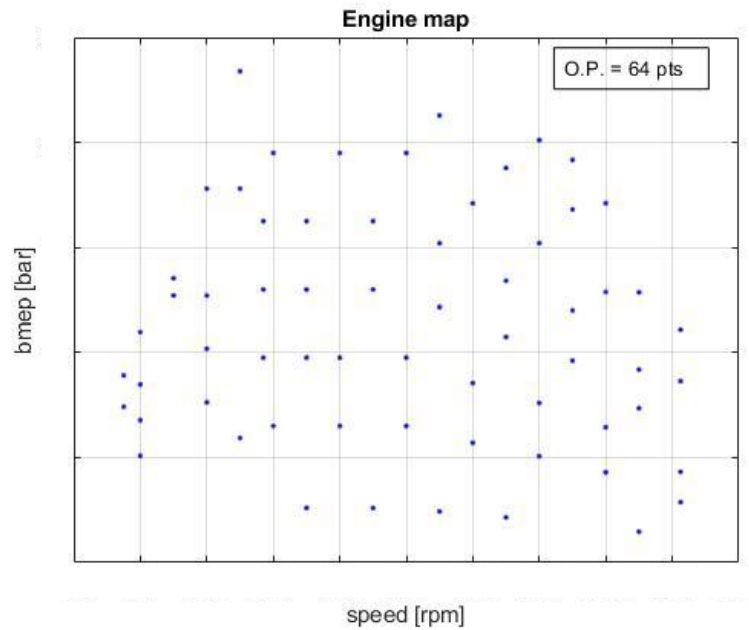


Fig. 76 – Operating points used for DI Pulse calibration

The three calibration methods proposed in this work are:

- **Sweep optimization for 64 operating points:** the optimization is performed in order to obtain a single set of multipliers valid for all the operating points.
- **Sweep optimization for 125 operating points:** like for the previous analysis, however the simulation is performed for all the points that pass non-predictive model consistency check. The output of this optimization will be only one set of multipliers, valid for all the cases.
- **Independent optimization for 125 operative points:** the optimization is performed in order to obtain a different set of multipliers for each of the 125 available operative points.

Other information of how these settings work is available in section 4.c. Below, the results of these analysis are discussed.

i. Sweep optimization for 64 operating points

This optimization process allows to obtain a single set of multipliers, valid for all the operating points. *Table 6* shows the results.

Multiplier set – 64 sweep	
Entrainment Rate Multiplier	1,5915
Ignition Delay Multiplier	0,3598
Premixed Combustion Rate Multiplier	0,8812
Diffusion Combustion Rate Multiplier	0,6347

Table 6 – Set of Multipliers obtained with a sweep optimization on 64 points

The optimization target was to obtain the best set of multipliers in order to minimize the *Improved Burn Rate RMS Error (Meas vs Pred)* parameter, which represents how much the predicted burn rate departs from the measured one. Fig. 77 shows this parameter's trend.

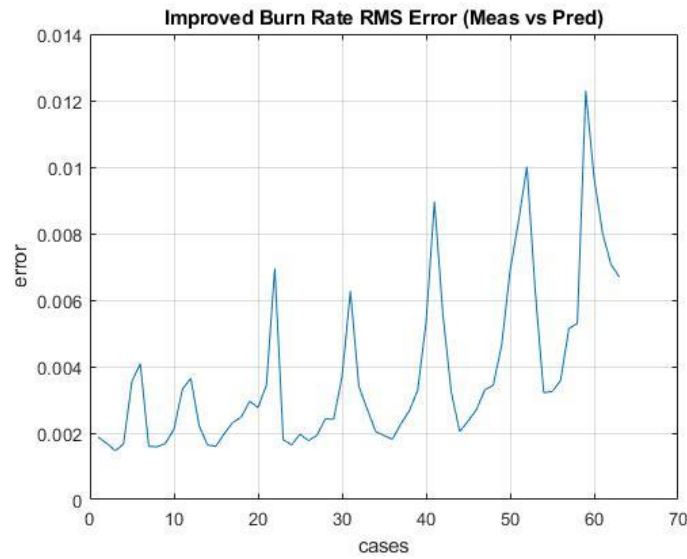


Fig. 77 – Improved Burn Rate RMS Error (Meas vs Pred)

Fig. 78 a)b) show the in-cylinder pressure traces and the burn rates obtained in the best case, the one with the lower error (Fig. 78 c)d)) and in the worst case, the case with the higher RMSE.

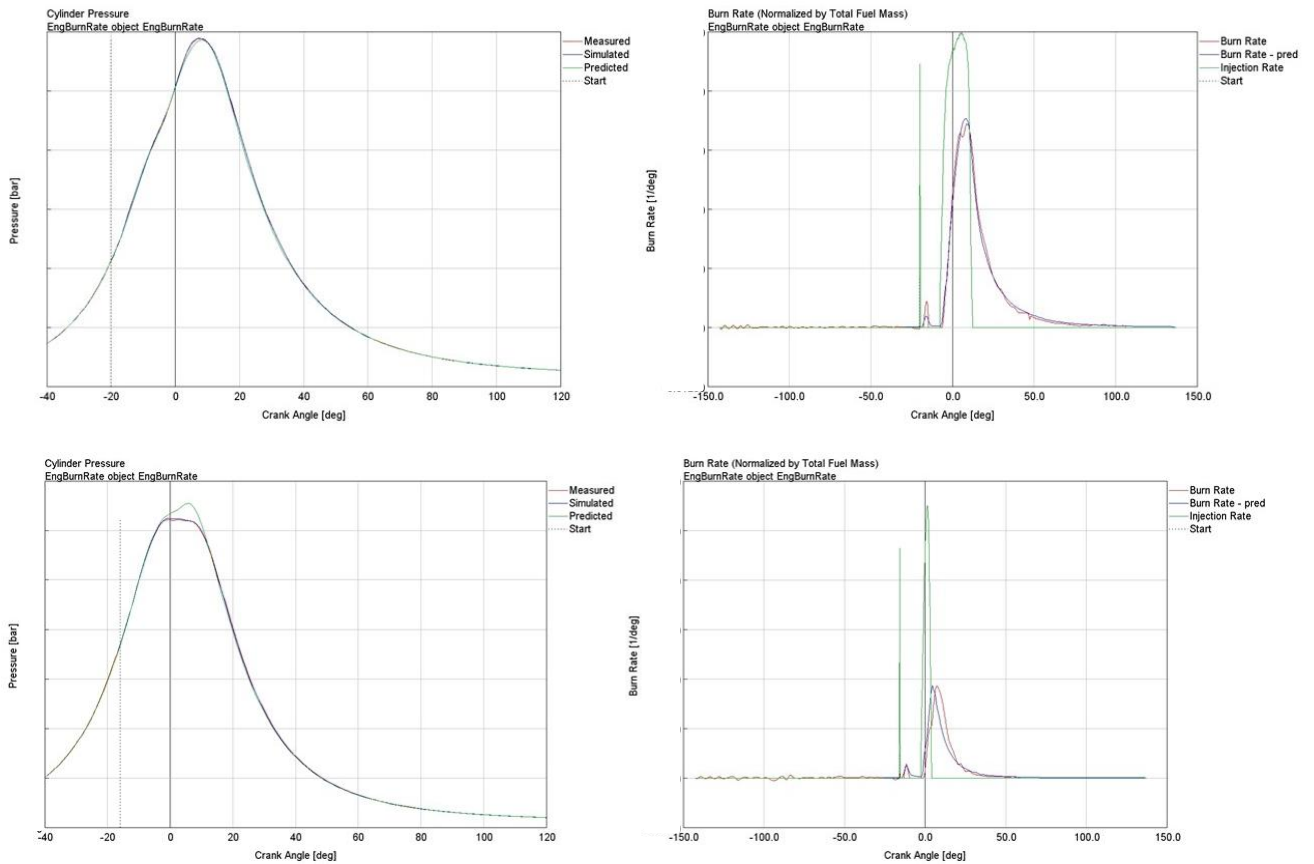


Fig. 78 – a) Pressure trends for the best case b) Burn Rate for the best case c) Pressure trends for the worst case d) Burn Rate for the worst case

Observing these figures, the source of error is clearly visible, in fact observing the worst case burn rates (*Fig. 78 c)d*), the predicted and the measured (respectively blue and red curves) curves are similar in shape, but they are not correctly phased, the predicted one is in advance with respect to the measured one, and this angular distance leads to a higher RMS error; furthermore, this discrepancy is also visible in the in-cylinder pressure traces (*Fig. 78 c*)), where the predicted one reaches higher value near its maximum with respect to the simulated and the measured ones. While for the best case (*Fig. 78 b*)), the burn rates are practically overlapped, lead to a lower RMS error.

Like suggested by the GT POWER Guide, further verifications on other combustion parameters are required, such as IMEP, MFB50 and maximum pressure, in order to check the presence of any anomalies in the calibration process results. For the IMEP, the error between the simulated and the predicted values is plotted in *Fig. 79*.

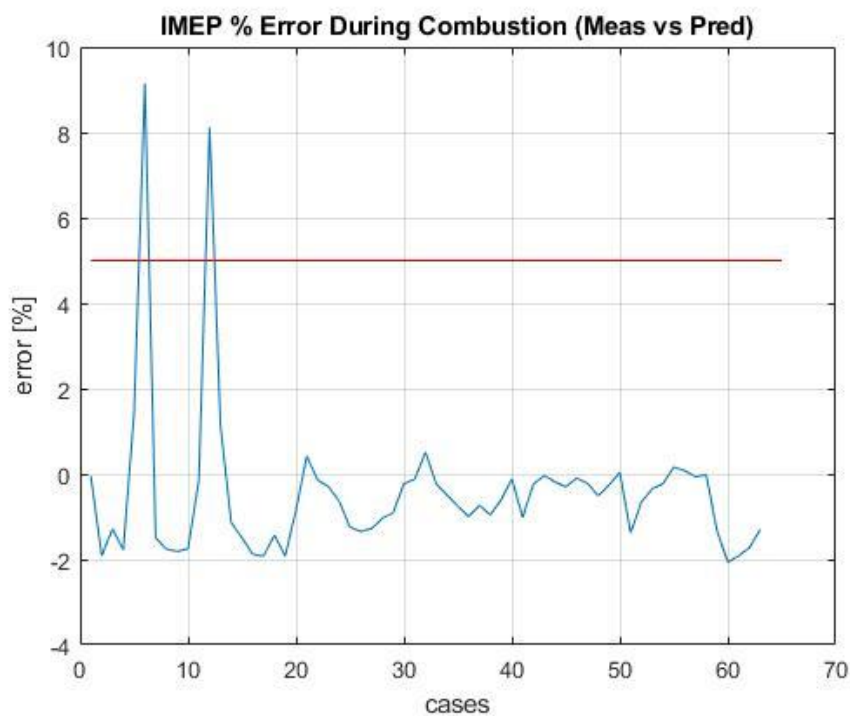


Fig. 79 – IMEP % Error During Combustion (Meas vs Pred)

The IMEP variation must be within the recommended limits $\pm 5\%$. In this case, only two cases have an error bigger than 5%. For the MFB50, the recommended limit is $\pm 2^\circ$ degrees; *Fig. 80* shows that no points exceed these limits.

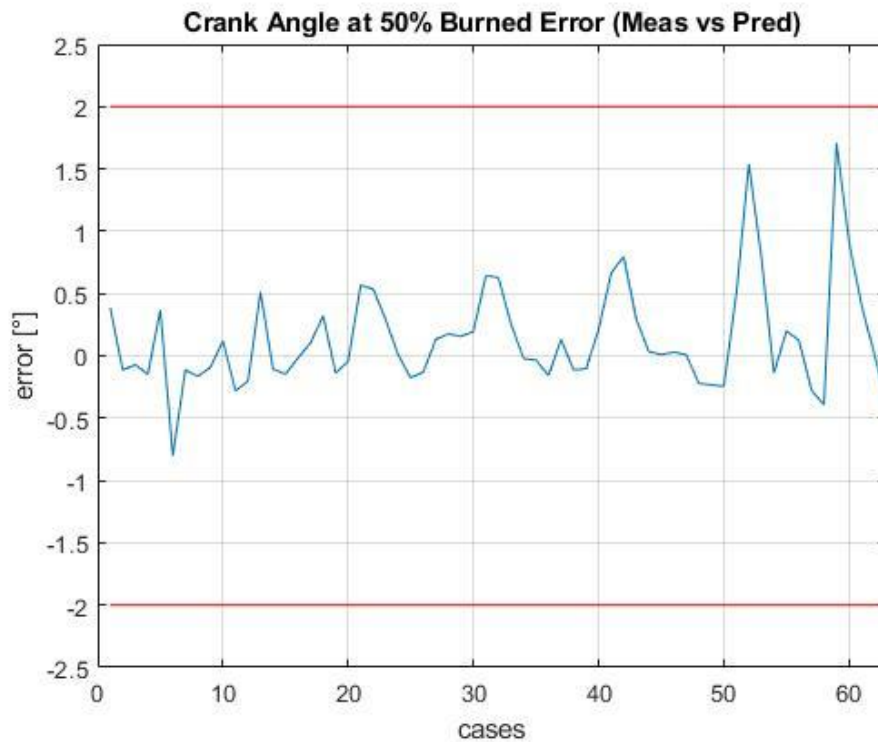


Fig. 80 – Crank Angle at 50% Burned Error (Meas vs Pred)

While for the maximum pressure the error between predicted and measured must be included in the range ± 5 bar (Fig. 81).

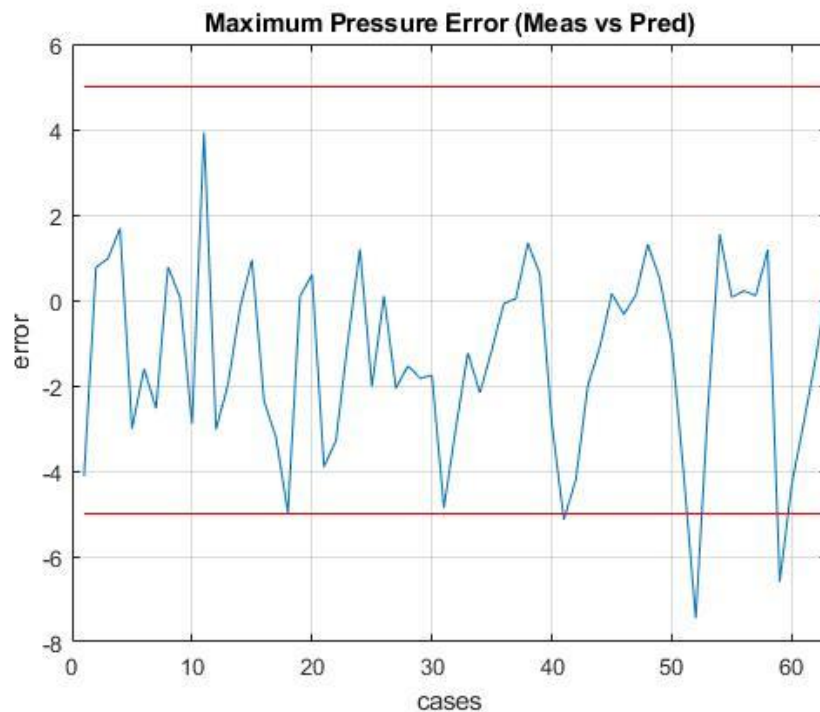


Fig. 81 – Maximum Pressure Error (Meas vs Pred)

Also, for this parameter, not all the points used for the calibration respect the imposed limit, in particular three operating points present an error bigger than five bars case (case 41, case 52, case 58).

It is interesting to understand why these operating points are affected by errors. *Table 7* shows the engine speed and the charge for each out-of-boundary case.

Op. conditions	BMEP [bar]	Speed [rpm]
6	13.53	700
12	10.97	600
41	5.94	550
52	3.67	2100
59	1.72	2000

Table 7 – Out-of-Boundary points

The first three points present a low engine speed at a middle load, while the last two points present high speed but at a low load. *Fig. 82 a)b)c)d)* show respectively case 12 and case 59.

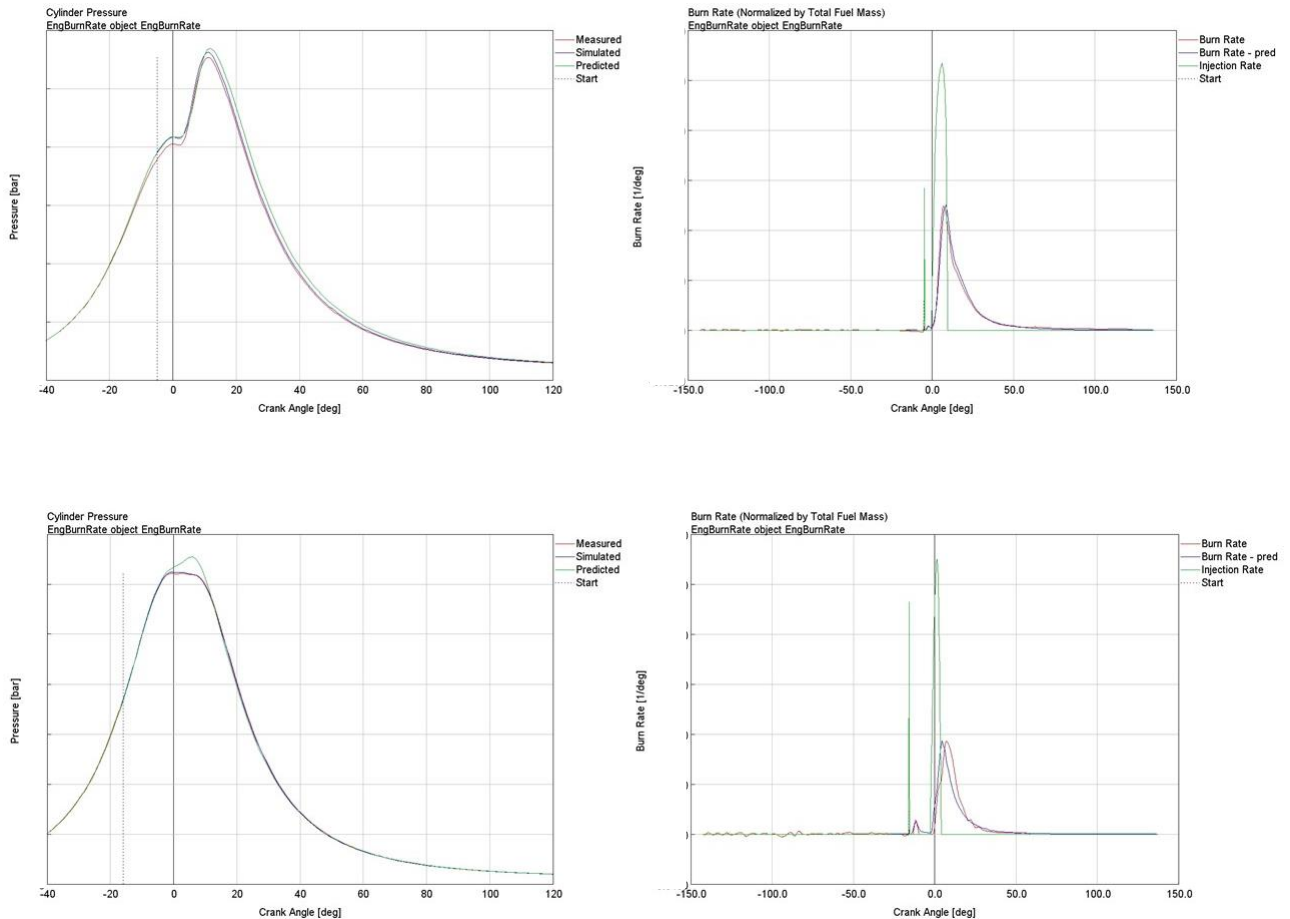


Fig. 82 – a) Pressure traces Case 12 b) Burn Rate Case 12 c) Pressure Traces Case 59 d) Burn Rate Case 59

Observing these data and expanding the analysis at the whole data set used for the calibration, it is not possible to find a correlation between the error and the operating condition at which the engine is running, this because beyond speed and load other parameters (boost pressure, EGR fraction, etc.) strongly influence the in-cylinder pressure trend and the heat exchange between gas and chamber's walls. Furthermore, these errors occur at limit operating conditions

(i.e., low load or low speed) where the combustion process is affected by many variables, so they can be considered isolated errors.

ii. Independent optimization for 125 operating points

Independent optimization allows to obtain a different set of multipliers for each case. Also in this case, the chosen parameter to minimize is the *Improved Burn Rate RMS Error (Meas vs Pred) parameter*, however in the independent optimization the output sets of multipliers are obtained with a higher accuracy, because every set fits the best for each case, with respect to a sweep optimization where the unique set must be the best compromise between the various operating conditions (*Fig. 83 a)b)c)d)*).

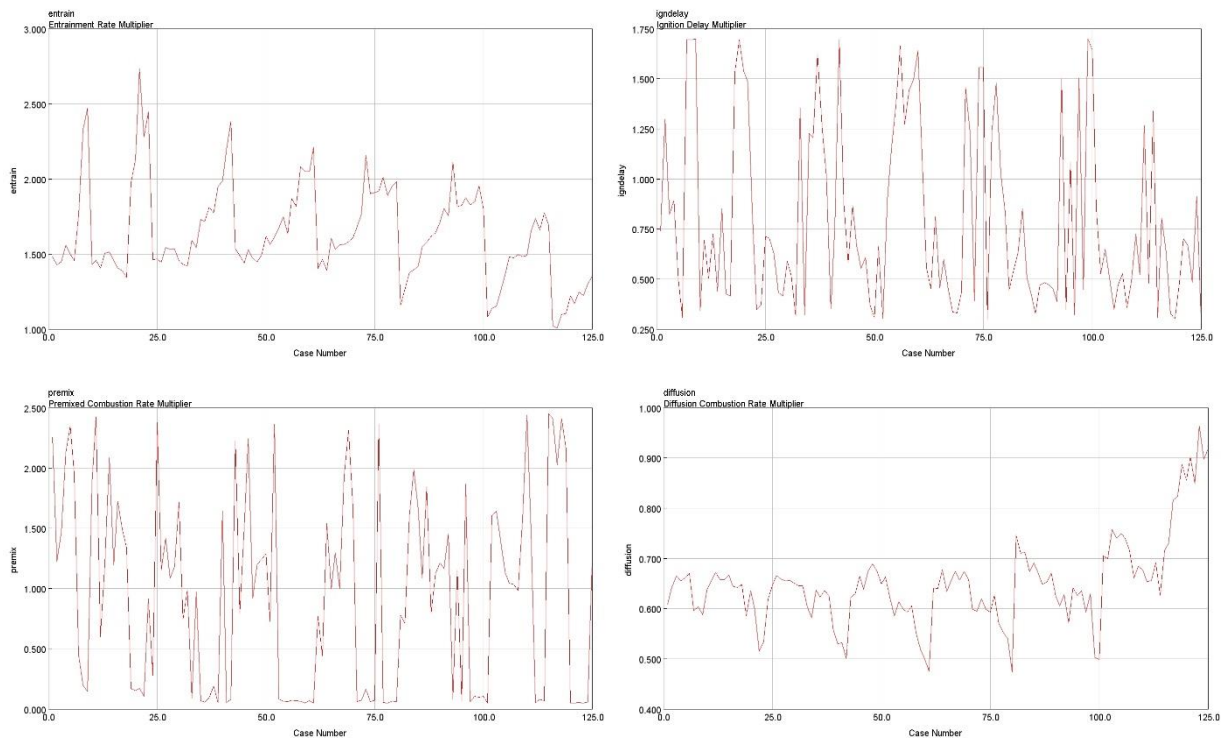


Fig. 83 – Independent Optimization Results a) Entrainment Multiplier b) Ignition Delay Multiplier c) Premixed Multiplier d) Diffusion Multiplier

A better accuracy for each case brings to a lower RMS error between measured and predicted combustion burn rates, like visible in *Fig. 84*.

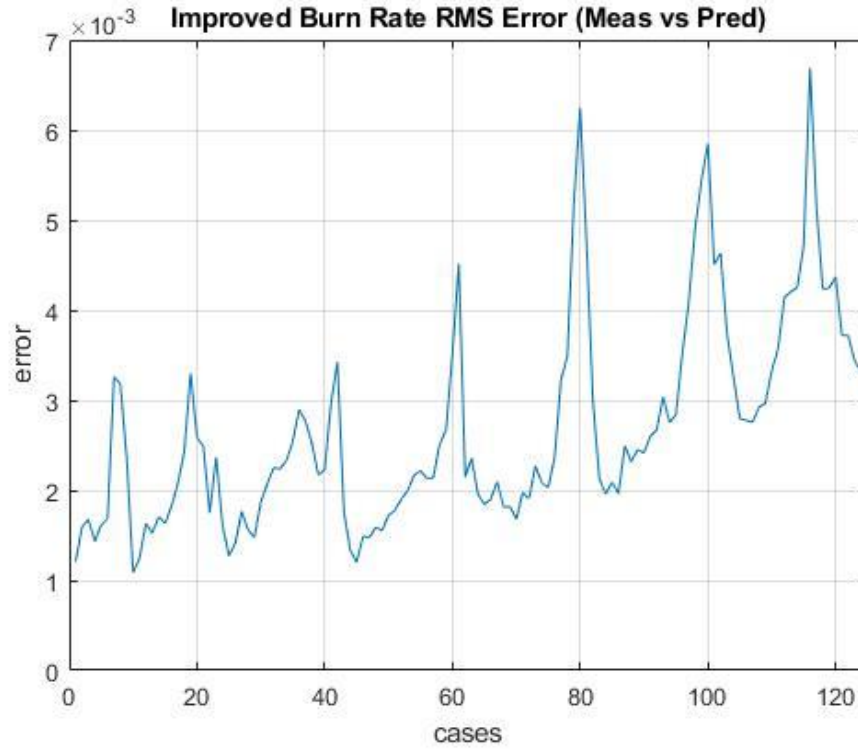


Fig. 84 – Improved Burn Rate RMS Error (Meas vs Pred)

Comparing those results with the one obtained in the previous simulation (Fig. 77) it is clearly visible that the independent ones are about one tenth with respect to the sweep ones. This is also reflected in pressure traces and burn rates where predicted and measured traces match better. Fig. 85 a) b) show these quantities for the ‘worst’ case of independent optimization.

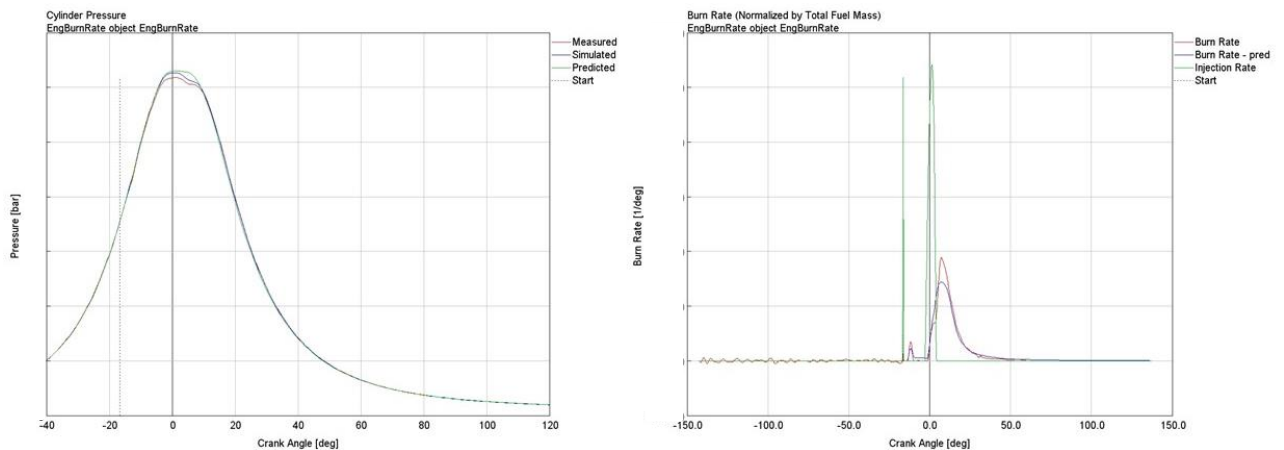


Fig. 85 – Worst case results a) Pressure traces b) Burn Rate

Even if this is the worst case of all the simulation, Fig. 85 a)b) show anyway a good match between predicted and measured both for in-cylinder pressure and combustion heat release. Like for the previous simulation, IMEP, MFB50 and maximum pressure must be checked within the imposed limits (Fig. 86, Fig. 87, Fig. 88).

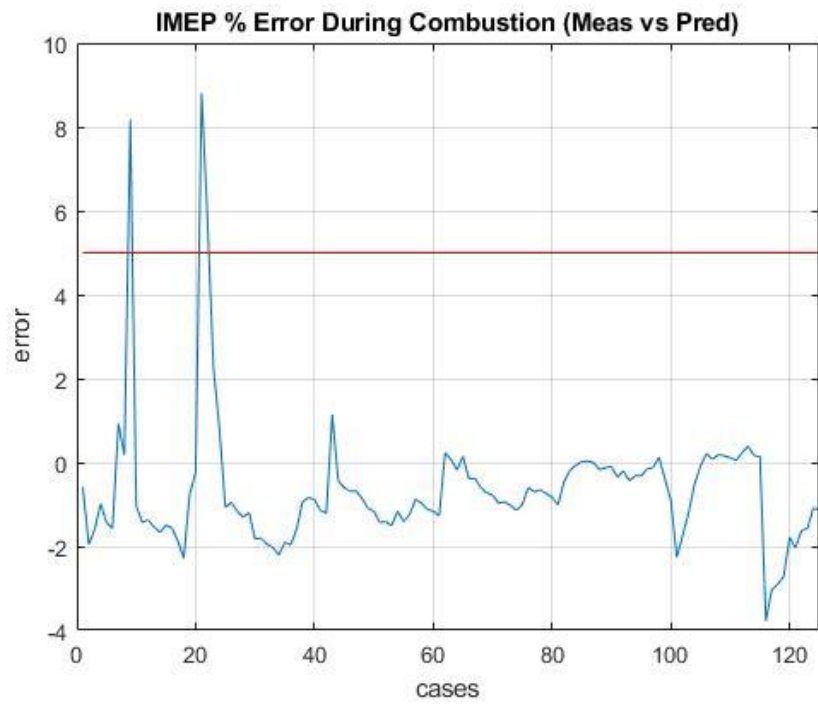


Fig. 86 – IMEP % Error During Combustion (Meas vs Pred)

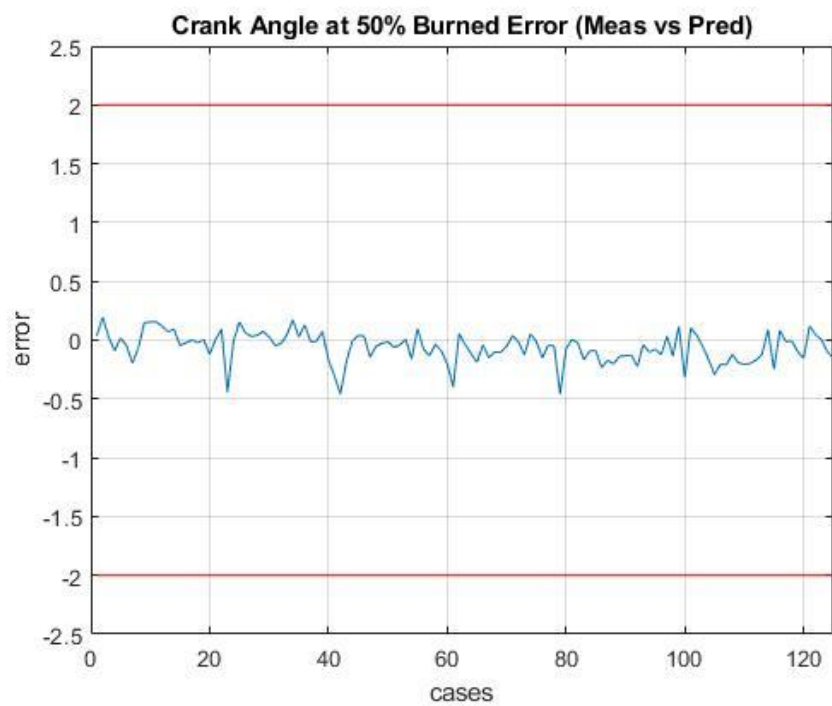


Fig. 87 – Crank Angle at 50% Burned Error (Meas vs Pred)

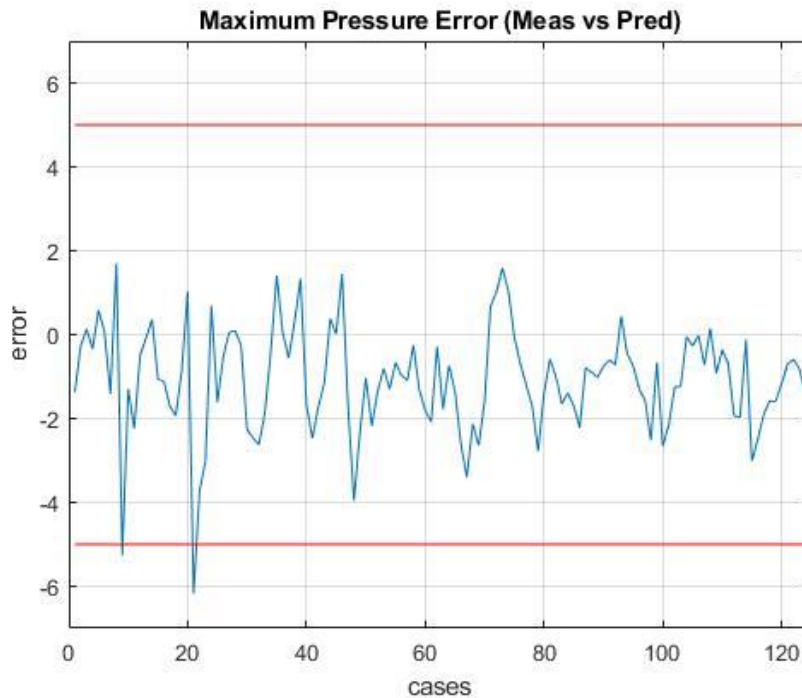


Fig. 88 – Maximum Pressure Error (Meas vs Pred)

Usually, the independent optimization results are better with respect to the sweep optimization results, because the set of multipliers is optimized for each case in order to find the best fit instead of being mediated on the whole case number to find the best compromise. However, observing the results obtained in this work, there is no big difference with respect to the previous, the results in independent optimization seem to fluctuate less, but in both cases, they are within the recommended limits, less than few negligible exceptions. These results open up to interesting implications in the next validation step.

iii. Sweep optimization for 125 operating points

Sweep optimization has been already described above, however in this case the simulation is performed for all the 125 available operating points. The procedure is the same, so in this sub-chapter are exposed only the obtained results.

Multiplier set – 64 sweep	
Entrainment Rate Multiplier	1,5683
Ignition Delay Multiplier	0,4058
Premixed Combustion Rate Multiplier	0,9598
Diffusion Combustion Rate Multiplier	0,6425

Table 8 – Set of Multipliers obtained from a Sweep Optimization with 125 Operating Points

Table 8 shows the set of multipliers valid for each case; comparing these values with the ones obtained in the sweep optimization for 64 points, it is clearly visible that the results seem to be very similar. This is an important result, because it means that the model is very strong, in fact it requires a few bunch of points for the calibration in order to obtain very solid results. Furthermore, calibration process requests a long computational time in order to reach the convergence in the iterative process, and this time increases with the number of point used as input. So, obtaining strong results with a minor number of operating points allows to perform

calibration process in less time. This result opens to another interesting question, that is how strong is this model, how much the number of points can be reduced in order to still have good results in term of set of multipliers. So, after this calibration a last sweep optimization process is performed using 32 operating points, in order to verify if the results are consistent yet, or the number of points is too little. 32 points calibration and validation are exposed in next section c.i. Anyway, these results are quite positive, and will be better discussed in the validation section c. Like for the previous simulations, *Fig. 89 a)b)c)d)* shows the errors on Burn Rate, IMEP, MFB50 and maximum pressure.

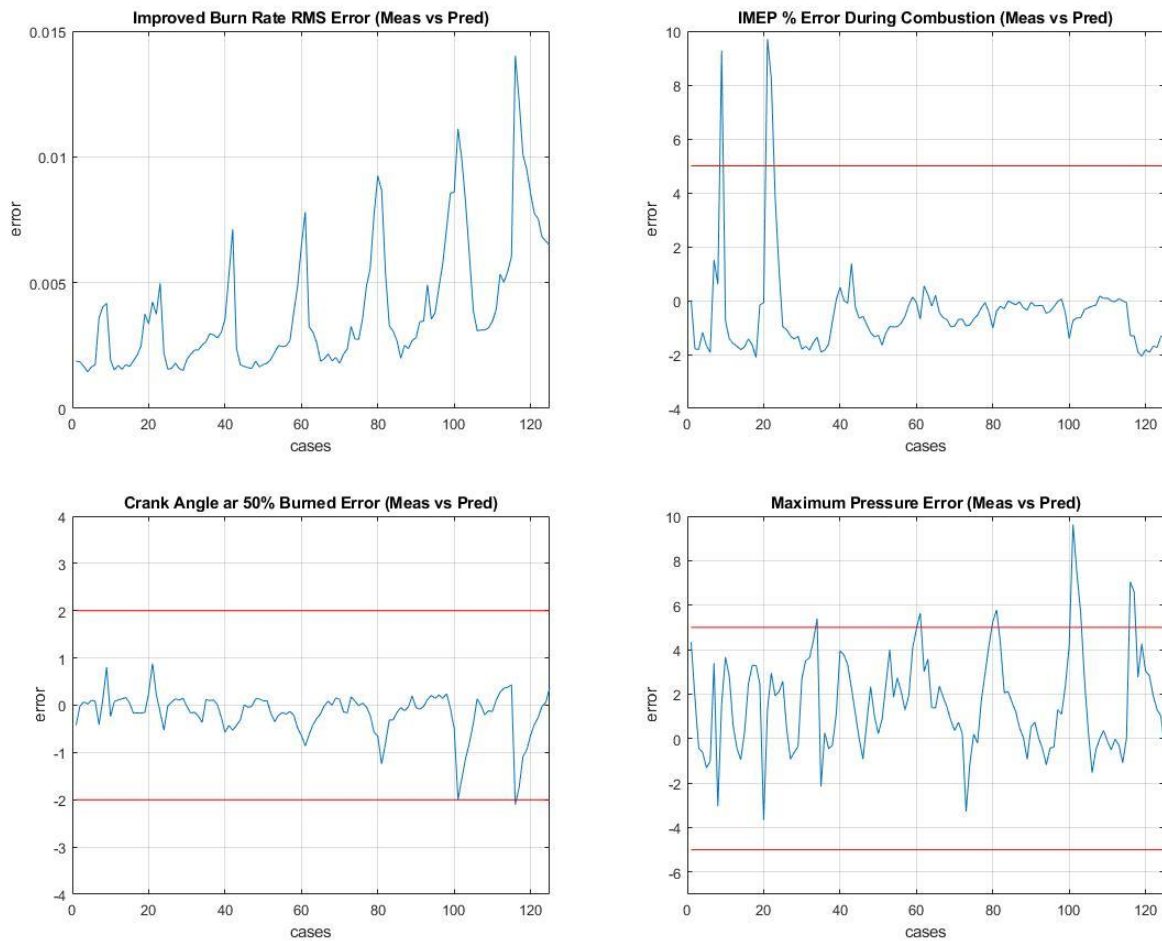


Fig. 89 – a) Improved Burn Rate RMS Error (Meas vs Pred) b) IMEP % Error During Combustion (Meas vs Pred) c) Crank Angle at 50% Burned Error (Meas vs Pred) d) Maximum Pressure Error (Meas vs Pred)

The trends in the figures are totally confrontable with the 64 points sweep simulation results, due to the similar values assumed by the four multipliers. Even in this simulation some points have an error bigger than the recommended limit and, like for the previous simulation, these errors are due engine conditions that in these points works near to idling.

c. DI Pulse validation results

Once the calibration process is ended, the next step is the validation of the DI Pulse combustion model. So, the set of multipliers obtained by the calibration are uploaded for each case (the same for all in sweep, one different for each case in independent) in the case setup of the full engine model. The validation of a model consists in understand how GT POWER simulation

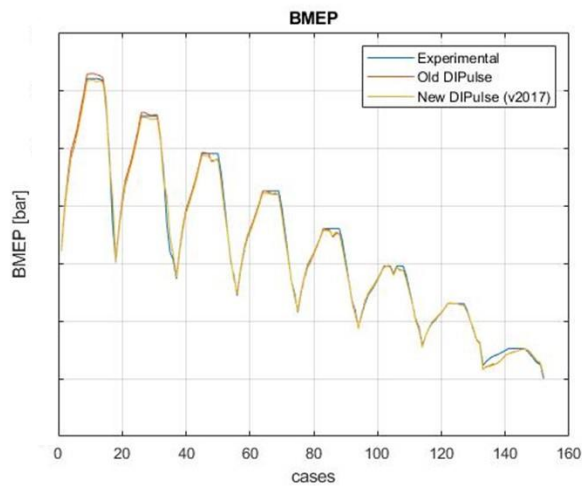
results fit with engine data obtained by rig tests, in order to test the model robustness. This validation is performed on different engine quantities, some quantities are directly linked with the combustion process, while other quantities are not directly linked, but their trend is strongly affected by the combustion process. These quantities are:

- BMEP
- MFB50
- IMEP720
- IMEP360
- FMEP
- PMEP
- In-cylinder maximum pressure
- Peak pressure position
- Intake manifold temperature and pressure
- Exhaust manifold temperature and pressure
- Air mass flow
- EGR mass flow

A description of these quantities is reported in section 3.2. In this work the results obtained using the now calibrated DI Pulse model (v2017) is compared not also with the experimental data, but also with the precedent DI Pulse model (v75) provided with the engine model at the beginning of this thesis work, to verify if this newer version brings better results with a higher accuracy. Furthermore, the validation process is performed for each calibration process tuned in the precedent section, so:

- Sweep optimization for 64 operating points
- Sweep optimization for 125 operating points
- Independent optimization for 125 operating points

And then these three validations are compared between them to find the best calibration settings. In order to have a quantitative overview on the results, two statistic indexes R2 and RMSE are evaluated for each simulation. These quantities synthesize the data robustness and highlight the correlation between the experimental data and the simulated ones. R2 and RMSE workings are explained in section 3.2. The following figures (*Fig. 90 a) to n)*) show the comparison between the experimental data and the simulated data and the tables on the right (*Fig. 90 a) to n)*) show the RMSE and R2 index values for each calibration process performed. Observing the tables of each analysed quantity it is possible to see different index values, in fact R2 and RMSE are evaluated not only on all the provided points, but also on some sub-sets of points: in particular, these statistic indexes have been evaluated for all the points used for calibration, and also for the points that in the non-predictive model do not pass the consistency check. For the same validation result, comparing the data's accuracy on different set of points allows to evaluate the consistency of the model: a good model, if correctly tuned, is able to provide comparable results whatever is the number of points used for its calibration.



Sweep 64 points

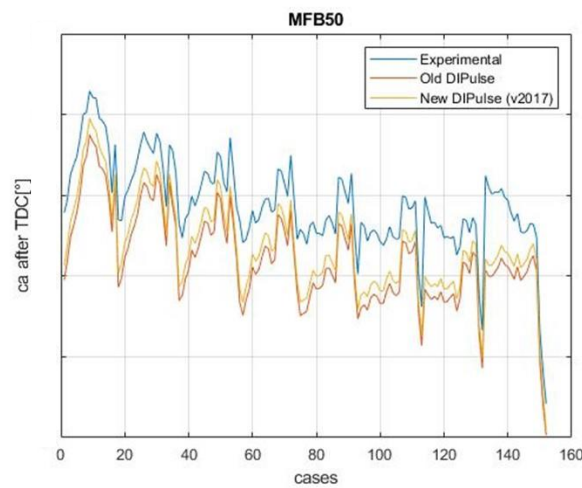
	R squared	RMSE
All Points (Old)	0,9968	0,411
All Points (New)	0,9972	0,3716
Cal. + Not Cal. (125)	0,9951	0,3916
Cal. (64)	0,9947	0,405
Not Valid (27)	0,9996	0,2598

Sweep 125 points

	R squared	RMSE
All Points (152)	0,9971	0,3845
Cal. (125)	0,9948	0,4052
Not Valid (27)	0,9995	0,2691

Independent 125 points

	R squared	RMSE
Cal. (125)	0,9952	0,3896



Sweep 64 points

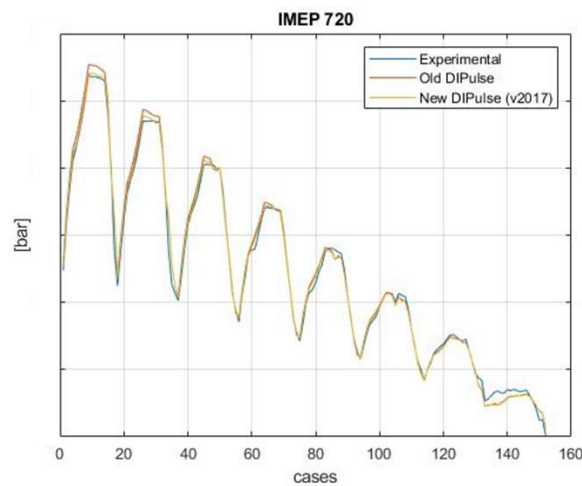
	R squared	RMSE
All Points (Old)	0,9224	3,4158
All Points (New)	0,9335	2,7001
Cal. + Not Cal. (125)	0,9048	2,7937
Cal. (64)	0,8928	2,8326
Not Valid (27)	0,9714	2,2159

Sweep 125 points

	R squared	RMSE
All Points (152)	0,9348	2,7274
Cal. (125)	0,9079	2,8226
Not Valid (27)	0,9728	2,234

Independent 125 points

	R squared	RMSE
Cal. (125)	0,8338	2,9289



Sweep 64 points

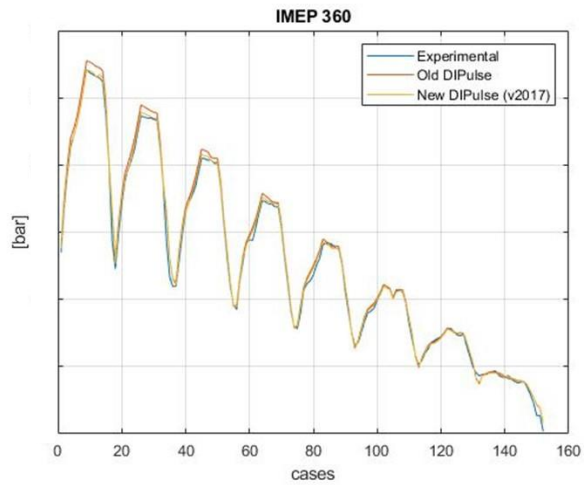
	R squared	RMSE
All Points (Old)	0,996	0,7436
All Points (New)	0,9964	0,4452
Cal. + Not Cal. (125)	0,9943	0,4532
Cal. (64)	0,9939	0,4724
Not Valid (27)	0,9988	0,4065

Sweep 125 points

	R squared	RMSE
All Points (152)	0,9962	0,4492
Cal. (125)	0,994	0,4551
Not Valid (27)	0,9988	0,4207

Independent 125 points

	R squared	RMSE
Cal. (125)	0,9943	0,4549



Sweep 64 points

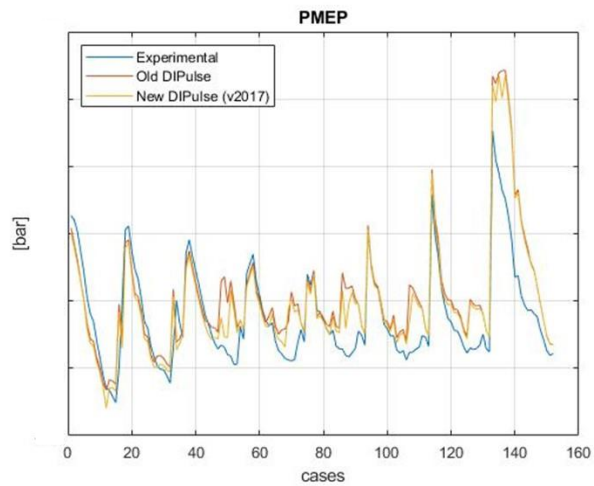
	R squared	RMSE
All Points (Old)	0,998	0,7396
All Points (New)	0,998	0,3468
Cal. + Not Cal. (125)	0,9969	0,3541
Cal. (64)	0,9965	0,3759
Not Valid (27)	0,9994	0,3107

Sweep 125 points

	R squared	RMSE
All Points (152)	0,998	0,346
Cal. (125)	0,9968	0,3526
Not Valid (27)	0,9994	0,3135

Independent 125 points

	R squared	RMSE
Cal. (125)	0,9968	0,3523



Sweep 64 points

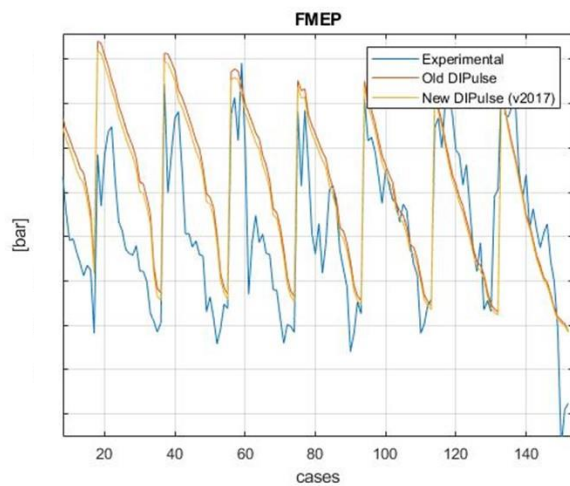
	R squared	RMSE
All Points (Old)	0,6967	0,2852
All Points (New)	0,725	0,2528
Cal. + Not Cal. (125)	0,6416	0,249
Cal. (64)	0,6519	0,2513
Not Valid (27)	0,9287	0,2697

Sweep 125 points

	R squared	RMSE
All Points (152)	0,7159	0,2603
Cal. (125)	0,6307	0,2547
Not Valid (27)	0,9268	0,2847

Independent 125 points

	R squared	RMSE
Cal. (125)	0,66	0,241



Sweep 64 points

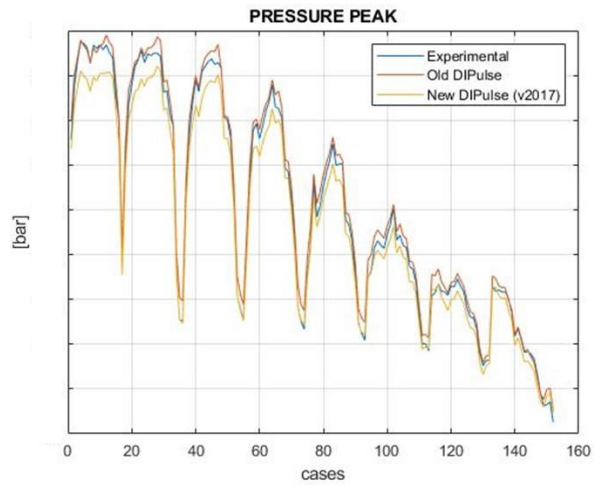
	R squared	RMSE
All Points (Old)	0,3696	0,5535
All Points (New)	0,582	0,2937
Cal. + Not Cal. (125)	0,6136	0,2819
Cal. (64)	0,6288	0,2893
Not Valid (27)	0,4229	0,3429

Sweep 125 points

	R squared	RMSE
All Points (152)	0,5814	0,2939
Cal. (125)	0,6135	0,2818
Not Valid (27)	0,4208	0,3441

Independent 125 points

	R squared	RMSE
Cal. (125)	0,6257	0,2889



Sweep 64 points

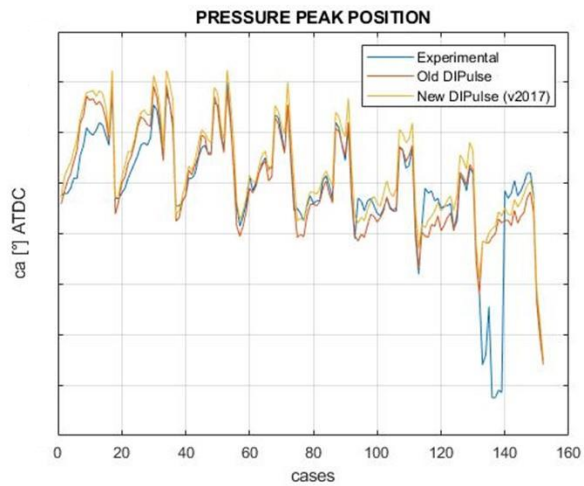
	R squared	RMSE
All Points (Old)	0,997	4,7447
All Points (New)	0,9973	6,9144
Cal. + Not Cal. (125)	0,9969	6,7147
Cal. (64)	0,9966	6,7269
Not Valid (27)	0,9981	7,7725

Sweep 125 points

	R squared	RMSE
All Points (152)	0,9974	6,8593
Cal. (125)	0,9971	6,7262
Not Valid (27)	0,9982	7,4448

Independent 125 points

	R squared	RMSE
Cal. (125)	0,9982	6,7457



Sweep 64 points

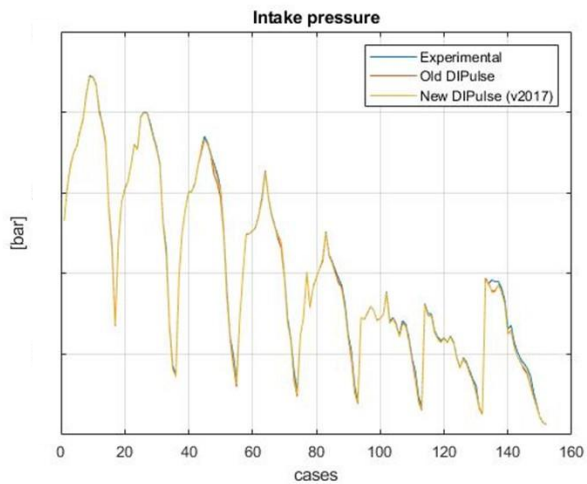
	R squared	RMSE
All Points (Old)	0,6664	1,4025
All Points (New)	0,6954	1,4631
Cal. + Not Cal. (125)	0,6731	1,2131
Cal. (64)	0,6597	1,2417
Not Valid (27)	0,7586	2,2886

Sweep 125 points

	R squared	RMSE
All Points (152)	0,6864	1,4943
Cal. (125)	0,6661	1,2377
Not Valid (27)	0,7467	2,3407

Independent 125 points

	R squared	RMSE
Cal. (125)	0,9517	0,6017



Sweep 64 points

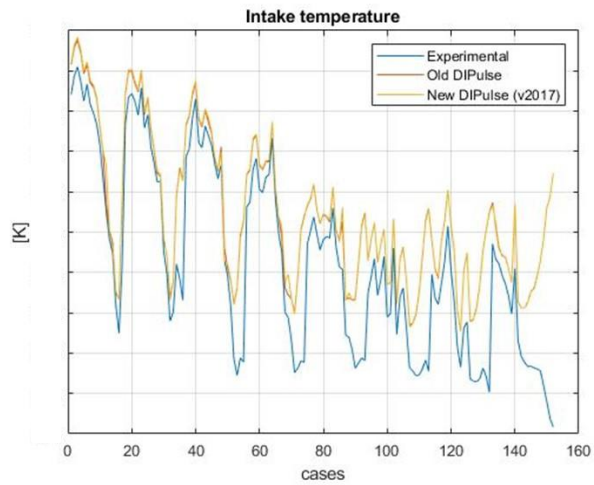
	R squared	RMSE
All Points (Old)	0,9992	0,0211
All Points (New)	0,9996	0,0163
Cal. + Not Cal. (125)	0,9994	0,0155
Cal. (64)	0,9996	0,0144
Not Valid (27)	0,9997	0,0197

Sweep 125 points

	R squared	RMSE
All Points (152)	0,9995	0,0176
Cal. (125)	0,9993	0,0171
Not Valid (27)	0,9997	0,0196

Independent 125 points

	R squared	RMSE
Cal. (125)	0,9996	0,0137



Sweep 64 points

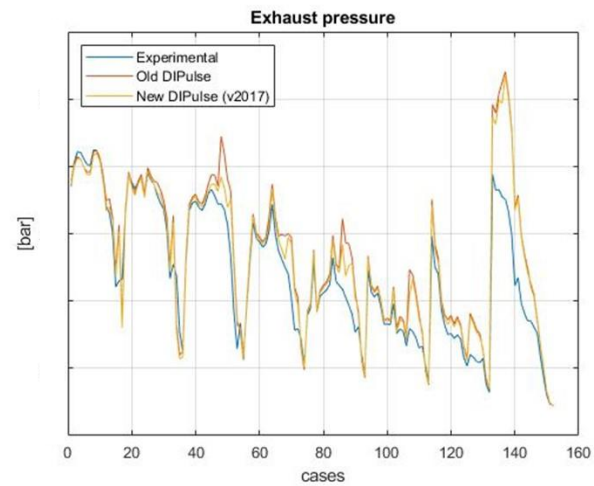
	R squared	RMSE
All Points (Old)	0,7825	3,2585
All Points (New)	0,7885	3,2669
Cal. + Not Cal. (125)	0,8795	2,7176
Cal. (64)	0,8784	2,7637
Not Valid (27)	0,5047	5,0885

Sweep 125 points

	R squared	RMSE
All Points (152)	0,787	3,2635
Cal. (125)	0,8783	2,7116
Not Valid (27)	0,5226	5,0907

Independent 125 points

	R squared	RMSE
Cal. (125)	0,8768	2,739



Sweep 64 points

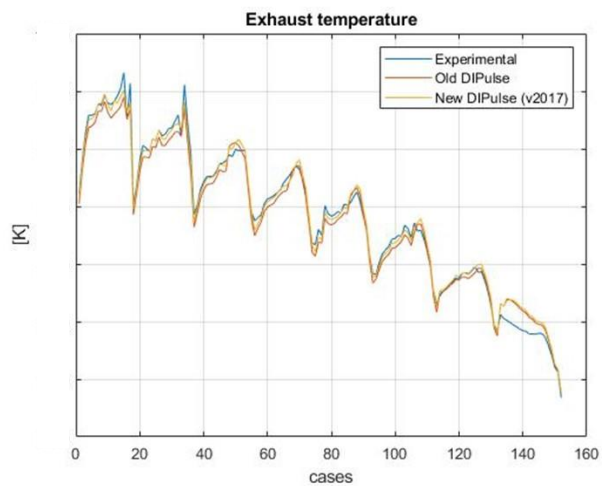
	R squared	RMSE
All Points (Old)	0,8573	0,2561
All Points (New)	0,8714	0,2235
Cal. + Not Cal. (125)	0,8493	0,2176
Cal. (64)	0,8521	0,2196
Not Valid (27)	0,9138	0,2491

Sweep 125 points

	R squared	RMSE
All Points (152)	0,8684	0,2324
Cal. (125)	0,8473	0,2255
Not Valid (27)	0,9089	0,262

Independent 125 points

	R squared	RMSE
Cal. (125)	0,859	0,2112



Sweep 64 points

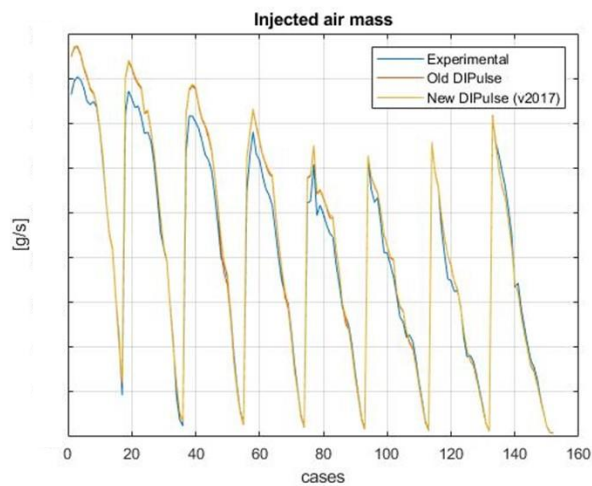
	R squared	RMSE
All Points (Old)	0,989	17,2322
All Points (New)	0,9914	13,5588
Cal. + Not Cal. (125)	0,9872	13,3087
Cal. (64)	0,988	13,4356
Not Valid (27)	0,997	14,6616

Sweep 125 points

	R squared	RMSE
All Points (152)	0,9906	14,3307
Cal. (125)	0,9861	13,9504
Not Valid (27)	0,9964	15,974

Independent 125 points

	R squared	RMSE
Cal. (125)	0,9886	13,1098



Sweep 64 points

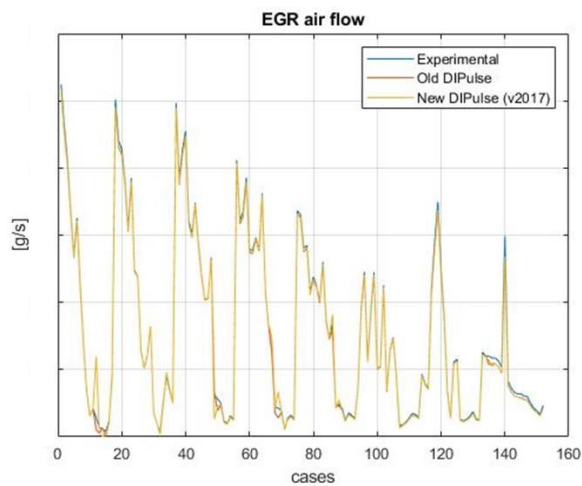
	R squared	RMSE
All Points (Old)	0,9926	16,7147
All Points (New)	0,9926	17,7114
Cal. + Not Cal. (125)	0,9932	19,2009
Cal. (64)	0,994	19,2924
Not Valid (27)	0,9975	7,6908

Sweep 125 points

	R squared	RMSE
All Points (152)	0,9927	17,543
Cal. (125)	0,9933	19,0119
Not Valid (27)	0,9975	7,6918

Independent 125 points

	R squared	RMSE
Cal. (125)	0,9941	19,3171



Sweep 64 points

	R squared	RMSE
All Points (Old)	0,999	0,6131
All Points (New)	0,9953	0,963
Cal. + Not Cal. (125)	0,9985	0,6382
Cal. (64)	0,9974	0,7856
Not Valid (27)	0,8836	1,8261

Sweep 125 points

	R squared	RMSE
All Points (152)	0,9954	0,9594
Cal. (125)	0,9982	0,6787
Not Valid (27)	0,8928	1,7467

Independent 125 points

	R squared	RMSE
Cal. (125)	0,9977	0,7745

Fig. 90 – Validation Results for all the calibration processes with related statistic indexes a) BMEP b) MFB50 c) IMEP720 d) IMEP360 e) FMEP f) PMEP g) In-cylinder Max Pressure h) Peak Pressure Position i) Intake Manifold Pressure j) Intake Manifold Temperature k) Exhaust Manifold Pressure l) Exhaust Manifold Temperature m) Air Mass Flow n) EGR Mass Flow

All the figures show three different trends, the blue one is the experimental one, while the orange and the yellow are respectively the quantity trend obtained with the old DI Pulse and with the now calibrated DI Pulse; these ones are obtained with the sweep optimization using 64 operating points. The results obtained by the other two simulations have not been reported in graphic form but only in analytic form as R2 and RMSE values, because their trends are very similar to each other and in a diagram like this the small differences are not visible. However, by observing the statistic indexes it is possible to get information in order to understand which model is the best. By comparing the old DI Pulse with the new one, is clearly visible that the yellow curve seems to fit better the experimental data curve, and this better fit is also appreciable by observing the indexes, where the R2 index is higher using the just calibrated DI Pulse (R2 is better when its value is as closer to one as possible – R2 equal to one indicates that experimental and simulated data are identical) while RMSE index

results to be minor (RMSE evaluates the error between simulated and experimental data, so, in reverse with respect to R^2 , a lower RMSE value means that the committed error is minor). Observing the results obtained with the 64 sweep optimization process it is possible to note an improvement: even if for the most part of the analysed quantities the old one DI Pulse already reaches quite satisfying results, the new DI Pulse seems to achieve even better results; for other quantities instead (such as MFB50, FMEP, PMEP) this improvement is even more visible, because in these cases the old DI Pulse is not able to follow the experimental data correctly, while the new one even if there are still some problems due to external factors achieves better results. However, for each investigated quantities bigger problems are visible in the last 25-30 cases, cases where the engine works in idling conditions: for these cases both DI Pulses fail to follow the experimental trend. This discrepancy is probably due to the flap valve in exhaust manifold that, even if in all the 152 operating points used for this work is always completely opened, increases the backpressure causing fluctuations in the data, especially at very low conditions in engine running. Flap valve using is described better in section 3.1.

Focalizing then on the results provided by the sweep optimization using the whole set of operating points that pass the consistency check, it is possible to see that the statistic indexes confirm a good match between the experimental data and the simulated ones. Furthermore, comparing their accuracy with the previous validation (sweep with a 64 points) it is visible that the two simulations are very consistent, because they both provide very similar results. This is an excellent goal of this work, because this confirm that the model is well generalized: obtaining about the same results on 152 point by calibrating with 64 rather than 152 operating points means that the model is very robust, and then it can be used in general on a wider range of operating points in any operating condition of the engine, always providing reliable results. This analysis confirms as said in the calibration step, where both the calibration using 64 points and 125 points provides about the same set of multipliers.

The last simulation is performed using the calibration results of 125 operative points, with independent optimization settings. Independent optimization provides 125 different sets of multipliers, one for each operating points. This single set of multipliers is evaluated specifically for each engine operative condition, while the sweep optimization works by finding the best compromise for all the considered cases: so, independent optimization is able to provide higher accuracy in the results with respect to a sweep optimization, at least theoretically. However, by observing statistic indexes R^2 and RMSE visible in *Fig. 90 a) to n)*, it is possible to see that the data accuracy is for almost all the quantities (FMEP and PMEP present the worst matches) very high, with a higher R^2 and a lower RMSE, but if compared with the validation obtained with the single set of multipliers (sweep optimization with 64 points), the accuracy is lower or at least, in some quantities, is equal. In reality, for the pressure peak position quantity in *Fig. 90 h)* independent optimization validation presents a much greater accuracy with respect to the other cases, however this quantity is particularly affected by the flap valve problem discussed before, so for the last cases the real peak pressure position is not correctly evaluating (a strange trend is visible in this zone) due to this problem, so it is not possible to evaluate the correct accuracy of the model. This is a further confirmation about the model robustness: obtaining a higher accuracy with a single DI Pulse set of multipliers means that, like said before, this model could work with a higher number of operating points, and therefore in whatever engine operating conditions, and still obtaining consistent results.

By analysing the results, this model shows a particular flexibility, mostly in calibration phase where comparable accuracies in output quantities are achieved using 125 and 64 operating points. So, can be interesting to test this flexibility, by reducing the number of operating points needed for the calibration process, still using optimization sweep settings in order to obtain a single set of multipliers. For these last test, 33 operating points all over the whole engine map are used: a further calibration points reduction cannot be done because GT POWER suggests using for DI Pulse model calibration at least 25 operative points.

i. Sweep optimization using 33 operating points

In this last calibration & validation test, the robustness of the model is tested by obtaining a single set of multiplier (sweep optimization) reducing the operating points from 64 to 33; also in this case, the points are selected all over the engine map, in order to cover all the engine operating conditions.

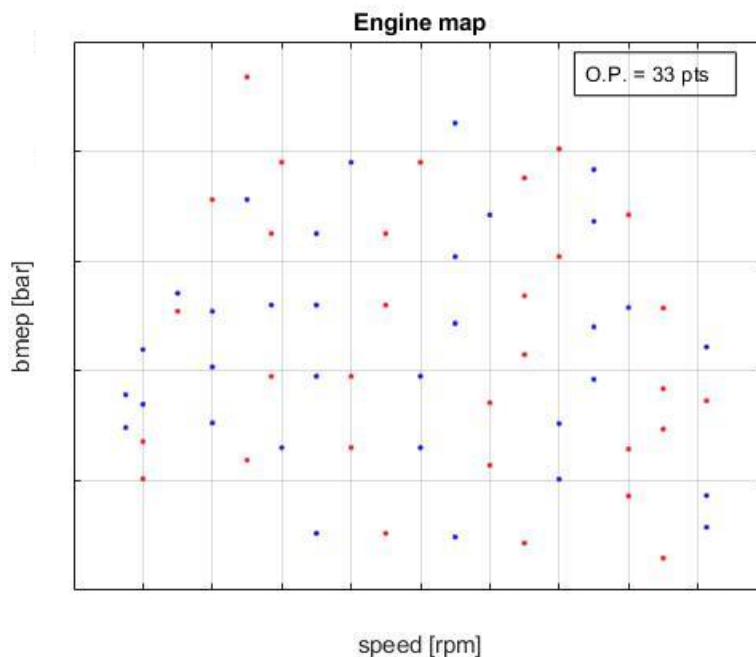


Fig. 91 – Operating points used for the calibration

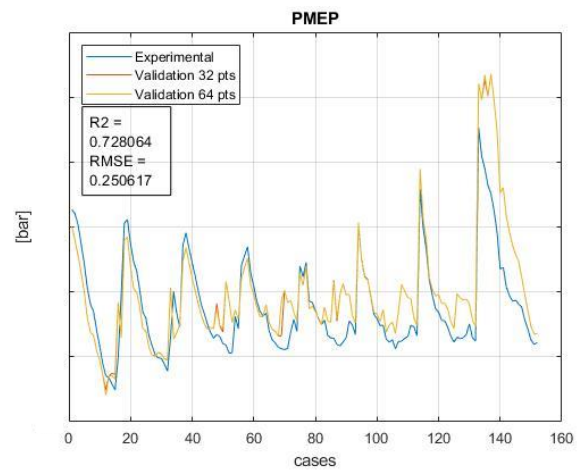
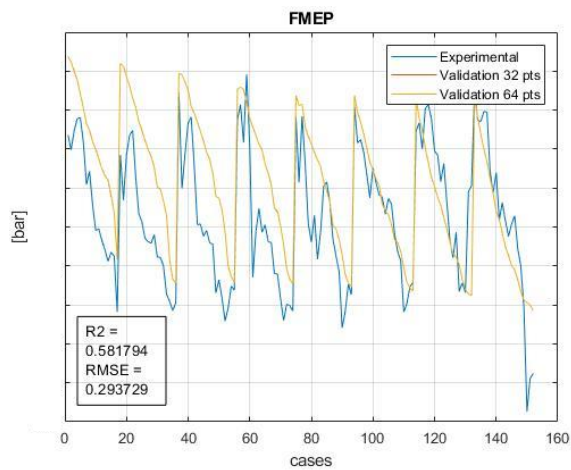
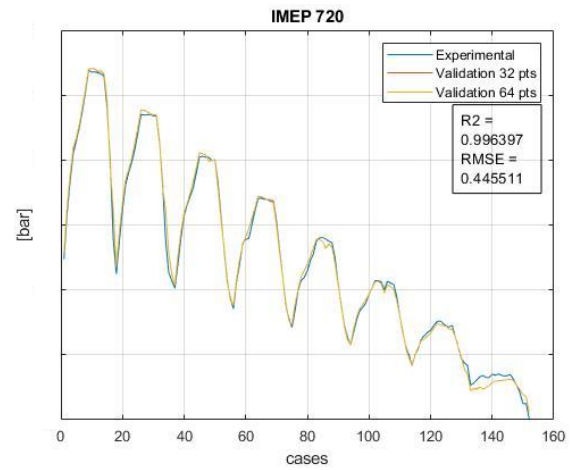
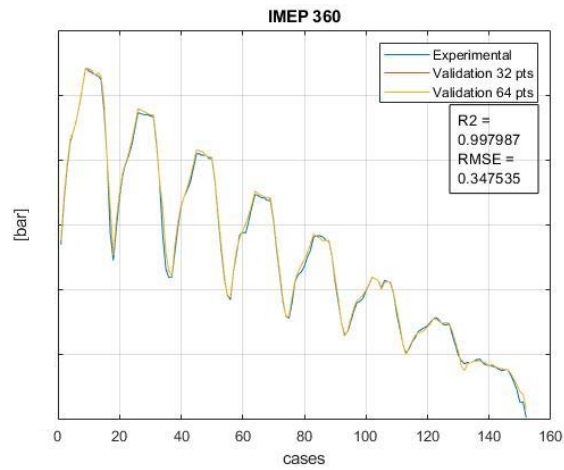
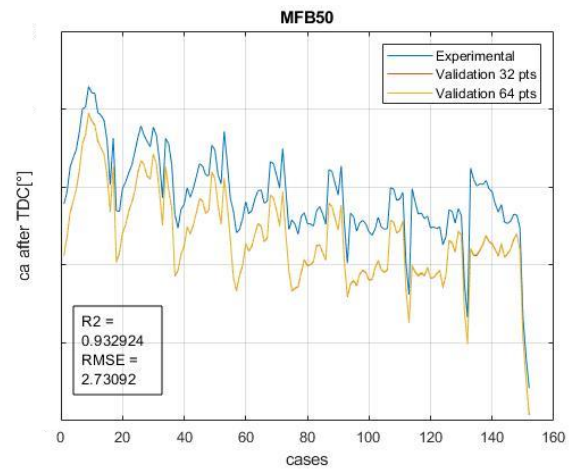
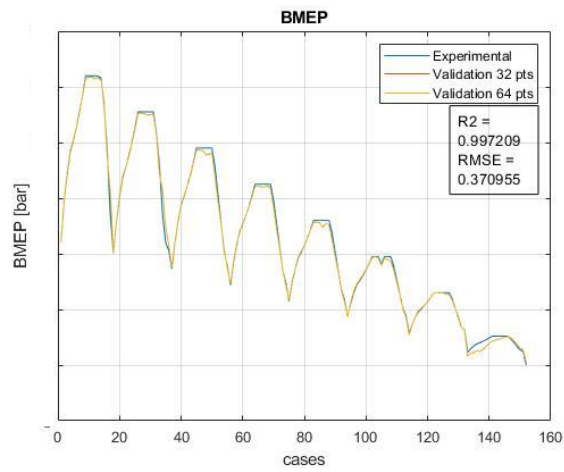
Fig. 91 shows the 33 operating points used for the calibration process, chosen from the 64 available from the first process (the blue ones are the chosen). All the optimization settings are completely identical with respect to the precedent calibration exposed in this work. The set of multipliers obtained is listed in Table 9:

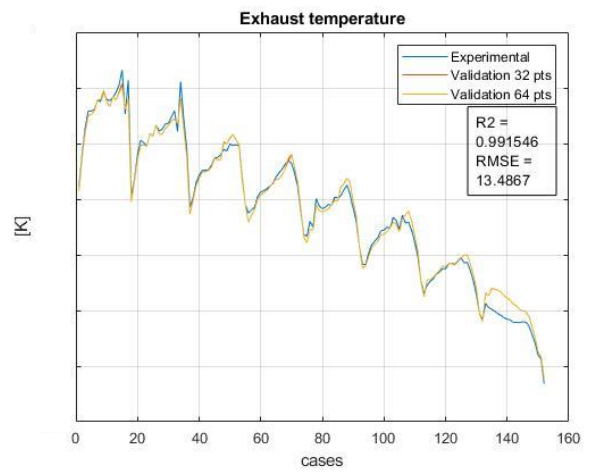
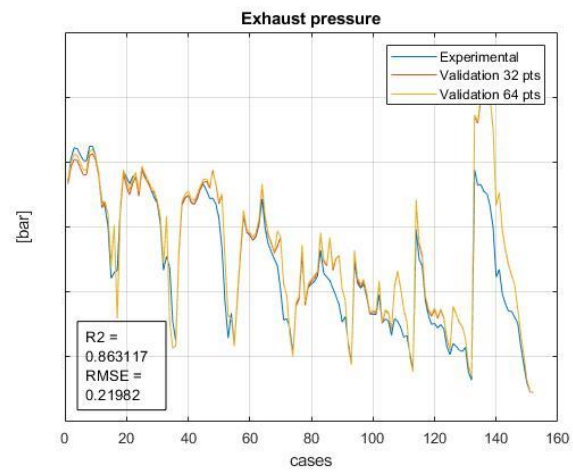
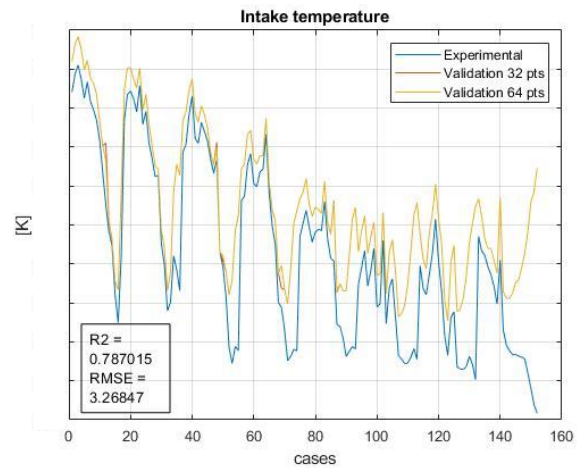
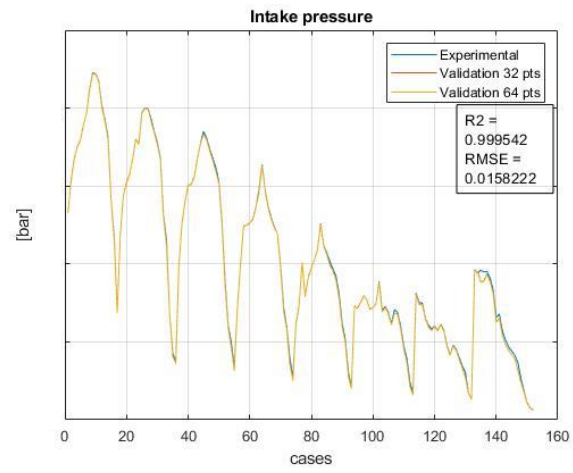
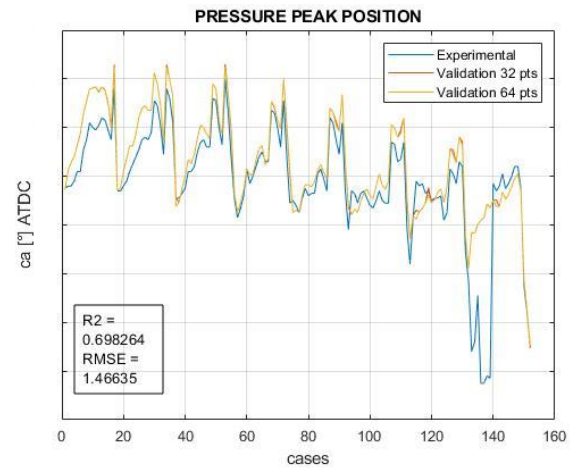
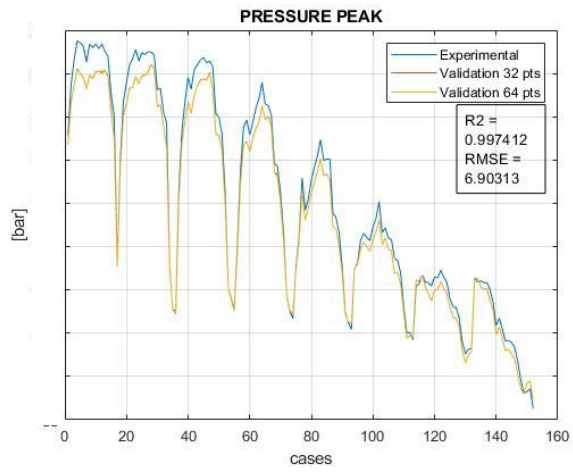
Multiplier set – 64 sweep	
Entrainment Rate Multiplier	1,5708
Ignition Delay Multiplier	0,4149
Premixed Combustion Rate Multiplier	0,9612
Diffusion Combustion Rate Multiplier	0,6386

Table 9 – Set of Multipliers obtained from a Sweep Optimization with 33 Operating Points

Comparing these results with the ones obtained in the other calibration processes (Table 9), it is possible to note that the multiplier values deviate a little with respect to the ones obtained using a huger number of points. With these values, the full engine model is validated using the same

quantities used for previous validations. *Fig. 92* from a) to n) show the results obtained, with their respective R2 and RMSE statistic index values.





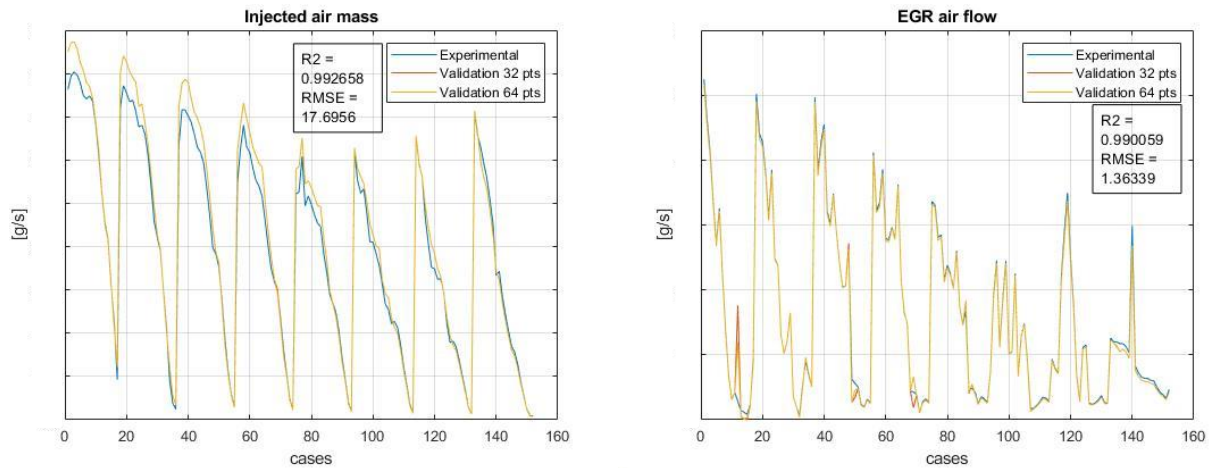


Fig. 92 – Validation Results a) BMEP b) MFB50 c) IMEP360 d) IMEP720 e) FMEP f) PMEP g) In-cylinder Max Pressure h) Peak Pressure Position i) Intake Manifold Pressure j) Intake Manifold Temperature k) Exhaust Manifold Pressure l) Exhaust Manifold Temperature m) Air Mass Flow n) EGR Mass Flow

These figure plot the results obtained in this section (orange trend) with the ones obtained in the simulation using 64 operating points (yellow trend), the blue curves represent the experimental quantities. The result is very interesting, because observing the quantity trends, as well as comparing the static index values, it is possible to confirm that even by using a smaller amount of operating points for the calibration process, the model seems to adapt in order to provide good results. In fact, for each analysed quantities, besides some punctual fluctuations, the trends are totally overlapped, and so the R2 values are completely comparable. This last DI Pulse calibration & validation test confirm what has been said in the previous sections, that is, that this model manages to deliver very truthful results with a single set of DI Pulse multipliers, whatever the number of calibrating points is.

However, this last test is reported only in order to further confirm the model robustness: in fact, in this particular case the available points that passed the consistency check are many, so it is not necessary to select only 33 cases on 125 available, a calibration using 64 points (about a half of the total) is the best solution.

6. CONCLUSIONS

At first, the aim of this project was to upgrade the predictive combustion model DI Pulse in GT POWER on a 11 liters Diesel engine, 6 cylinders, direct injection, supercharged for heavy duty applications from an old v76 GT POWER version to a newer v2017 version in order to obtain several improvements during the validation.

However, during the first validation of the old DI Pulse, analyzing the match between the simulated data and the ones provided by FPT Industries it turned out that several errors could come from a wrong pressure trace phasing, since even 1° degrees before or after the real TDC position can bring up to 10% evaluation error on IMEP and from 5% to 25% error on the heat released by combustion event. So, in order to verify the correct phasing or finding the correct one, three different TDC phasing methods were carried out: the results of these methods was that the provided pressure traces must be shifted forward by $0,2^\circ$ degrees.

Then, with these new pressure traces, the v2017 DI Pulse model can be tuned. However, before to calibrate a predictive model, the operating points available for the calibration must be checked in order to exclude any anomalous points: so, for this aim a non-predictive model must be used. GT POWER provides two different non-predictive models, which differ according to the available data for the setup: CPOA (Cylinder Pressure Only Analysis) which needs only the in-cylinder pressure trace in order to evaluate the combustion burn rate, and TPA (Three Pressure Analysis) which, beyond the in-cylinder pressure trace, also requires intake and exhaust manifold pressure. Both methods have drawbacks, however the results at the end must be the same. In this work both non-predictive models are tested.

The operating points that passed the non-predictive model Consistency Check have been then used for the DI Pulse model calibration. DI Pulse calibration consists in optimizing a certain quantity in order to obtain the best set of four multipliers, which govern four crucial steps of Diesel combustion (Entrainment, Ignition Delay, Premixed Combustion, Diffusion Combustion). The quantity to minimize suggested by GT POWER manual is the *Improved Burn Rate RMS Error (Meas vs Pred) parameter*. GT POWER allows to perform two different optimization processes: sweep optimization, which gives a single set of multipliers for all the available case, and independent optimization, which gives a different set of multipliers for each case. In this work, three different calibrations have been performed in order to find the best settings: a sweep optimization process using 125 cases (all the consistency check-passed cases), a sweep optimization process using a half of the total amount of points, and an independent optimization on all the provided points. Then, the obtained set of multipliers from the calibration process must be uploaded in the full model engine: this second step is called model validation. The results of the model validation must be compared with the data provided by rig tests in order to verify if the model is able to simulate the engine performances. The obtained results are very satisfying: all the simulations seem to obtain a good correspondence between simulated and measured data, which means that the model is correctly tuned. Furthermore, the best results came from the sweep optimization calibration, which means by using a single set of multipliers. This result is very positive, because it means that the model is very robust and even by calibrating with a few bunch of points it can works with different points, even in transitory, and still provides excellent results.

7. BIBLIOGRAPHY

- [1] C. F. Taylor, The Internal-Combustion Engine in Theory and Practice Volume 2 - Combustion, Fuels, Materials, Design, Second ed., vol. 2, The M.I.T. Press, 1985.
- [2] F. Millo, Design of Engine and Control System course's material.
- [3] G. Ferrari, Motori a Combustione Interna, Bologna: Società Editrice Esculapio, 2016.
- [4] E. Spessa, Engine Emission Control course's material.
- [5] J. E. Dec, "A Conceptual Model of DI Diesel Combustion Based on Laser-Sheet Imaging," *SAE Technical Paper 970873*, 1997.
- [6] E. Spessa, Design of Engine and Control System course's material.
- [7] Gamma Technologies, GT-SUITE: Flow Theory Manual, 2017.
- [8] Gamma Technologies, Engine Performances Application Manual, 2017.
- [9] A. B. Emiliano Pipitone, "Determination of TDC in internal combustion engines by a newly developed thermodynamic approach," in *Applied Thermal Engineering*, Palermo, 2010, pp. 1914-1926.
- [10] P. Tunestal, "TDC Offset Estimation from Motored Cylinder Pressure Data based on Heat Release Shaping," *IFP Energies nouvelles*, 2011.
- [11] O. L. C. S. R. M. Tazerout, "TDC Determination in IC Engines Based on the Thermodynamic Analysis of the Temperature-Entropy Diagram," *SAE Technical Paper 1999-01-1489*, 1999.
- [12] J. R. Jaye. Auburn Hills, MI (US) Patent US 6367317 B1, 2002.
- [13] M. J. R. B. T. B. Faisal Lodi, "Statistical Analysis of the Results Obtained by Thermodynamic Methods for the Determination of TDC Offset in an Internal Combustion Engine," *SAE Technical Paper 2020-01-1350*, p. 2020.
- [14] J. B. Heywood, Internal Combustion Engine Fundamentals, New York: McGraw-Hill, 1988.
- [15] F. M. G. B. a. M. R. Andrea Piano, "Assesment of the Predictive Capabilities of a Combustion Model for a Modern Common Rail Automotive Diesel Engine," *SAE Technical Paper 2016-01-0547*, 2016.
- [16] D. N. A. Dohoy Jung, "Multi-Zone DI Diesel Spray Combustion Model for Cycle Simulation Studies of Engine Performance and Emissions," *SAE Technical Paper 2001-01-1246*, 2001.
- [17] L. E. Ylva Nilsson, "Determining TDC Position Using Symmetry and Other Methods," *SAE Technical Paper 2004-01-1458*, 2004.

- [18] R. Finesso, "Fast calibration procedure of the DIPulse combustion object," 2018.
- [19] O. M. D. M. E. S. M. V. Y. Y. G. H. C. M. Roberto Finesso, "Development and Assessment of Pressure-Based and Model-Based Techniques," *SAE Technical Paper 1996-1073*, pp. 1538-1555, 2017.
- [20] E. Spessa, Combustione e gasdinamica delle macchine course's material.